

FINAL REPORT

NASA Grant #NGR 22-009-496

DSR #72406

"Spectral Study of Suggested Apollo Sites"

Thomas B. McCord
Principal Investigator
Department of Earth and Planetary Sciences
Massachusetts Institute of Technology

INTRODUCTION

This is the final report on two years of research which were conducted under the auspices of the National Aeronautics and Space Administration. A one-year telescopic spectral reflectivity analysis of proposed lunar landing sites was carried out beginning in April 1970. In March 1971 the project was extended for another year. A report was submitted on the first year's work (see attachment A); this is the report on the second year's work. Copies of the proposals for both years are also included (attachments B and C).

ACTIVITIES

Under the grant extension the following was accomplished:

1) a final report of the results of the project was completed and distributed; 2) the data have been reworked to include some minor corrections discovered to be useful; 3) an atlas of both graphic and numerical data has been prepared and is available to interested groups. In addition, this information has been widely disseminated by presentation at a conference at MSC-LSI in January, 1972, an article published in The Moon (see attachment D) and detailed reports sent to the MSC and USGS mapping personnel for use in planning the Apollo 16 and 17 missions. We prepared a presentation for the Apollo 16 and 17 astronaut teams. It was given to the 17 crew but was cancelled for the 16 crew due to astronaut sickness.

Dr. Thornton Page of MSC also suggested that the Apollo 17 television camera be used to attempt mapping for rock types and minerals. He thought that this would be possible since we had shown that the absorption bands present in the reflection spectrum

of lunar rocks and soils are diagnostic of the rock type and mineralogy (see attachment D). The principal investigator was asked to consult on this project as part of the grant extension; he agreed to advise on this matter, but not to organize or direct it.

It was suggested that the vidicon tube in the Apollo camera be changed from a SIT to a direct silicon target vidicon. This would extend the spectral response into the infrared where the mineral absorption bands exist. Further, it was suggested that a set of filters be used which would show contrasts between rock types and at the same time allow public viewing of the lunar surface. The blue and green filters were essentially the same as those used on other missions but the red filter was to be moved to near 0.95 microns so as to be positioned in the pyroxene absorption band.¹ Using this filter, the dramatic band strength changes from rock to rock (see attachment E) would be visible on the television monitor.

Several meetings were held at MSC with Dr. Page and an RCA representative to prepare a proposal for a change in the hardware on the forthcoming mission. It became apparent at this time that there was little sympathy within the Apollo program for such a change.

We also worked with the MSC Image Processing Group on an attempt to extract useful mineral information from the tape of the Apollo 15 television science experiment. The principal investigator met with several members of the MSC group to advise on data to be processed and analyses to be used. There were several false starts before some preliminary analysis was performed. The results were encouraging; several color features

were evident in the processed images. However, the services of the MSC group were withdrawn before any further work could be done.

In the mean time, RCA modified an Apollo camera by installing a silicon vidicon and a 0.90 - 1.00 micron filter. I was unable to attend the demonstration which was performed at MSC on 10 March 1972 because of a previous commitment. The report I received stated that the camera worked well and spectral "contrast" was seen for a variety of terrestrial materials including basalt but little or no contrast was seen for "two lunar materials."

I do not understand how the test was performed. It has been fully demonstrated by spectrometer measurements in several laboratories, television imaging in my laboratory and telescope observations of the moon that spectral contrast factors of 2 and 3 exist in the 0.90 to 1.0 micron spectral region for a variety of lunar samples. The lack of contrast in the MSC test must have been due to a technical problem or poor choice of samples.

A few weeks after this demonstration the grant year expired. There was no attempt made by MSC to extend the work and I considered the project dead.

FOOTNOTES

1. See Figure 2 , Attachment D.

ATTACHMENT A

SPECTROPHOTOMETRY (0.3 to 1.1 μ) OF VISITED
AND PROPOSED APOLLO LUNAR LANDING SITES

Thomas B. McCord
Michael P. Charette
Torrence V. Johnson
Larry A. Lebofsky
Carle Pieters

Planetary Astrology Laboratory
Department of Earth and Planetary Sciences
Massachusetts Institute of Technology
Cambridge, Massachusetts 02139

FINAL REPORT-NASA GRANT NGR-22-009-496

August 1, 1971

MITPAL Publication #47

CONTENTS

	<u>Page</u>
INTRODUCTION	1
OBSERVATION AND DATA PRESENTATION	3
ANALYSIS OF LUNAR SAMPLES FROM VISITED APOLLO LANDING SITES	
Introduction	7
Observations and results	7
Interpretation	11
ANALYSIS OF PROPOSED LANDING SITES	
Introduction	15
CENSORINUS	
Position map	16
Positional and geologic description	17
Relative spectral reflectivity data	18
Results, Interpretation, Discussion	19
COPERNICUS	
Position map	20
Positional and geologic description	21
Relative spectral reflectivity data	23
Results, Interpretation, Discussion	24
DAVY RILLE	
Position map	26
Positional and geologic description	27
Relative spectral reflectivity data	28
Results, Interpretation, Discussion	29

DESCARTES

Position map	31
Positional and geologic description	32
Relative spectral reflectivity data	33
Results, Interpretation, Discussion	34

HADLEY-APENNINES

Position map	36
Positional and geologic description	37
Relative spectral reflectivity data	38
Results, Interpretation, Discussion	39

HYGINUS RILLE

Position map	41
Positional and geologic description	42
Relative spectral reflectivity data	44
Results, Interpretation, Discussion	45

LITTROW

Position map	46
Positional and geologic description	47
Relative spectral reflectivity data	48
Results, Interpretation, Discussion	49

MARIUS HILLS

Position map	51
Positional and geologic description	52
Relative spectral reflectivity data	53
Results, Interpretation, Discussion	- 54

TYCHO	
Position map	55
Positional and geologic description	56
Relative spectral reflectivity data	57
Results, Interpretation, Discussion	58
SPECTRAL REFLECTIVITY MEASUREMENTS	60
Introduction	
Observations and results	
Interpretation	
ACKNOWLEDGEMENTS	62
REFERENCES	63
APPENDICES	
I. LUNAR SPECTRAL TYPES (1971)	
T.B. McCord, M.P. Charette, T.V. Johnson,	
L.A. Lebofsky, C. Pieters, and J.B. Adams	
II. ALTERATION OF LUNAR OPTICAL PROPERTIES: AGE	
AND COMPOSITIONAL EFFECTS (1971)	
J.B. Adams and T.B. McCord	
III. OPTICAL PROPERTIES OF MINERAL SEPARATES, GLASS	
AND ANORTHOSITIC FRAGMENTS FROM APOLLO MARE	
SAMPLES (1971)	
J.B. Adams and T.B. McCord	

INTRODUCTION

The color of the lunar surface has been a topic of study since the beginning of the century (for a review of early studies, see McCord, 1968a, 1970). Only in the past few years, however, have the spectral reflectance properties of small regions of the lunar surface been determined throughout the spectral region where reflected solar radiation is important, i.e., from 0.3μ to 2.5μ .

Sufficient spectral resolution and intensity precision has now been achieved in the $0.3\text{--}2.5\mu$ region to detect absorption bands in the lunar reflection spectrum. Of equal importance is the appearance in the reflection spectrum of differences in both the continuum shapes and absorption band strengths from place to place on the lunar surface (McCord, 1968a, 1969 ab; McCord and Johnson, 1969, 1970; McCord et al., 1970). These effects are important to our understanding of the moon, since according to laboratory studies, the reflection spectrum of solids is controlled primarily by mineralogy and composition. Although only provisional predictions were available before the Apollo 11 samples were returned (Adams, 1968; McCord, 1968a), studies of the lunar samples supported and greatly extended these early results (Adams and Jones, 1970; Adams and McCord, 1970, 1971 ab; Conel, 1970; Conel and Nash, 1970).

The basis for the interpretation of absorption bands in the spectra of silicates between 0.3μ and 2.5μ was developed through the application of crystal field theory to mineralogy (Burns, 1965; White and Keester, 1966). Transmission spectra of

oriented single crystals, using polarized light, led to later refinements in band assignments (Burns and Fyfe, 1967; Bancroft and Burns, 1967; White and Keester, 1967; Burns, 1970).

Absorption bands have also been studied in diffuse reflectance spectra of minerals and their powders (White and Keester, 1967; Adams and Filice, 1967), thus establishing a foundation upon which planetary surface composition can be determined (Adams, 1968).

This report discusses a study of the spectral reflectance of regions of the lunar surface containing most of the proposed Apollo landing sites. Using these measurements, information regarding surface properties such as composition and mineralogy can be obtained. Specifically 1), the presence of pyroxenes which causes an absorption band at 0.95μ in the lunar reflection spectrum; 2), the proportion of crystalline to glass present in the soil which is derived from the slope of the reflectivity curve between 0.4μ and 0.7μ and strength of the 0.95μ absorption band; 3), the presence of Ti^{3+} ions in the glosses on the lunar surface which effects the reflection spectrum at blue and ultraviolet wavelengths.

The study uses information gained by analysis of the spectral properties of lunar samples in the laboratory and telescope spectra of over 100 lunar areas to provide information regarding the composition and mineralogy of each proposed lunar landing site. Several of the previously cited papers which formed the basis for this study are included in the Appendices for the reader's convenience.

OBSERVATION AND DATA PRESENTATION

Several areas of the lunar surface, approximately 18 kilometers in diameter, were studied in the regions of the visited and proposed Apollo landing sites (see Figure 1 for region locations). The 24-inch (61 cm) and 60-inch (152 cm) telescopes on Mt. Wilson, California were used with a double-beam, filter photometer (McCord, 1968b) to obtain the data. The spectral reflectivity of each area was measured in the spectral region from 0.3μ to 1.1μ , using 24 narrowband interference filters. A detailed description of the equipment and technique used in this study is given in Appendix I.

The data are discussed in two sections. The measurements of sites from which samples have been returned to earth and analyzed are discussed first. Laboratory analyses of the spectral properties and mineralogy of returned samples allow detailed interpretation of the telescopic spectral reflectivity curves. Much of this work has been published earlier and is reviewed for completeness.

The telescopic data for the proposed Apollo landing sites are discussed in the second section. The format for each site consists of a topographic map showing the locations of the areas observed, a description of the local geology, a set of relative spectral reflectivity graphs for the observed areas, and a discussion of the results. The spectral reflectivity measurements are discussed in a separate section.

The topographic maps are taken from the Lunar Atlas Chart (LAC) series published by the U.S.A.F. Aeronautical Chart

PRECEDING PAGE BLANK NOT FILMED

and Information Center. The geologic descriptions have been derived from the U.S. Geological Survey's Geologic Atlas of the Moon and inspection of Lunar Orbiter and Apollo photographs.

The reflectivity data are presented in two forms. First, two graphs of the normalized relative spectral reflectivity, scaled to unity at 0.564μ , are given. These plots are obtained by dividing the reflectivity of a given area by the reflectivity of a standard area. The standard for the first plot is the Mare Serentatis 2 standard area, while the standard for the second plot is a selected area within the investigated region. This use of relative reflectivities reveals important compositional information, since the relative data are sensitive to the small differences which exist in the spectrum of the various lunar areas.

Secondly, graphs of the normalized spectral reflectivity scaled to unity at 0.564μ are plotted in a separate section before the Summary and Recommendations. The normalized spectral reflectivity is proportional to the ratio of light energy reflected from the lunar surface to the incident solar flux.

The precision of the spectral reflectivity measurements discussed in this report is usually about 1%, as indicated by the error bars. The accuracy of the measurements is dependent on several variables. A variation of 2-3% is caused by changes in the phase angle of the moon, depending on when observations were made. The lack of complete knowledge of the solar and stellar fluxes introduces a possible error of 4% in the curves from 0.3μ to 0.4μ ,

1-2% from 0.4μ to 0.9μ , and 2-3% from 0.9μ to 1.1μ . It should be noted, however, that the relative spectral reflectivity curve shapes are not affected by the inaccuracies cited here.

ANALYSIS OF LUNAR SAMPLES FROM VISITED APOLLO LANDING SITES

INTRODUCTION

The study of samples returned from the moon has greatly increased our knowledge of the landing sites and their immediate surroundings. However, our understanding of the vast areas beyond these sites is dependent, in large part, on remote measurements. Therefore, it is important that the returned samples be studied as ground truth for observations of proposed landing sites. The extension of the knowledge gained from these sample analyses to lunar areas not yet visited allows future landing sites of exceptional interest to be chosen. It also allows the study of large regions of the moon for which the cost of in situ study would be prohibitive.

OBSERVATIONS AND RESULTS

Telescopic measurements of the spectral reflectivity for areas 18 km in diameter containing the Apollo 11, 12, 14 and Luna 16 landing sites and for the standard reference area in Mare Serentatis (21.4E, 18.7N) are shown in Figure 2. All curves are scaled to unity at 0.564μ to make the shapes directly comparable with each other.

The spectral reflectivity for all areas shown in Figure 2 increases steadily toward the red end of the spectrum. An absorption band appears near 0.95μ in all curves. The curves are characteristic of most lunar areas which have been studied to date (McCord and Johnson, 1970; McCord et al., 1971, see Appendix I).

There are small but significant differences between the curves shown in Figure 2, but they are difficult to analyze as plotted. Therefore, the relative spectral reflectivity curves (as described earlier) for the areas shown in Figure 2 are plotted in Figure 3 to resolve these subtle differences. Thus, curve A in Figure 3 is the ratio of curve b to curve a in Figure 2. Note the expanded scale in Figure 3 as opposed to Figure 2.

It has been found (McCord, 1968a, 1969; McCord and Johnson, 1969; McCord, et al., 1971) that the shapes of the relative reflectivity curves can be used to identify several types of lunar material. Basically, all upland regions except bright craters and a few other anomalously bright areas have a single curve-type. Upland bright craters have curve-types which grade into upland material curves with increasing crater age. Mare regions illustrate a suite of curves within one general class. Mare bright craters have a distinct curve-type which grades into mare curves with increasing crater age.

Discussion of the above curve-types and lunar material identification is given in Appendix I. According to this spectral type classification, the Apollo 11, 12 and Luna 16 curves all have mare-type curves. The Apollo 11 curve is near the "blue" end member of the mare curve series, while the Apollo 12 curve falls near the "red" end member of the series. The Luna 16 landing site curve is intermediate between the two aforementioned curves. The Apollo 14 curve is a typical upland curve.

PRECEDING PAGE BLANK NOT FILMED

INTERPRETATION

Apollo 11: Laboratory reflectivity curves of Apollo 11 rock, breccia, and soil samples have been compared with earth-based telescopic measurements of the landing site and with petrologic analysis of the samples (Adams and McCord, 1970 ab; Birkebak, et al., 1970; Conel and Nash, 1970; McCord and Johnson, 1970). The telescopic curve for the Apollo 11 site agrees very closely with the laboratory curve for the bulk surface fines. From these data, it was concluded that: (1) the surface fines at Apollo 11 site are representative of the lunar surface material within ten or more kilometers of the landing area. (2) Lunar fines produce much weaker absorption bands than the rocks. (3) Exposed, crystalline rocks are not sufficiently abundant at the landing site to significantly influence the reflectivity curve of the site. (4) The single, weak band at 0.95μ in the telescope curve is due mainly to clinopyroxene, with a minor influence of olivine on the band position. (5) The low albedo of the lunar soil can be attributed to the presence of iron and titanium ions in the glass present in the lunar soil.

Apollo 12: The telescopic spectral reflectivity curve for the Apollo 12 landing site (Figure 2) shows an absorption band at 0.95μ , as does the Apollo 11 curve. Also, the Apollo 12 curve continuum is similar to the Apollo 11 continuum. As in the Apollo 11 curve, these data would indicate that the clinopyroxene and dark glass in the Apollo 12 soil strongly influence the reflectivity curves. Laboratory analysis of the Apollo 12 samples confirm these interpretations (Adams and McCord, 1971 ab, see

Appendix II and III).

The intensity of the absorption band and the slope of the telescopic reflectivity curve continuum for the 18 km region containing the Apollo 12 site differ slightly from those of the Apollo 12 soil samples. Laboratory analysis of surface and sub-surface soil samples, and of mineral separates from these samples, indicate that these differences are due to variations in the relative proportion of crystalline to glassy material in the soil. These same studies (Adams and McCord, 1971 ab; Conel and Nash, 1970) demonstrated that vitrification of lunar crystalline material changes the spectral properties of the material. These changes are observed when reviewing the range of telescopic curves from bright craters (more crystalline material, less glass) to mare surface material (less crystalline material, more glass) (McCord, et al., 1971).

Further studies of the Apollo 12 samples (Adams and McCord, 1971 ab) have revealed that the spectral region from 0.3μ to 0.6μ is affected by the amount of Ti^{3+} ions present in the lunar glass. Ti^{3+} ions in the crystalline material have been found to produce an absorption band at approximately 0.5μ and cause an increase in reflectivity in the ultraviolet. Ti^{3+} ions are also found in ilmenite, but the mineral is so opaque that almost no light which enters the crystal is reflected back into space. Thus, titanium in ilmenite has little effect on the spectral reflectivity curves.

Laboratory studies of titanium-rich lunar minerals and glasses, and of artificially generated glasses (Conel, 1970; Adams and McCord, 1970 ab, 1971 ab) show that the amount of titanium

present in the lunar glasses can be measured using spectral reflectivity curves. This information was used to predict the lower titanium content in the Apollo 12 samples over the Apollo 11 samples (Johnson and Soderblom, 1969).

Luna 16: The spectral reflectivity curve for the Luna 16 landing (Figure 2) has a 0.95μ absorption band and a positively sloping curve similar to those for the Apollo 11 and Apollo 12 landing site curves.

The Luna 16 relative spectral reflectivity curve (Figure 3) is a mare-type curve which is intermediate between the Apollo 11 and Apollo 12 curves (McCord, et al., 1971). The absorption band is similar to that found in the Apollo 11 curve, but the continuum is more similar to the Apollo 12 continuum. It can be inferred from these data that the crystal-to-glass ratio of the Luna 16 soil is similar to that of Apollo 11, but the titanium content is more similar to the Apollo 12 content. The Luna 16 sample analyses available to date bear out these interpretations.

Apollo 14: The spectral reflectivity curve for the Apollo 14 landing site has an absorption band near 0.95μ , but it is much shallower than in any landing site curve previously discussed. The overall curve shape suggests the presence of glasses but the much higher albedo of this upland area over the mare regions implies that a lower amount of Ti^{3+} and Fe^{3+} exists in the glasses of the region, i.e. less dark glass is present. The absorption band position again indicates clinopyroxenes as a major mineral present in the soil.

The relative spectral reflectivity curve (Figure 3) is a typical example of an upland curve (McCord, et al., 1971).

The shallowness of the absorption band at 0.95u can be clearly seen. The decrease in slope toward the ultraviolet indicates a much lower titanium content at the site than in the maria, especially the Apollo 11 site.

A preliminary study of the Apollo 14 fines reveals a good correlation between the laboratory and the telescopic spectral reflectivity curves. The detailed interpretation of the spectral properties of these samples is not yet available.

ANALYSIS OF PROPOSED LANDING SITES

Most of the lunar areas suggested as landing sites for the Apollo program are discussed in this section. The selection of areas to study was made more than one year ago. The changing nature of the Apollo program has made some of these sites at least temporarily uninteresting. In the meantime several sites not included here have been suggested seriously. The large amount of work inherent in a study of this nature requires production methods be adopted. Thus we were unable to keep up with the changing Apollo program and had to freeze our site selection early.

However, the information contained here will allow some extrapolation to other areas without direct measurements. A careful reader of this report and the material in the Appendices will develop a feel for the spectral analysis and he will be better able to judge other sites.

Presented in this section are maps showing observation area locations and size, plots of relative spectral reflectivity for each area and a discussion both of the site and its spectral properties. We have attempted to discuss the properties of each site only. We are not attempting to "sell" one site over another. Here are the data, do as you please with them.

CENSORINUS

<u>SPOT</u>	<u>LAT.</u>	<u>LONG.</u>	<u>UNIT</u>	<u>DATE</u>	<u>RUNS</u>	<u>PHASE</u>
A	0°05'N	30°30'E	Em	10-17-70	3	+35°
B	1°10'N	33°15'E		10-17-70	3	+35°
C	0°25'S	32°30'E	Cs	10-17-70	3	+35°

CENSORINUS A: A region of mare material northwest of Censorinus J. The albedo is moderate, the crater density is moderate to heavy, with the subdued craters indicating a regolith depth similar to the Apollo 11 landing site.

CENSORINUS B: An area of rough, hummocky material east of Mashe-lyne C. Crater density is low and the regolith appears to be moderately deep.

CENSORINUS C: A region centered on the crater Censorinus. The crater has very steep slopes and a sharp rim, with ray material of high albedo radiating from the crater. Extensive radial lineation (-10m.) exist within 10 km. of Censorinus, and the regolith appears to be moderately deep. Boulders (10-30m.) are extensive within 2 km. of Censorinus.

CENSORINUS

RESULTS

The CENSORINUS A curve illustrates a typical mare curve (see Appendix I) which is very much like the Luna 16 landing site curve. CENSORINUS B, on the other hand, shows a typical uplands curve, which is similar to the Apollo 14 landing site curve. CENSORINUS C has an uplands, bright crater curve which is similar to the curves for TYCHO C and DESCARTES A.

INTERPRETATION

We find that CENSORINUS A probably has a bulk surface soil composition which is very similar to that found at the Luna 16 landing site. CENSORINUS B seems to have a composition similar to the Apollo 14 landing site. CENSORINUS C is typical of areas where freshly-exposed rock and breccia is predominant.

DISCUSSION

Our results indicate that soil with a higher ratio crystalline to glassy material and exposed rock and/or breccia exists within the region of Censorinus crater. Radar (Zisk, et al., 1970) and thermal (Shorthill, 1970) studies also confirm the existence of exposed rock in the region. The sampling of a locale where freshly exposed material of greater than usual amounts of crystalline material predominates has not occurred to date (except possibly at cone crater) and could provide baseline data for interpretation of the aforementioned spectral curve series.

PRECEDING PAGE BLANK NOT FILMED

COPERNICUS

<u>SPOT</u>	<u>LAT.</u>	<u>LONG.</u>	<u>UNIT</u>	<u>DATE</u>	<u>RUNS</u>	<u>PHASE</u>
A	10°00'N	22°00'W	Ccrh	1-9-71	2	-27°
B	9°50'N	21°20'W	Cs	1-9-71	5	-27°
C	10°00'N	20°20'W	Ccfs	1-9-71	6	-27°
D	9°15'N	19°45'W	Ccfh	1-9-71	4	-27°
E	10°05'N	19°35'W	Ccfh	1-9-71	5	-27°

COPERNICUS A: An area of high, local relief, with discontinuous hills and valleys somewhat concentric to Copernicus, on the western side of the crater. Numerous lineations, radial to Copernicus, exist in this area. A high crater density and relative sharpness of the features indicate a relatively shallow regolith.

COPERNICUS B: A region of terraced walls on the western slope of Copernicus, with rolling hills and extensive hummocks. A system of concentric ridges is evident, with lineations radial to the crater floor superposed on the system. Many features are subdued and the regolith is fairly deep, with a concentration of boulders (10-20 m.) and talus at the bottom of the slope furnishing evidence of gravity slumping.

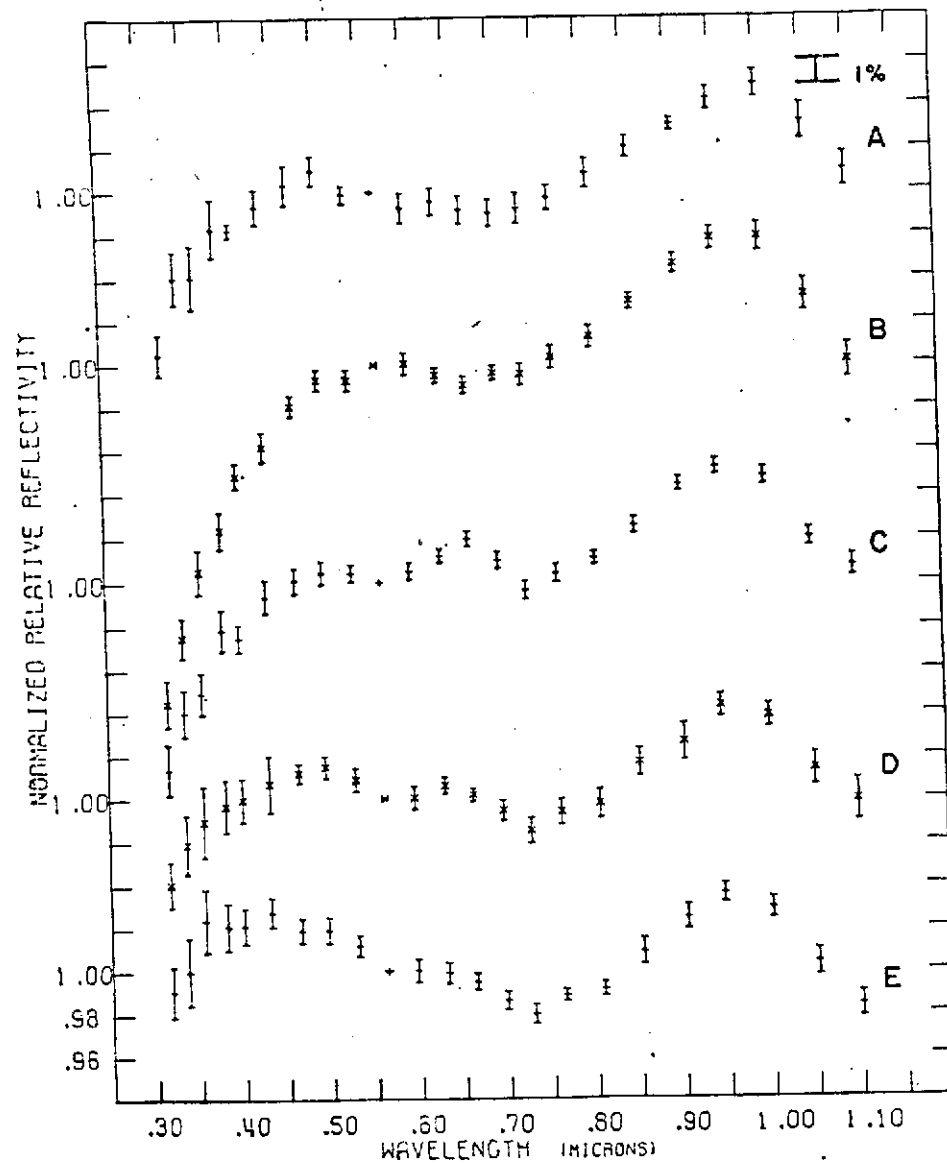
COPERNICUS C: A surface of relatively level terrain, with a few bulbous domes (200-700 m.) which have concentrations of boulders (5-15 m.) strewn on their summits, in the northwest quadrant of the Copernicus.

A large amount of faulting and nondirectional lineation (75-100 m.) is observed in this region. The regolith appears to be shallow, and the crater density is relatively high.

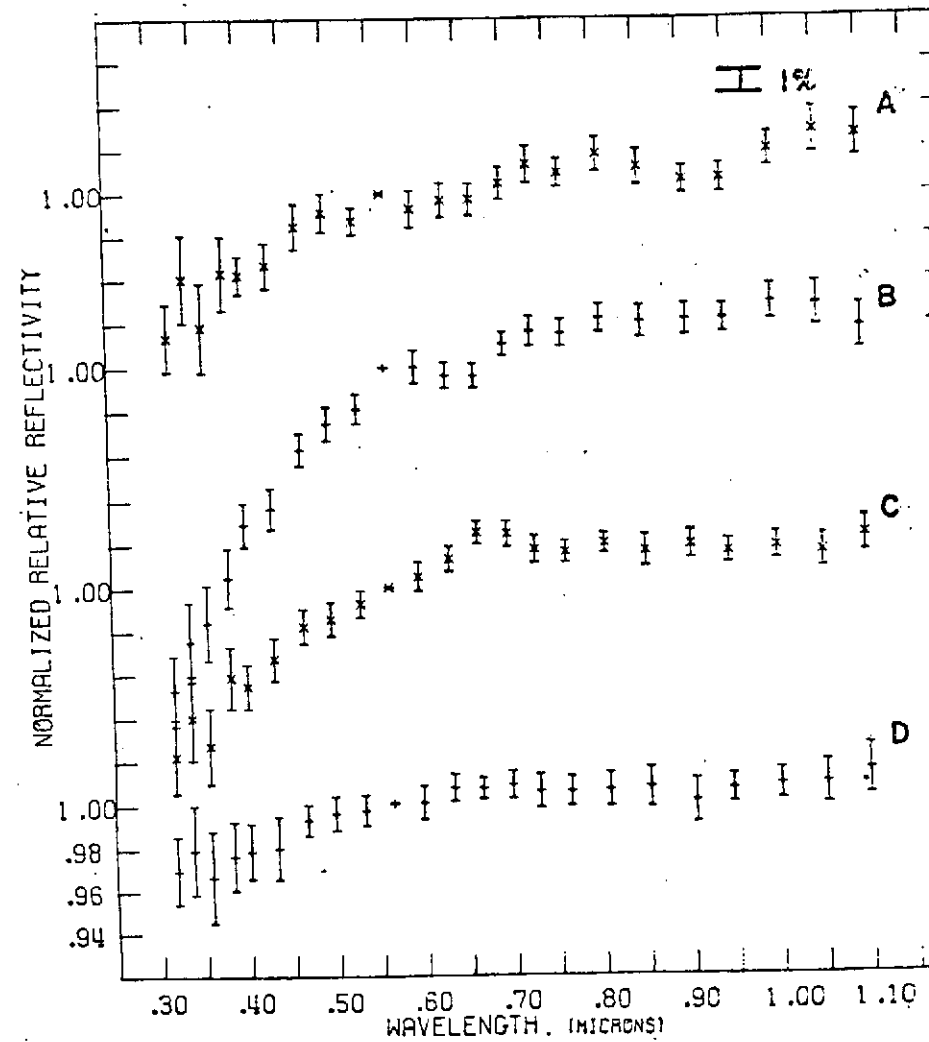
COPERNICUS D: An area of irregular hills (.5-1.0 km.), with an elevation higher than COPERNICUS C, south of the central peaks. The surface features are greatly subdued, indicating a rather deep regolith. The crater density is low relative to the rest of the floor.

COPERNICUS E: A surface of low, irregular hills (.5-1.0 km.), in the northeast quadrant of the Copernicus floor. Very extensive faulting and nondirectional lineation is evident, although small scale features (~100 m.) are subdued. Many bulbous domes with boulders (10-20 m.) on the summits and slopes are observed here.

COPERNICUS



COPERNICUS AREAS vs. NS 2



COPERNICUS AREAS vs. COPELUS E

COPERNICUS

RESULTS

All of the areas observed in the Copernicus region illustrates typical uplands curves with minor differences. The COPERNICUS A curve is quite similar to the Apollo 14 landing site curve. The curve for the COPERNICUS B area is similar to the COPERNICUS A curve, but the downward slope in the ultraviolet region is the greatest of any Copernicus area observed. The COPERNICUS C curve has an 0.95μ absorption band of similar intensity to COPERNICUS D and E, but has a slightly steeper downturn in the ultraviolet. The COPERNICUS D and E curves are quite similar to each other, and both are similar to the DESCARTES C curve.

INTERPRETATION

The bulk surface soil composition at COPERNICUS A and B are probably similar to that of the Apollo 14 landing site. The downturn in the ultraviolet at COPERNICUS B is perhaps a function of differing exposed material at the various levels on the Copernicus slopes. The composition of the soil at COPERNICUS C, D and E is probably similar to the Apollo 14 landing site material.

DISCUSSION

The Copernicus area has been shown to be an uplands region, and is quite similar to the Apollo 14 landing site in its

spectral reflectivity. We believe that although Copernicus is situated in the mare, the event which formed the crater penetrated through the mare fill to the upland material (McCord, et al., 1971).

DAVY RILLE

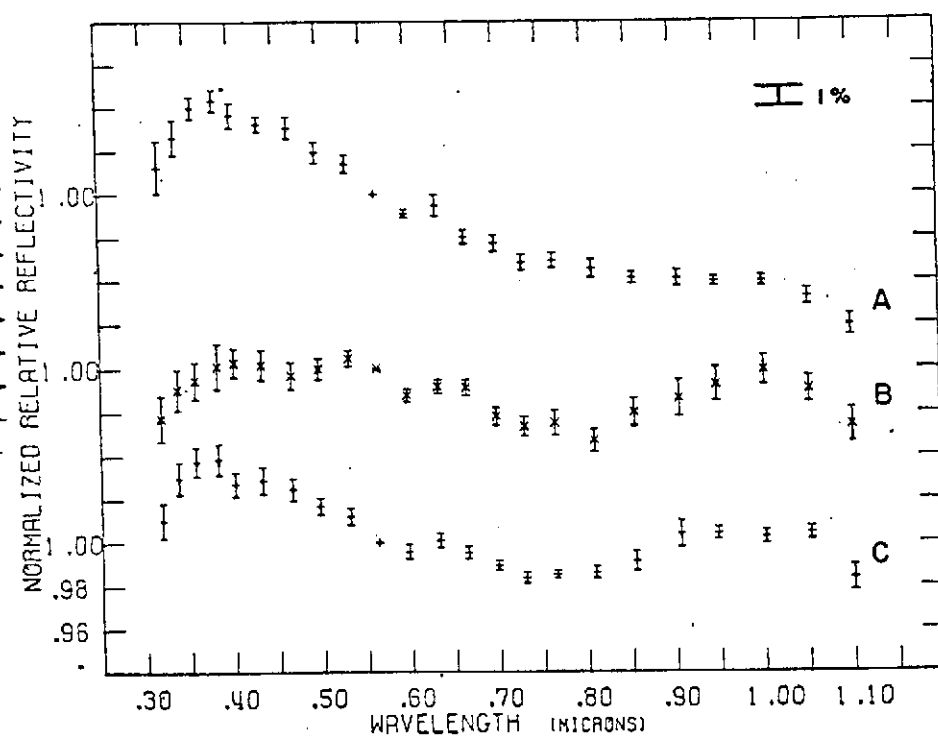
<u>SPOT</u>	<u>LAT.</u>	<u>LONG.</u>	<u>UNIT</u>	<u>DATE</u>	<u>RUNS</u>	<u>PHASE</u>
A	10°25'S	5°05'W	CEch	1-11-71	4	-4°
B	10°50'S	5°05'W	CEch	1-11-71	4	-4°
C	13°00'	6°55'W	Ica	1-11-71	4	-4°

DAVY RILLE A: An uplands region centered on the crater Davy G, this crater has high albedo, sharp rim, and very smooth, steep walls.

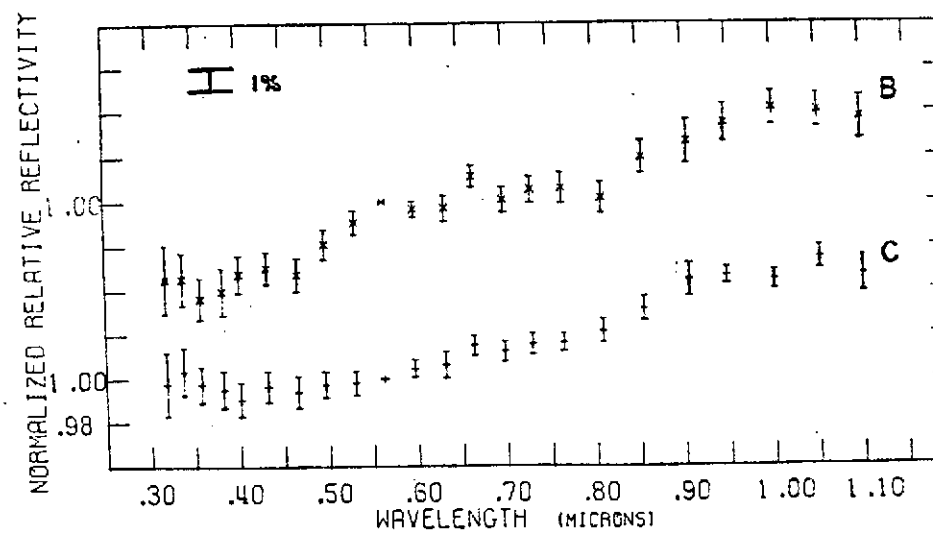
DAVY RILLE B: An uplands region centered on the crater Davy GA, which is adjacent to Davy G. Davy GA has a sharp rim and smooth walls. Some uplands material is included in the sample region.

DAVY RILLE C: An area of intermediate albedo and high crater density, with numerous ghost craters and deep regolith.

DAVY RILLE



DAVY RILLE AREAS vs. MS 2



DAVY RILLE AREAS vs. DAVY RILLE A

DAVY RILLE

RESULTS

DAVY RILLE A has a rather weak upland bright crater curve, with a rise at 0.40μ that is not as great as the TYCHO C or CENSORINUS C curves. DAVY RILLE B shows a rather ill-defined mare curve. The DAVY RILLE C curve exhibits both the uplands characteristics of a weak 0.95μ absorption band and the bright crater characteristics of a maxima in the ultraviolet.

INTERPRETATIONS

The DAVY RILLE A area probably contains some freshly exposed, high crystalline material. In the DAVY RILLE B region, the bulk soil composition is probably similar to that of a low-titanium uplands region. The DAVY RILLE C area probably contains uplands material in the form of Imbrium ejecta. It may also contain some freshly exposed, crystalline material which may be similar to that at DAVY RILLE A, or material which may have been ejected from the crater-chain. However, the spatial resolution of the data tends to make such an interpretation very tenuous at best.

DISCUSSION

The bulk surface soil composition in the observed areas is probably not substantially different from uplands material. However, sufficiently high spatial resolution data were not obtained to determine the characteristics of the crater chain itself. Therefore, the worth of detailed investigation of the crater chain cannot be determined from the study. These data do establish

several areas where bright crater and uplands material interfaces probably exist. The interface between such areas would be extremely interesting to investigate.

PRECEDING PAGE BLANK NOT FILMED

DESCARTES

RESULTS

The Descartes region, with the exception of DESCARTES A, exhibits a typical uplands curve. The DESCARTES B, C and E curves are all very similar to the Apollo 14 landing site curve, except for small intensity variations in the 0.95μ absorption band. The curve for DESCARTES D has a much weaker 0.95μ band and a stronger downturn near 0.30μ than the Apollo 14 landing site curve.

DESCARTES A is quite anomalous to this region and its curve is similar to the TYCHO B and CENSORINUS C curves.

INTERPRETATIONS

It can be inferred from these data that DESCARTES B, C and E have bulk surface soil compositions which are similar to that at the Apollo 14 landing site. DESCARTES D may have less pyroxene and greater titanium content than the Apollo 14 landing site.

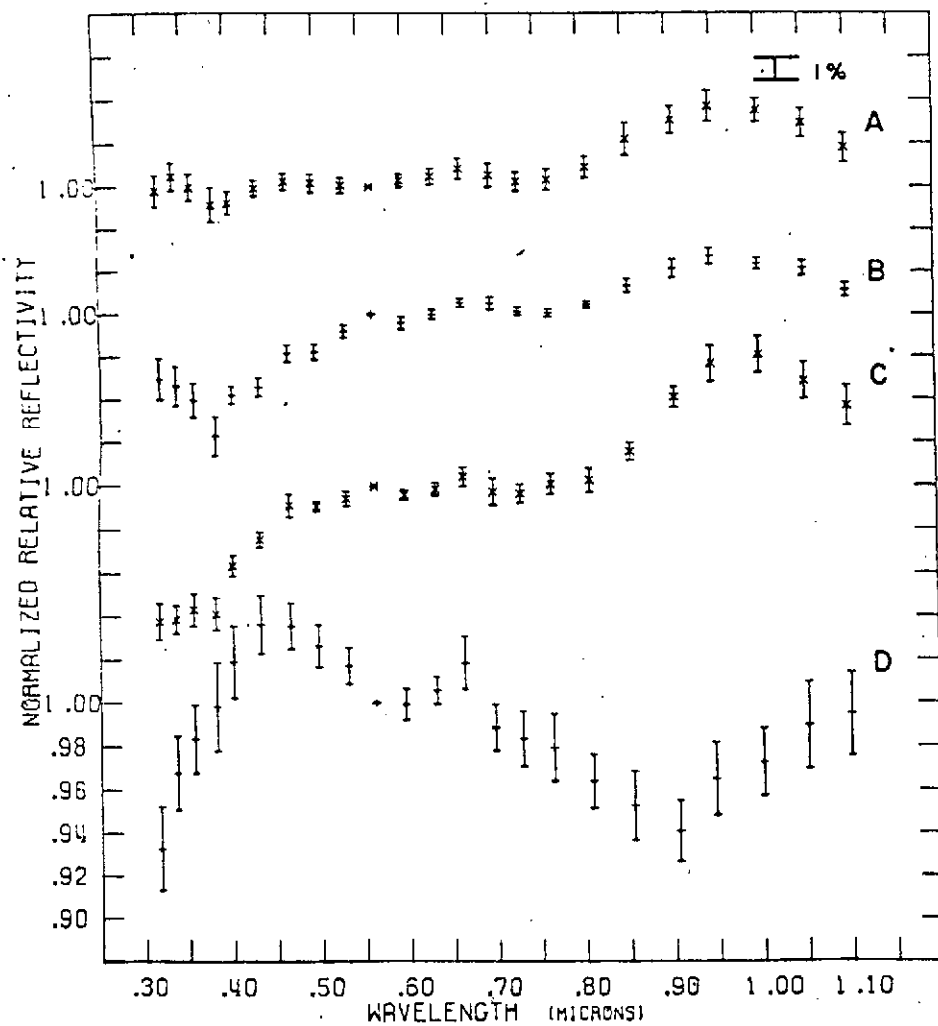
DESCARTES A is centered on the Kant Plateau, which has been described as volcanic in origin (Milton, 1968). The similarity of the DESCARTES A curve to that of TYCHO B and CENSORINUS C indicates that the surface material is highly crystalline, probably freshly exposed, and contains much less dark glass than the surrounding uplands material. Radar backscatter at 3.8 cm is greater in this area than surrounding regions (Zisk, 1970). Both results imply a (relatively) recent event, not obviously associated with any crater, exposed fresh material in this area.

DISCUSSION

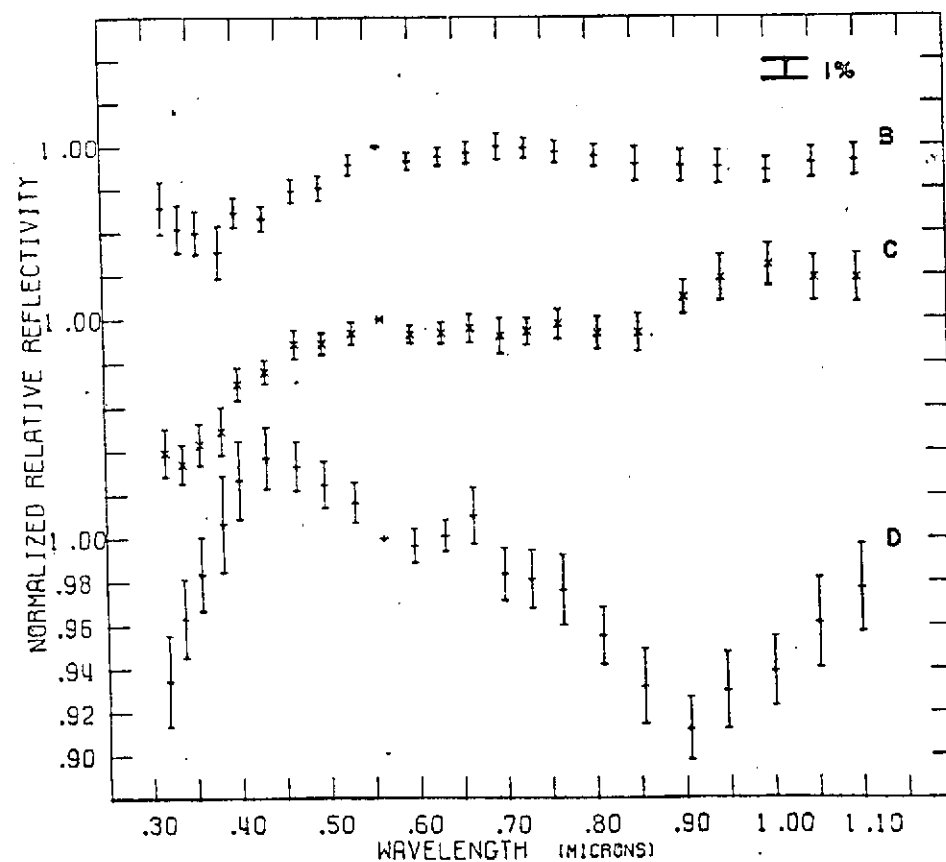
Although most of the Descartes area is composed of upland material similar to the Apollo 14 landing site, the Kant Plateau region is extraordinary in its exposure of fresh material. In view of the above data, it is important to sample the Kant Plateau region during a Descartes mission. We feel that such sampling will provide the best chance to study an area where processes other than cratering may have recently occurred. The contact between the Kant Plateau region and the surrounding upland regions, occupied by the so called Cayley Formation, could also yield important information on 1) the structural relations between these two regionally important upland units, 2) origin of the bright Descartes plateau material, 3) origin of the Cayley Formation and 4) the mixing of different lunar soils.

In our opinion, a mission to this region without strong emphasis on sampling Kant Plateau material would probably be scientifically undesirable, since the type of upland material which surrounds the Kant Plateau, i.e. the Cayley Formation and the more subdued appearing parts of the Descartes Formation, have probably been previously sampled.

HADLEY - APENNINES



HADLEY - APENNINES AREAS vs. MS 2



HADLEY - APENNINES AREAS vs. HADLEY - APENNINES A

HADLEY-APENNINE

RESULTS

The HADLEY-APENNINE A area has a curve which is similar to the Apollo 12 landing site curve except for a weaker 0.95μ absorption band. The HADLEY-APENNINE B curve is somewhat similar to the HADLEY-APENNINE A curve except for a lower reflectivity in the ultraviolet. HADLEY-APENNINE C's curve is similar to the Apollo 14 landing site curve. HADLEY-APENNINE D illustrates a bright upland material curve.

INTERPRETATION

The HADLEY-APENNINE A area probably has a soil composition similar to the non-ray material (Adams and McCord, 1971a) found at the Apollo 12 landing site in the ratio of crystalline to glass in the soil. HADLEY-APENNINE B's soil composition is most likely similar to that found at HADLEY-APENNINE A except for a decrease in the titanium content. The HADLEY-APENNINE C region probably contains uplands material similar to that found at the Apollo 14 landing site. The HADLEY-APENNINE D area probably contains freshly exposed, higher-crystalline material. The exposure may have been the result of gravity-slumping on the slopes of the Apennine Front.

DISCUSSION

The Hadley-Apennine region probably contains material which has been previously sampled during the mare and upland mission. However, it would be worthwhile to sample the area at the edge of Hadley Delta, since it could reveal important information

regarding the interface between mare and uplands regions. Also, the similarity between the Hadley Delta and Apollo 14 landing site material, as seen in the telescopic spectra, could support the hypothesis of a common Imbrium event producing Fra Mauro Formation material.

The difference between the reflectivities of HADLEY-APENNINE C and D cannot be explained at present, and radar measurements offer no clue (Zisk, et al., 1971), since both features are strongly enhanced.

PRECEDING PAGE BLANK NOT FILMED

HYGINUS RILLE

<u>SPOT</u>	<u>LAT.</u>	<u>LONG.</u>	<u>UNIT</u>	<u>DATE</u>	<u>RUNS</u>	<u>PHASE</u>
A	8°20'N	5°40'E	CEch	1-10-71	4	-15°
B	8°05'N	6°15'E	CId	1-10-71	5	-15°
C	7°45'N	6°15'E	CEch	1-10-71	5	-15°
D	7°25'N	6°10'E	CId	1-10-71	4	-15°
E	7°25'N	7°55'E	CEch	1-10-71	4	-15°

HYGINUS RILLE A: An area, centered on the northwest part of Hyginus Rille, containing crater chain material of moderate albedo. Extensive talus with blocks (10-40 m.) emanate from exposed, stratified layers on the crater chain walls. The crater density within the chain and outside the chain is equal, with larger craters subdued as a result of the heavy regolith.

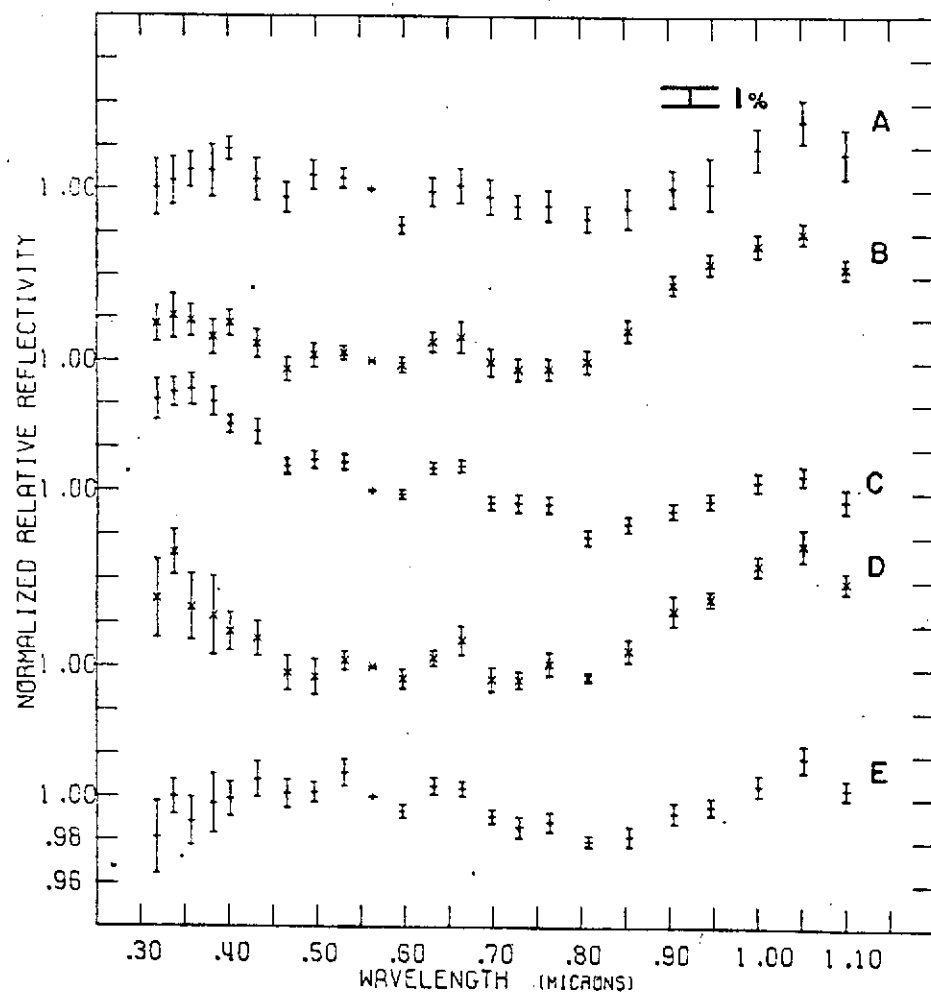
HYGINUS RILLE B: A region of flat, mare material, north of the crater Hyginus, with very low albedo. The crater density is high and most features are subdued.

HYGINUS RILLE C: An area, encompassing the floor and walls of Hyginus Crater, with low to moderate albedo. The walls have steep slopes and blocks (10-20 m.) for talus at the floor-wall contact. The crater density is the same as at MARIUS HILLS A and B, and most features are subdued.

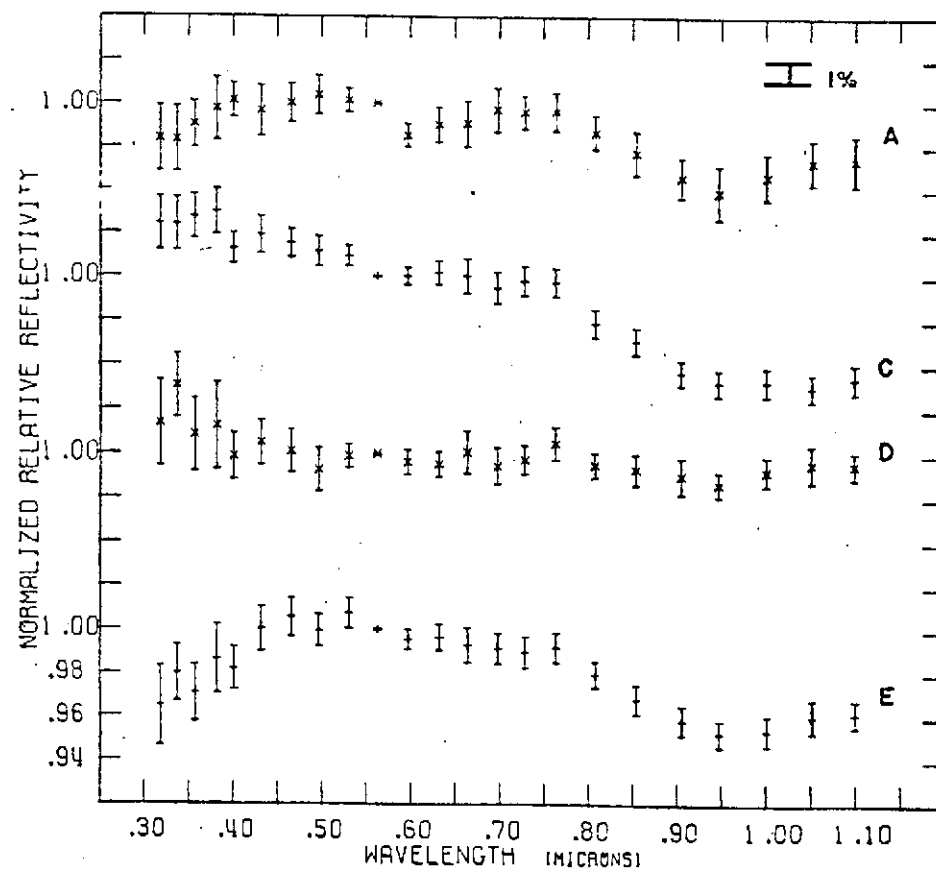
HYGINUS RILLE D: A region of flat, mare material, south of Hyginus, with very low albedo. Very similar to HYGINUS RILLE B.

HYGINUS RILLE E: An area, centered on the southeastern part of Hyginus Rille, with very high albedo. A large amount of talus, similar to that observed at HYGINUS RILLE A, is evident on the bottom of the chain-crater.

HYGINUS RILLE



HYGINUS RILLE AREAS vs. MS 2



HYGINUS RILLE AREAS vs. HYGINUS RILLE B

HYGINUS RILLE

RESULTS

The HYGINUS RILLE A, C and E curves are quite similar to each other, and are both similar to the HADLEY-APENNINE A region. The curves for HYGINUS RILLE B and D are similar to the LITTROW B curve, and some resemblance to the LITTROW A curve.

INTERPRETATION

The HYGINUS A, C and E areas probably contain mare material that has been previously sampled during the Apollo 12 mission and perhaps will be sampled during the Apollo 15 mission. The HYGINUS RILLE B and D regions' surface soil composition probably is the same as HYGINUS A, C and E except for a marked increase in the dark glass content.

DISCUSSION

Although most of the material in the Hyginus Rille region probably has been previously sampled, the dark material at HYGINUS B and D are anomalous in their high reflectivity in the ultraviolet and the near-infrared, and in their low depolarized radar backscatter values (Zisk, et al., 1970). This material is part of a dark mare series whose end member is LITTROW A, and whose origin may be relatively recent (see Littrow analysis).

PRECEDING PAGE BLANK NOT FILMED

LITTROW

<u>SPOT</u>	<u>LAT.</u>	<u>LONG.</u>	<u>UNIT</u>	<u>DATE</u>	<u>RUNS</u>	<u>PHASE</u>
A	21°15'N	29°40'E	CId	1-11-71	4	-3°
B	21°40'N	29°45'E	Cc	1-11-71	3	-3°
C	22°05'N	29°45'E	Cc	1-11-71	3	-3°
D	21°40'N	29°00'E	Im	1-11-71	3	-3°

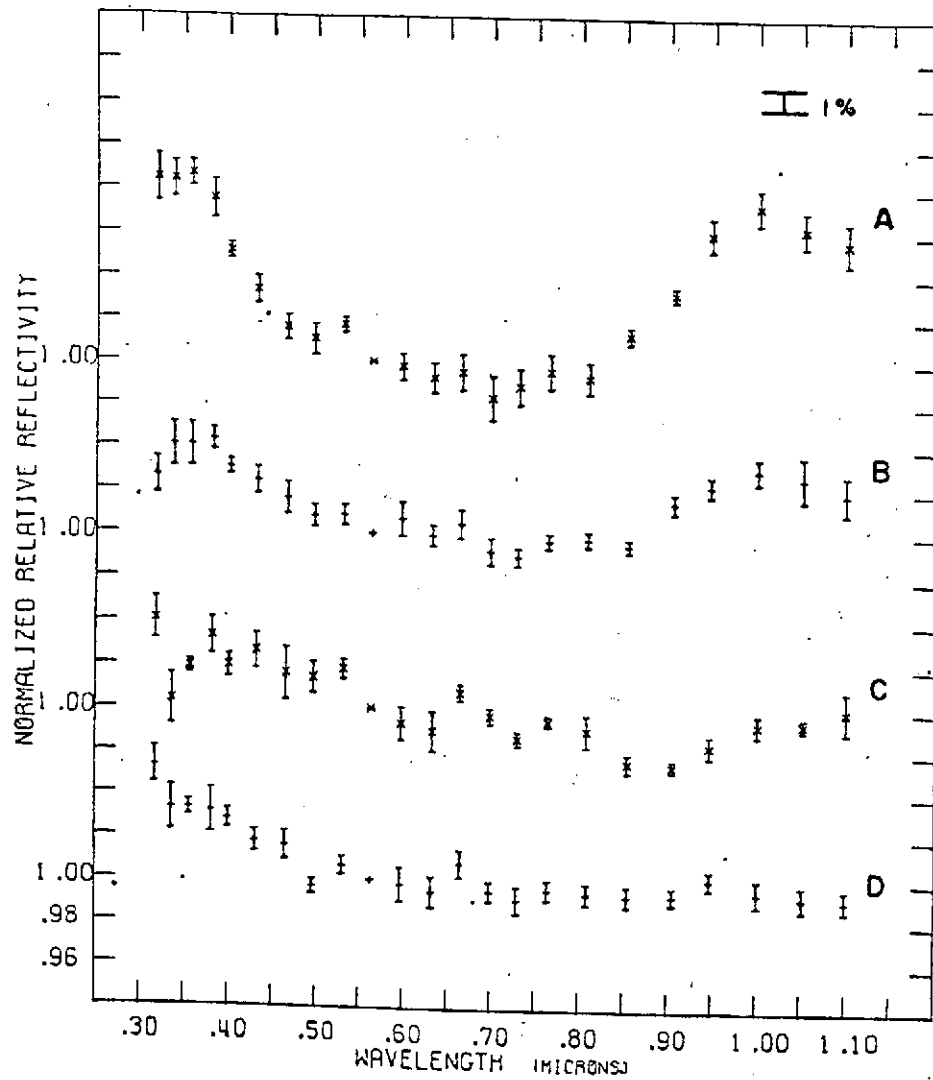
LITTROW A: Littrow Rilles I, III, and IV pass through the area, which has very low albedo (0.05-0.055). Topography is smooth and level, with numerous shallow-rimmed, subdued craters and thick regolith evident.

LITTROW B: Area is centered on the crater Littrow B, which is sharp-rimmed and exhibits slumping of its walls. The surrounding terrain is considerably hummocky, with heavy overlaying regolith evident and high albedo (0.10)

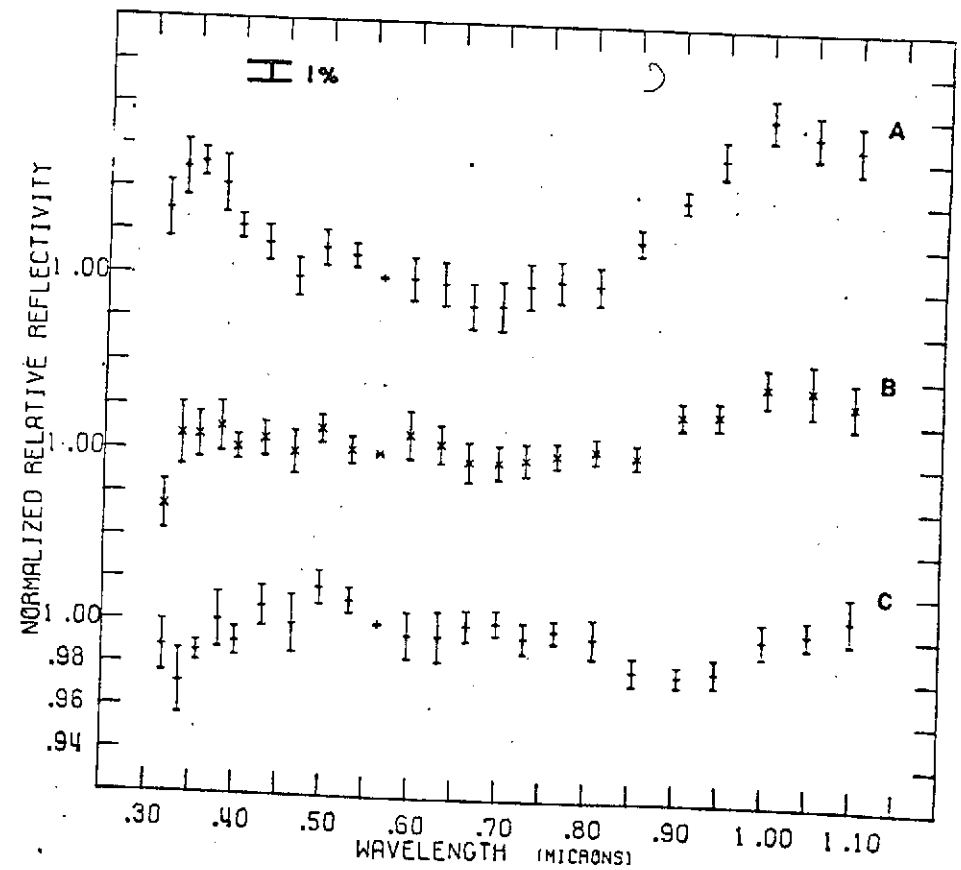
LITTROW C: Area is centered on the crater Littrow BA, which has a rocky floor. Surrounding area is extremely hummocky and has high albedo, along with a low crater density.

LITTROW D: Area has relatively smooth topography and low ridges, with moderately low albedo (0.064-0.066). The crater density in this region is high.

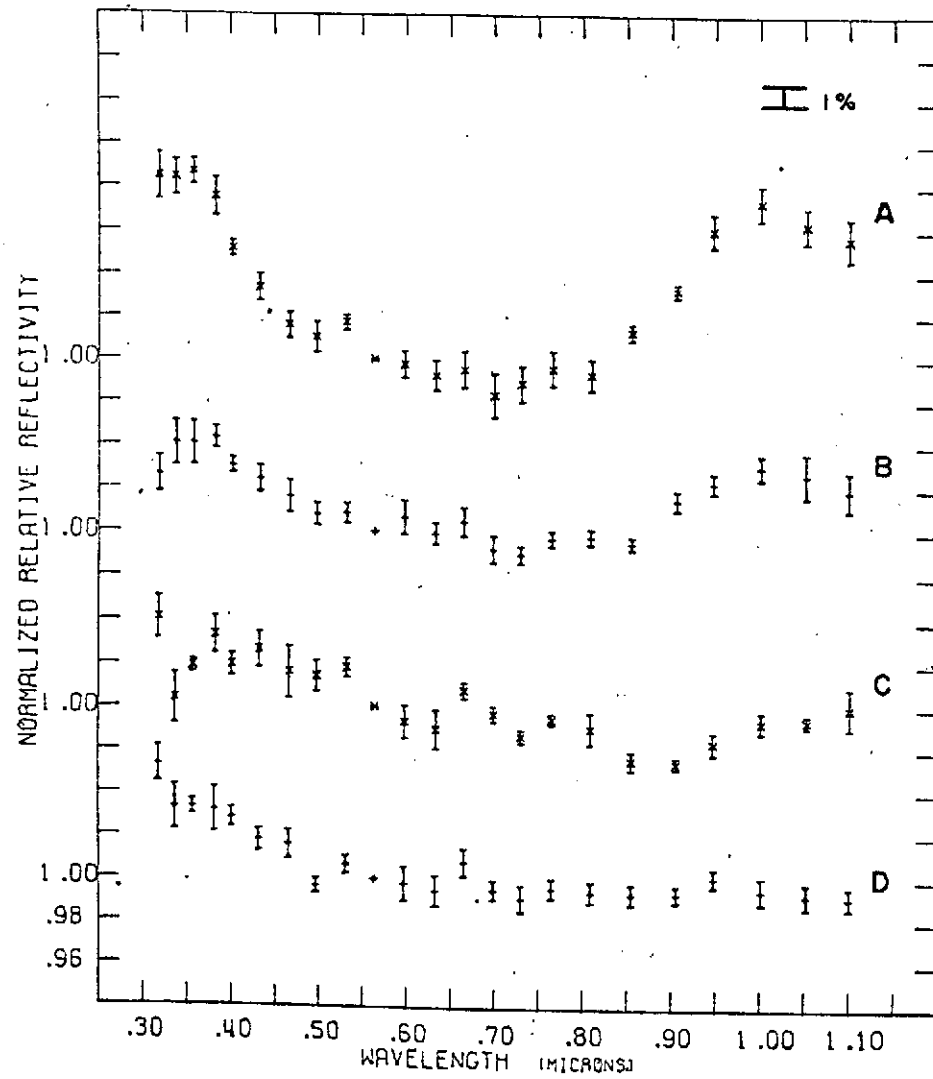
LITTROW



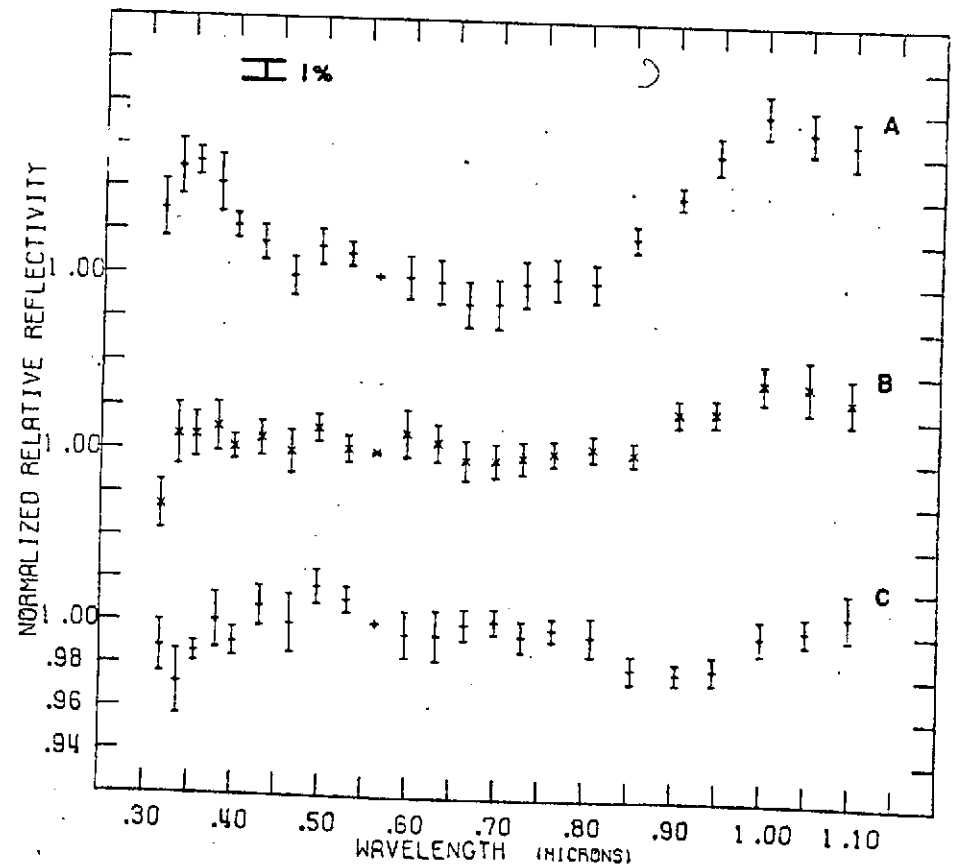
LITTROW AREAS vs. MS 2



LITTROW AREAS vs. LITTROW D



LITTROW AREAS vs. MS 2



LITTROW AREAS vs. LITTROW D

LITTROW

RESULTS

The LITTROW A curve has some similarity to the Apollo 11 landing site curve. However, the strong reflectivity in both the ultraviolet and the near-infrared indicate that this material is different from the normal mare material.

Both the LITTROW B and C curves illustrate mare curves which resemble the Luna 16 landing site curve. The LITTROW D curve is like the Apollo 12 landing site curve, except for an upturn in the ultraviolet.

INTERPRETATION

The LITTROW A region probably has an extraordinary amount of titanium-rich glass on the surface and little or no exposed rock. Both LITTROW B and C appear to exhibit curves which have mare-like compositions. The LITTROW D area probably has a soil composition similar to the Apollo 12 landing site except for a higher titanium content.

DISCUSSION

Most of the Littrow region appears to have a soil composition which is similar in some ways to previously sampled mare material. The high albedo craters of LITTROW B and BA apparently have not penetrated beyond the mare fill to uplands material, as can be seen from the curves.

The LITTROW A area is quite anomalous to the Littrow region in its low albedo, high ultraviolet and near-infrared

reflectivity, and very low depolarized radar backscatter values (Zisk, et al., 1970). The localized nature of this anomaly would tend to rule out a concentrated impact vitrification which would yield large amounts of glass. Some form of local event, such as volcanism, could have produced such a rock-free surface. The possibility that the material in this region is relatively young, and the fact that it is an anomaly in many ways, should cause this site to be seriously considered for a future sampling mission.

MARIUS HILLS

<u>SPOT</u>	<u>LAT.</u>	<u>LONG.</u>	<u>UNIT</u>	<u>DATE</u>	<u>RUNS</u>	<u>PHASE</u>
A	13°45'N	56°45'W	Emp	1-15-71	3	+44
B	13°45'N	56°05'W	Emp	1-15-71	3	+44
C	13°45'N	55°30'W	Emp	1-15-71	2	+44

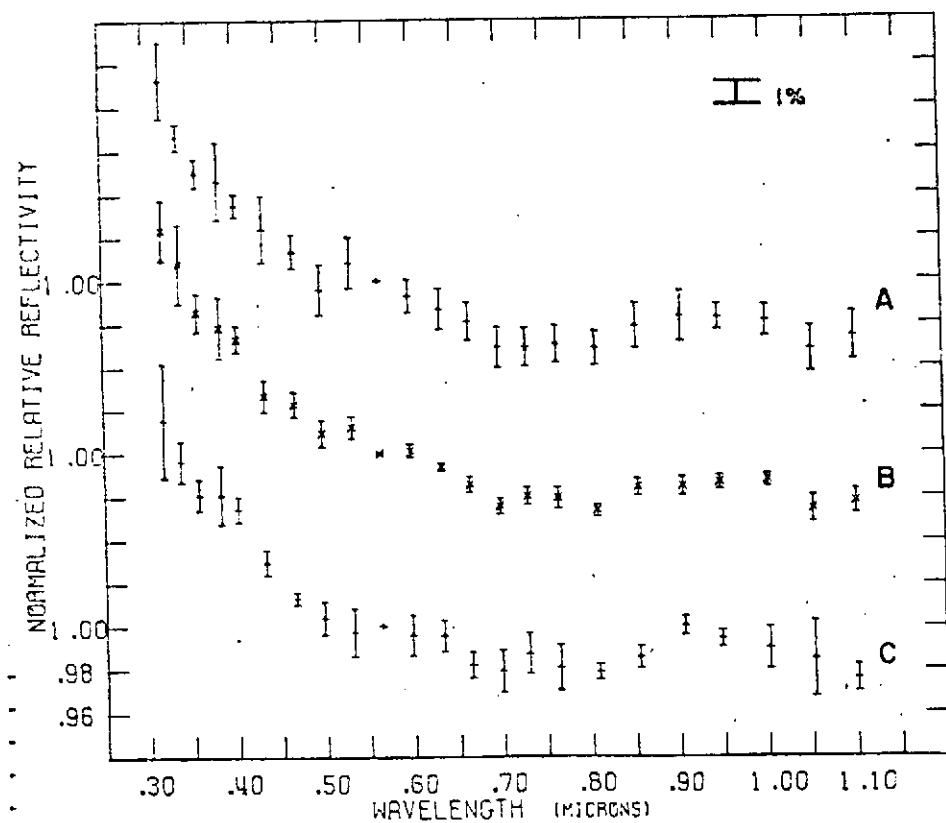
MARIUS HILLS A: An area of smooth, undulating material with low domes, north of Galilaei M. Extensive lineations are observed, apparently as a result of slumping of heavy regolith. All features in this area are subdued.

MARIUS HILLS B: A region of wrinkle ridges and domes, centered on a rille system northeast of Galilaei M. All features are subdued by the heavy regolith.

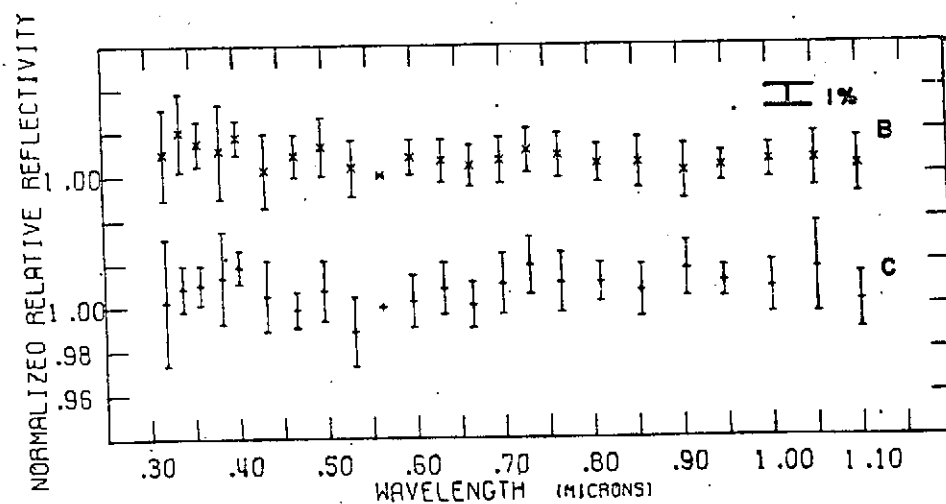
MARIUS HILLS C: An area of flat, mare material with a high crater density. Numerous ghost craters exist, although the regolith seems to be thinner than at either MARIUS HILLS B or C.

PRECEDING PAGE BLANK NOT FILMED

MARIUS HILLS



MARIUS HILLS vs. MS 2



MARIUS HILLS AREAS vs. MARIUS HILLS A

MARIUS HILLS

RESULTS

All three sample area curves are quite uniform among themselves, and have slopes from 0.3μ to 0.6μ which are similar to the curves for the Luna 16 landing site (although somewhat steeper) and the Apollo 11 landing site.

INTERPRETATION

It can be inferred from these data that Marius Hills site is intermediate in bulk soil composition between the Luna 16 and Apollo 11 landing site. The composition is probably closer to the Apollo 11 site but with perhaps less titanium. These spectral reflectivities are also similar to other areas in Oceanus Procellarum (McCord, 1968).

DISCUSSION

As with Davy Rille, high spatial resolution measurements of suspected volcanic features were not performed, and the possibility of small, localized areas of very different material exists. On the basis of these spectral reflectivity measurements, it is recommended that the Marius Hills region be placed as low-priority for a manned mission, as it is similar to previously sampled material in bulk soil composition and the surrounding mare.

PRECEDING PAGE BLANK NOT FILMED

TYCHO

<u>SPOT</u>	<u>LAT.</u>	<u>LONG.</u>	<u>UNIT</u>	<u>DATE</u>	<u>RUNS</u>	<u>PHASE</u>
A	41°05'S	11°05'W	Ccrr	11-11-70	3	-26°
B	41°55'S	11°20'W	Ccw	11-11-70	3	-26°
C	42°55'S	10°40'W	Ccfh	11-11-70	3	-26°
D	43°15'S	11°20'W	Ccp	11-11-70	2	-26°

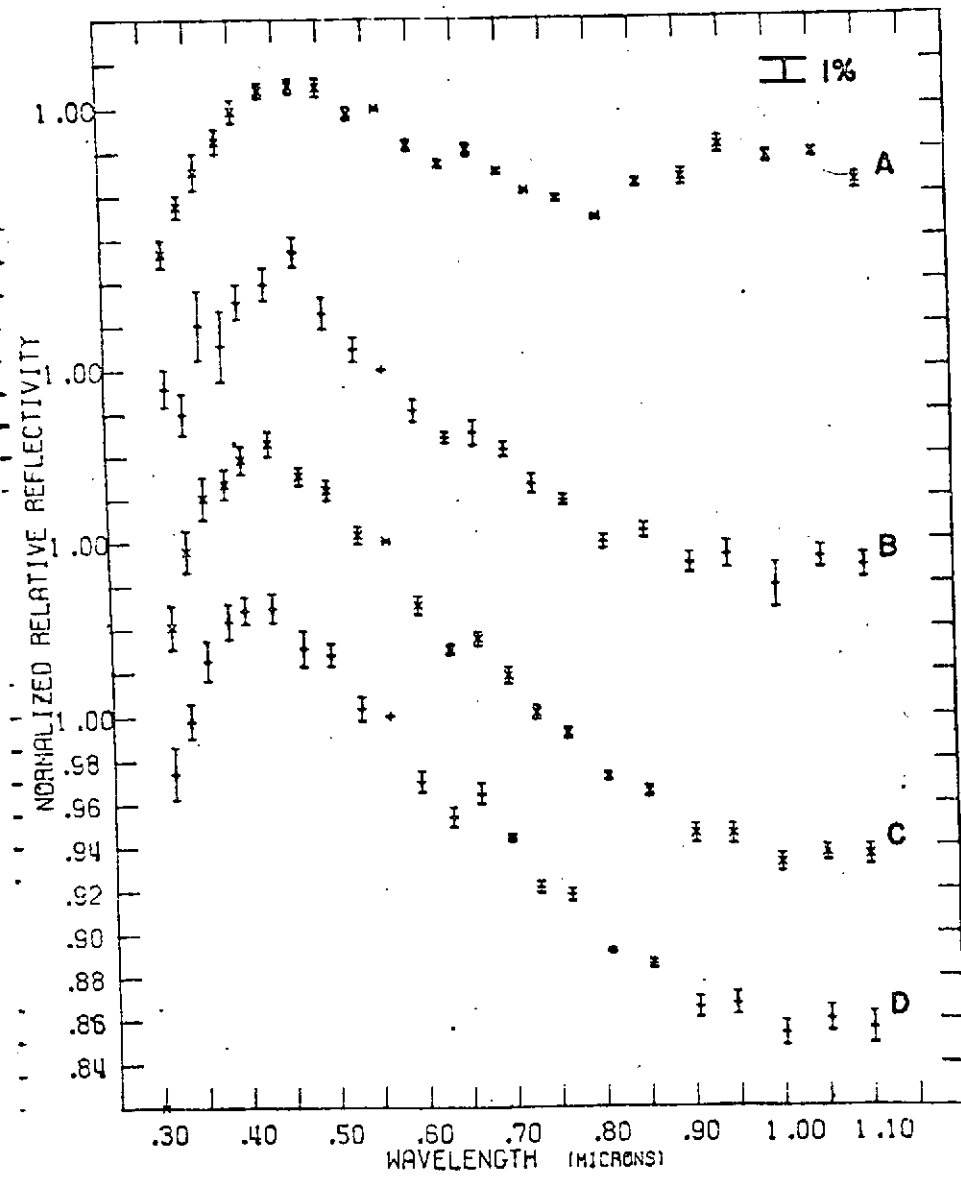
TYCHO A: An area with lower albedo than the surrounding terrain, north of Tycho, containing the Surveyor 7 landing site. Region has rolling, hummocky material which is radial to the crater. Some ponds of smooth material with extensive fissures exist between hummocks.

TYCHO B: A region of rough, angular hummocks on a terraced wall, with a much higher albedo than TYCHO A. Lineations concentric to Tycho are abundant, with much-exposed rock and boulders (20-30 m.) evident. Many ponds of smooth material exist between hummocks, and to a greater extent than TYCHO A.

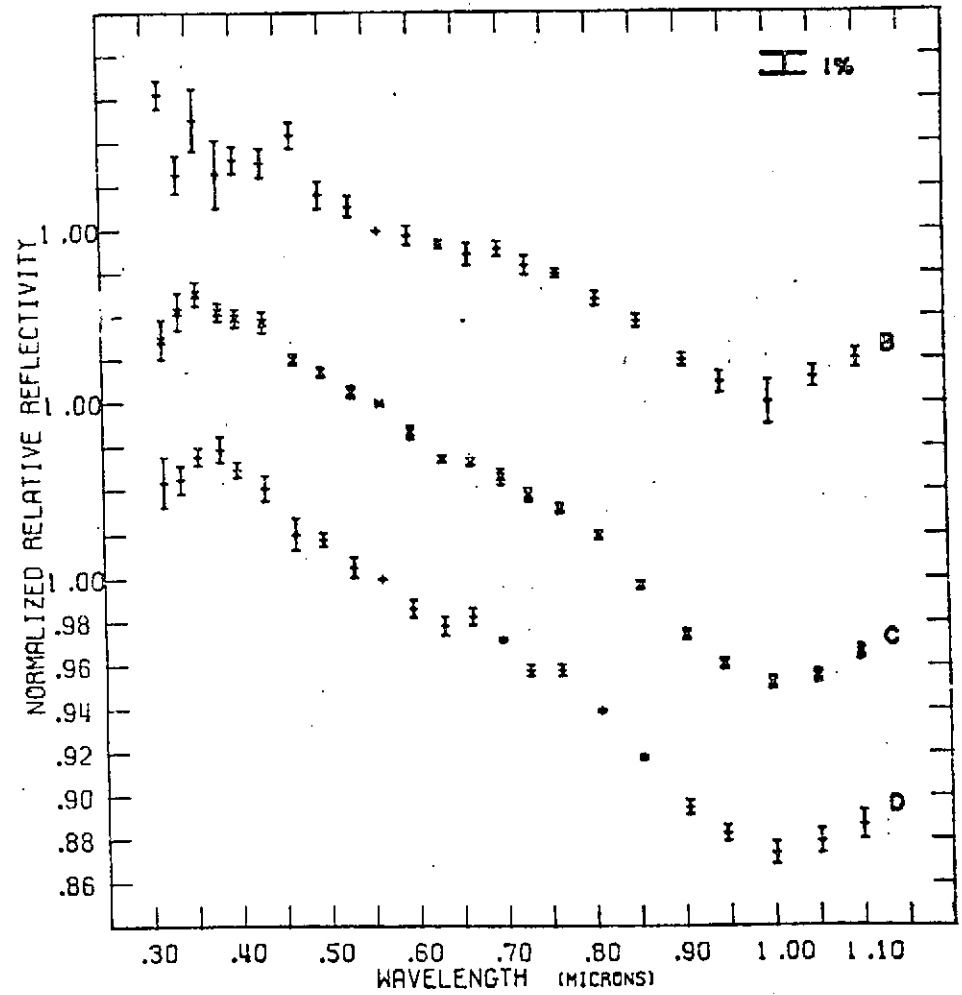
TYCHO C: An area containing an extremely rough, non-directional hummock and ridge system, in the northeast quadrant of the Tycho floor. Numerous fissures, tens of meters wide, exist throughout the locale. Albedo is intermediate with the crater density lower here than on the rim.

TYCHO D: A region of angular peaks and ridges with fairly smooth, steep slopes, at the center of the Tycho floor. Albedo is relatively high.

TYCHO



TYCHO AREAS vs. NS 2



TYCHO AREAS vs. TYCHO A

TYCHO

RESULTS

The TYCHO A curve has features which are decidedly uplands in nature and can be found in the Fra Mauro and Descartes (primarily at DESCARTES C) regions. The curve for TYCHO B is the same as the TYCHO C and D curve, except for a weaker 0.95μ absorption band. The TYCHO C and D curves are practically the same as for TYCHO B in shape and intensity. These latter three curves are "end members" of the bright crater series.

INTERPRETATION

The TYCHO A area probably contains some form of uplands material which is similar to the Apollo 14 landing site soil. The TYCHO B area contains more crystalline, exposed material. The variation of the 0.95μ band relative to TYCHO C and D is perhaps a function of different material in the exposed layers on the slopes of Tycho, although contamination by TYCHO A material within the observed area cannot be ruled out. Both TYCHO C and D have similar curves, thus indicating that the surfaces of the floor and central peaks have the same amount of crystalline material.

DISCUSSION

The Tycho region is extremely interesting since it contains a large amount of higher crystalline material over a vast surface area. This region should be sampled, inasmuch as an area where such high crystalline rocks predominate has yet to be

visited. Such a manned mission would yield samples which could establish a baseline for this "end member" of the bright crater series, and thus allow interpretation of bright crater spectra for other areas of the moon.

The TYCHO A area, which contains material of the dark "halo ring", is quite anomalous to the Tycho region. The processes that cause this area to appear as uplands material cannot be explained at this time.

It should be noted that a manned mission to the contact between the dark "halo ring" and the bright, exposed material at the rim probably would have the potential for a maximum scientific return.

SPECTRAL REFLECTIVITY MEASUREMENTS

INTRODUCTION

In the last section the relative spectral reflectivities of several areas near each of the proposed landing areas were discussed. These relative curves are derived by dividing the reflectivity of the area of interest by that of a standard area. Two standard areas were used for each region studied:

- (1) The area in Mare Serenitatis was used for all regions, and
- (2) an area within the region studied. The spectral reflectivity curve for the Mare Serenitatis standard area is given in Figure 2. The spectral reflectivity curves for the regional standard areas are given in this section.

OBSERVATIONS AND RESULTS

The spectral reflectivity curves scaled to unity at 0.564μ and one area from within each lunar region studied are given in Figure 22. As was shown in Figure 2, the curve for almost all lunar areas are quite similiar and one must resort to the relative curves to show the small but significant differences between the spectral properties of different lunar areas. All curves have a positive slope toward the red spectral region and show the absorption band near 0.95μ .

INTERPRETATION

The overall curve slopes (the red color) for all areas is an expresion of the colored glass content of the lunar soil (Adams and McCord, 1970, 1971ab; Conel, 1970;

Conel and Nash, 1970). The curve slopes less (less red color) and becomes less linear as the proportion of glass to crystalline material in the soil becomes smaller. The depth of the absorption band also follows this parameter to some extent (more glass, less band). From this and the curves in Figure it is apparent that colored glass is a significant component of the soil everywhere we observed. Bright crater material is more crystalline than other regions.

The absorption band near 0.95μ is an expression of the clinopyroxenes in the soil. The band appears at about the same wavelength position with varying strengths in all curves. These clinopyroxenes must be a major component of the lunar soil almost everywhere.

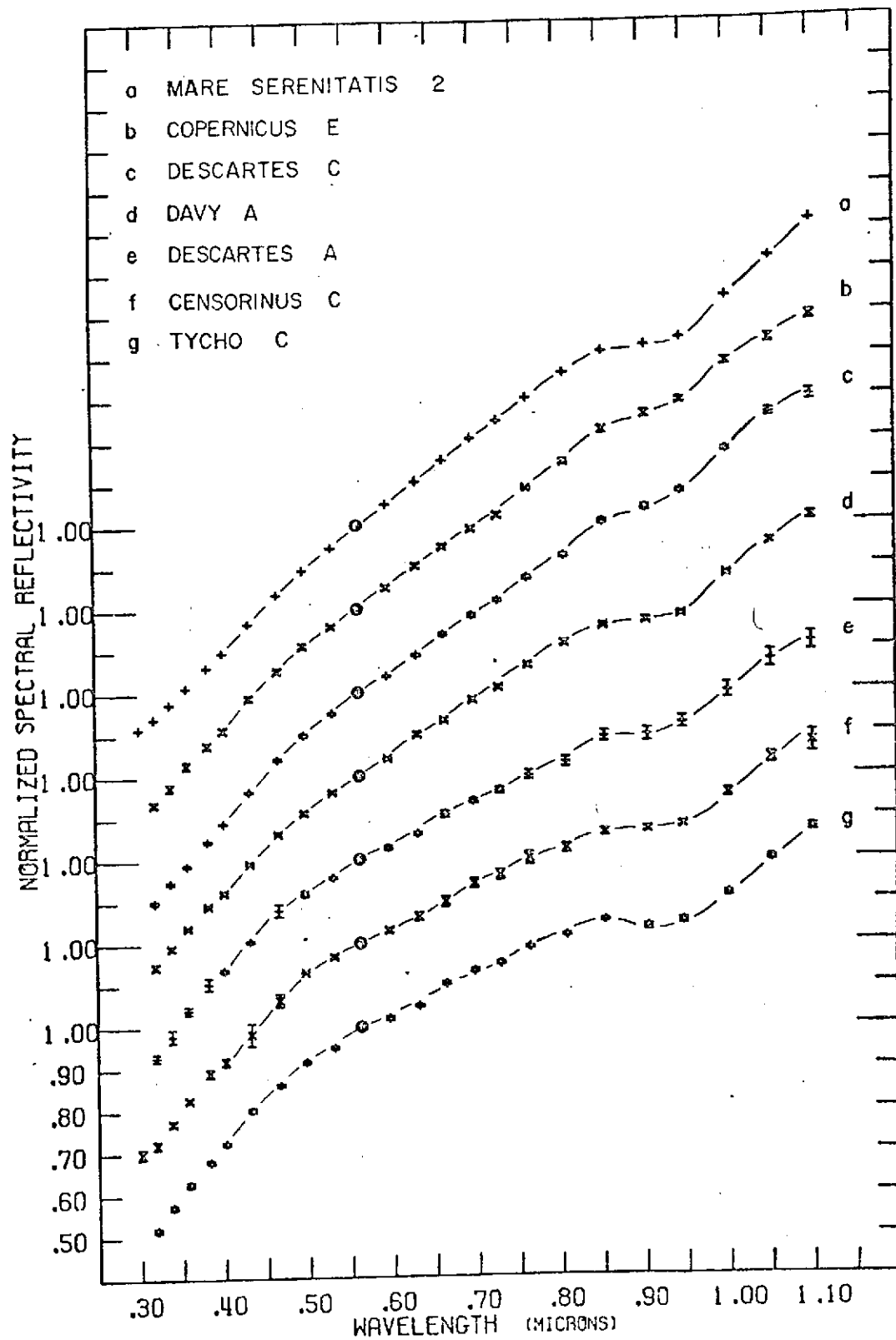


Figure 22a

+ = LITTROW 1/SUN

1/11/71

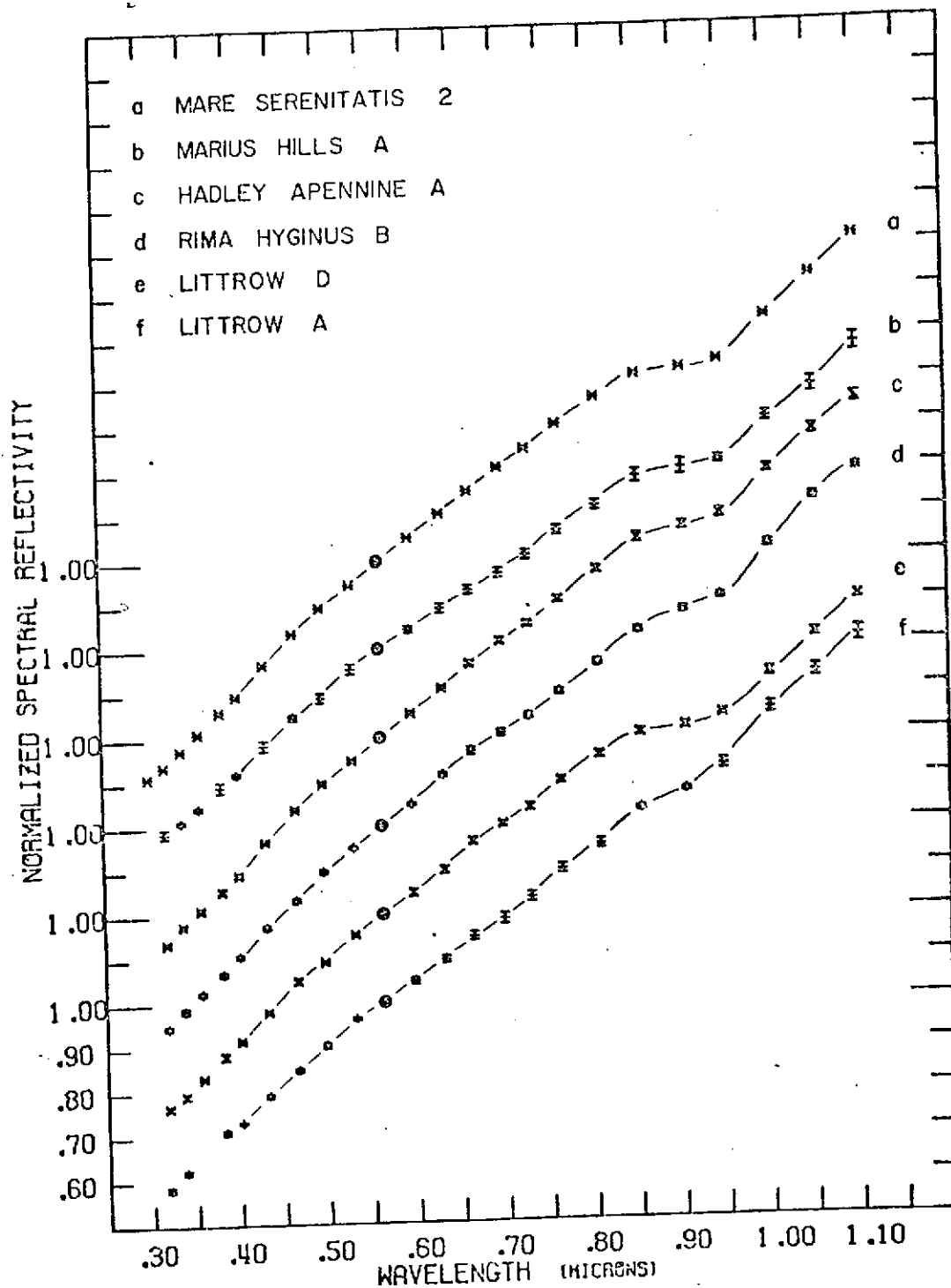


Figure 22b

ACKNOWLEDGEMENTS

We wish to thank Dr. John B. Adams of the College of the Virgin Islands and Dr. Thomas R. McGetchin of M.I.T. for many useful discussions.

This research was carried out under NASA Grant: NGR-22-009-496.

REFERENCES - LUNAR LANDING SITES

- Adams, J.B. and Filice, A.L., Spectral Reflectance from 0.4u to 2.0u of Silicate Rock Powders, J. Geophys. Res., 72, 5705-5715, 1967.
- Adams, J.B., Lunar and martian surfaces: petrologic significance of absorption bands in the near-infrared, Science, 159, 1453-1455, 1968.
- Adams, J.B. and Jones, R.L., Spectral reflectivity of lunar samples, Science, 167, 737-739, 1970.
- Adams, J.B. and McCord, T.B., Remote sensing of lunar surface mineralogy: Implications from visible and near-infrared reflectivity of Apollo 11 samples, Proceedings of the Apollo 11 Lunar Science Conference (Suppl. 1, Geochim. Cosmochim. Acta), 3, 1937-1945, 1970.
- Adams, J.B. and McCord, T.B., Alteration of lunar optical properties: Age and composition effects, Science, 171, 567-571, 1971a.
- Adams, J.B. and McCord, T.B., Optical properties of mineral separates, glass, and anorthositic fragments from Apollo mare samples. Submitted to Proceedings of the Apollo 12 Lunar Science Conference, 1971b.
- Bancroft, G.M. and Burns, R.G., Interpretation of the electronic spectra of iron in pepoxenes. Amer. Mineralogist, 52, 1278-1287, 1967.

- Birkebak, R.C., Cremers, C.J., and Dawson, J.P., Directional spectral and total reflectance of lunar materials. Proceedings of the Apollo 11 Lunar Science Conference (Suppl. 1, Geochim. Cosmochim. Acta), 3, 1993-2000, 1970.
- Burns, R.G., Electronic spectra of silicate materials: Application of crystal-field theory to aspects of geochemistry, Ph.D. Dissertation, University of California, Berkeley, 1965.
- Burns, R.G. and Fyfe, W.S., Crystal-field theory and the geochemistry of transition elements. In Researches in Geochemistry (editor P.H. Abelson) Vol. 2, 259-285, 1967.
- Burns, R.G., Mineralogical Applications of Crystal-Field Theory, Cambridge University Press, Cambridge, 1970.
- Conel, J.E., Coloring of synthetic and natural lunar glass by titanium and iron, Jet Propulsion Laboratory Space Programs Summary, 3, 26-31, 37-62.
- Conel, J.E. and Nash, D.B., Spectral reflectance and albedo of Apollo 11 lunar samples: effects of irradiation and vitrification and comparison with telescopic observations. Proceedings of the Apollo 11 Lunar Science Conference (Suppl. 1, Geochim. Cosmochim. Acta), 3, 2013-2023, 1970.
- Johnson, T.V. and Soderblom, L.A., Relative reflectivity (0.4u to 1.1u) of the lunar landing site Apollo 7. J. Geophys. Res., 74, 6046-6048, 1969.

McCord, T.B., Color differences in the lunar surface, Ph.D.

Dissertation, California Institute of Technology, Pasadena,
1968.

McCord, T.B., A double-beam astronomical photometer, Appl. Opt.,
7, 475, 1968b.

McCord, T.B., Time dependence of lunar differential color, Astron.
J., 74, 273-278, 1969.

McCord, T.B. and Johnson, T.V., Relative spectral reflectivity
0.4-2.5u of selected areas of the lunar surface. J.Geophys.
Res., 74, 4395-4401, 1969.

McCord, T.B., The spectral reflectivity of the moon and Apollo
11 lunar samples: to be published in The Geophysical Inter-
pretation of the Moon (Ed. Gene Simmons), 1970.

McCord, T.B. and Johnson, T.V., Lunar spectral reflectivity
(0.30u to 2.50u) and implications for remote mineralogical
analysis. Science, 169, 855-858, 1970.

McCord, T.B., Charette, M.P., Johnson, T.V., Lebofsky, L.A.,
Pieters, C., and Adams, J.B., Lunar spectral types. Sub-
mitted to J. Geophys. Res., 1971.

Milton, D.J., Geologic map of the Theophilus quadrangle of the
moon: U.S.G.S. geologic atlas of the moon I-546, 1968.

Shorthill, R.H., "Brief description of Apollo landing sites in terms of earth-based infrared observations". Boeing, Technical Note 016, April 1970.

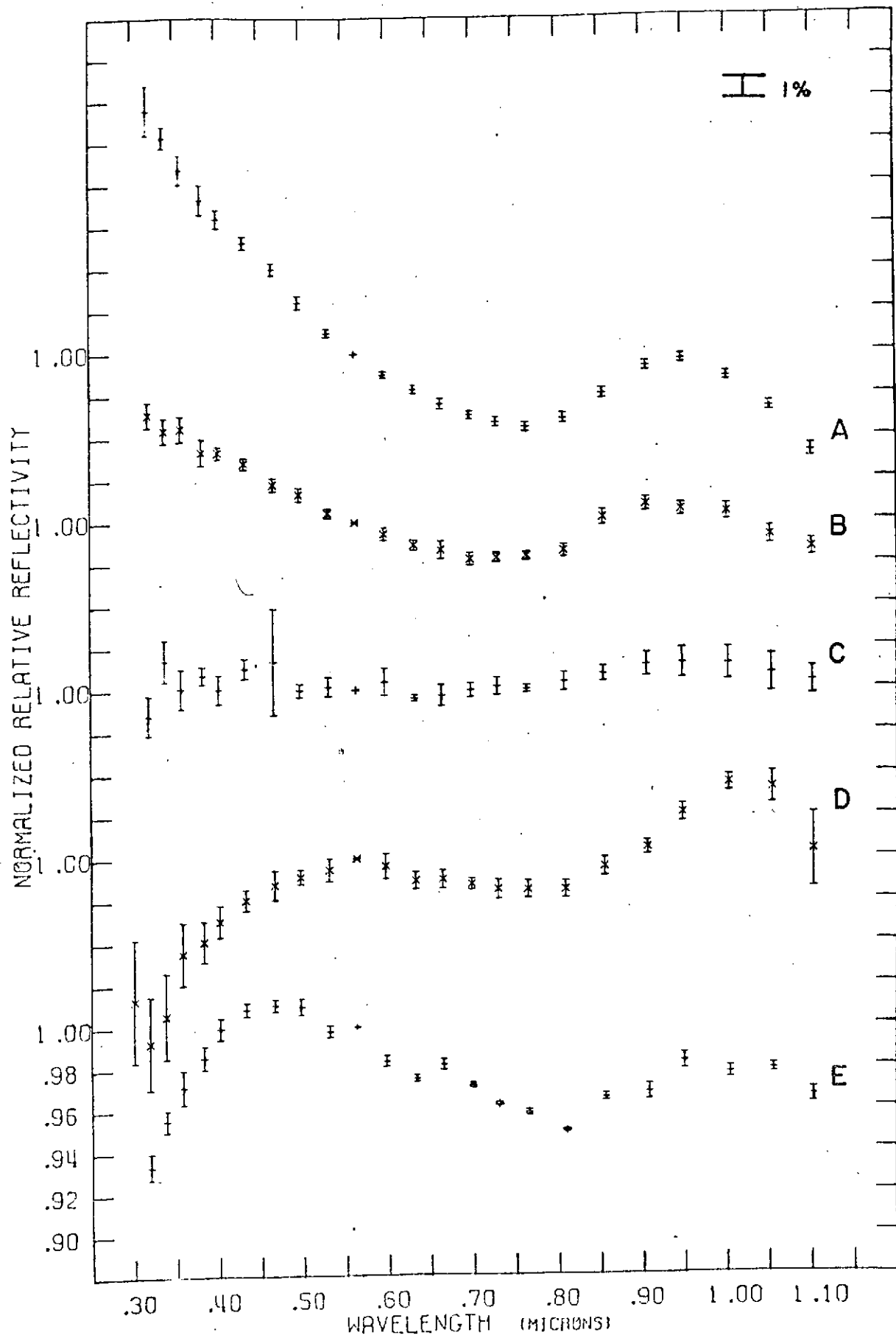
Soderblom, L. A., The distribution and ages of regional lithologies in the lunar maria, Ph.D. Dissertation, California Institute of Technology, 1970.

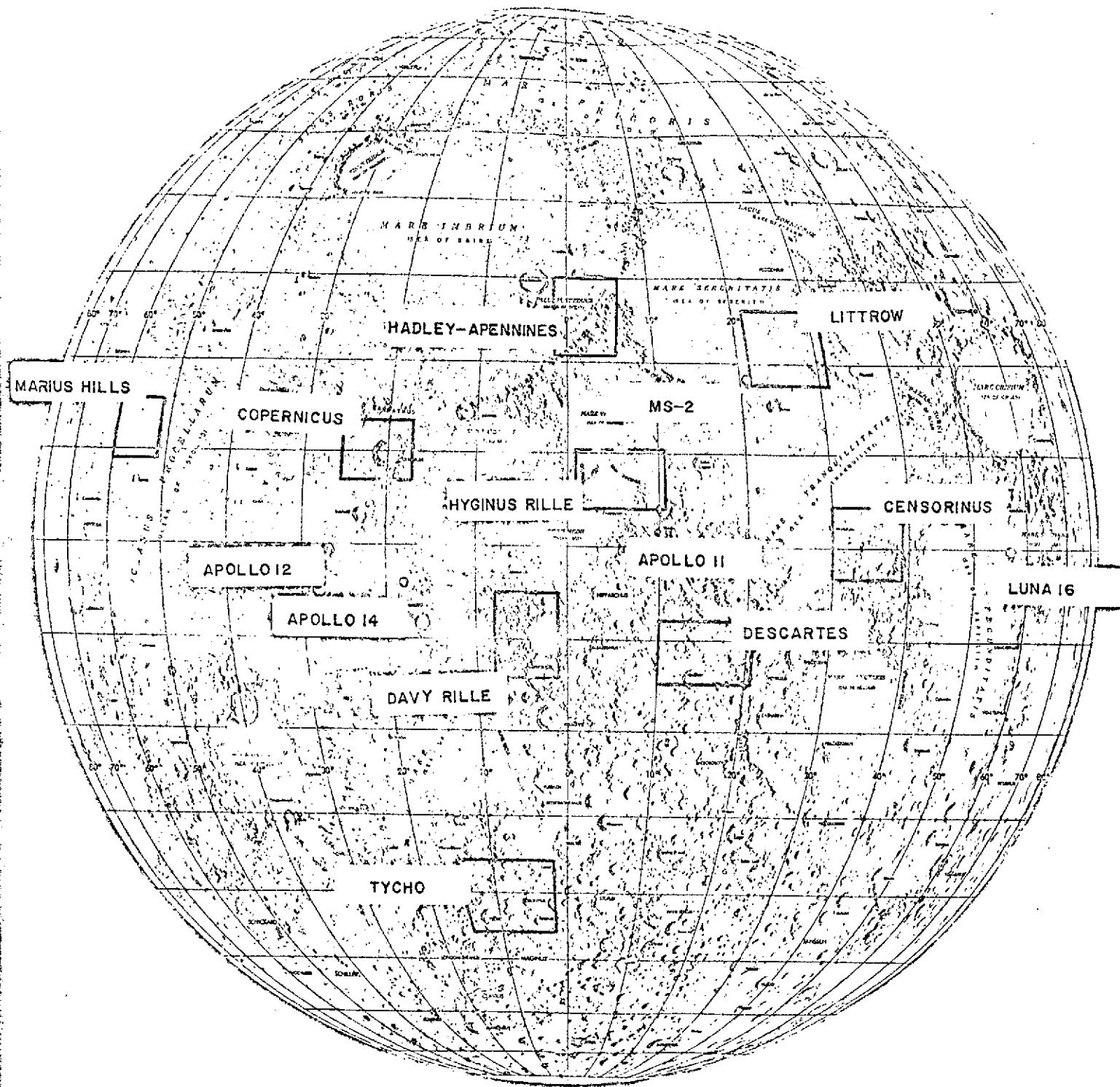
White, W.B. and Keester, K.L., Optical absorpition spectra of iron in the rock-forming silicates. Amer. Mineralogist, 51, 774-491, 1966.

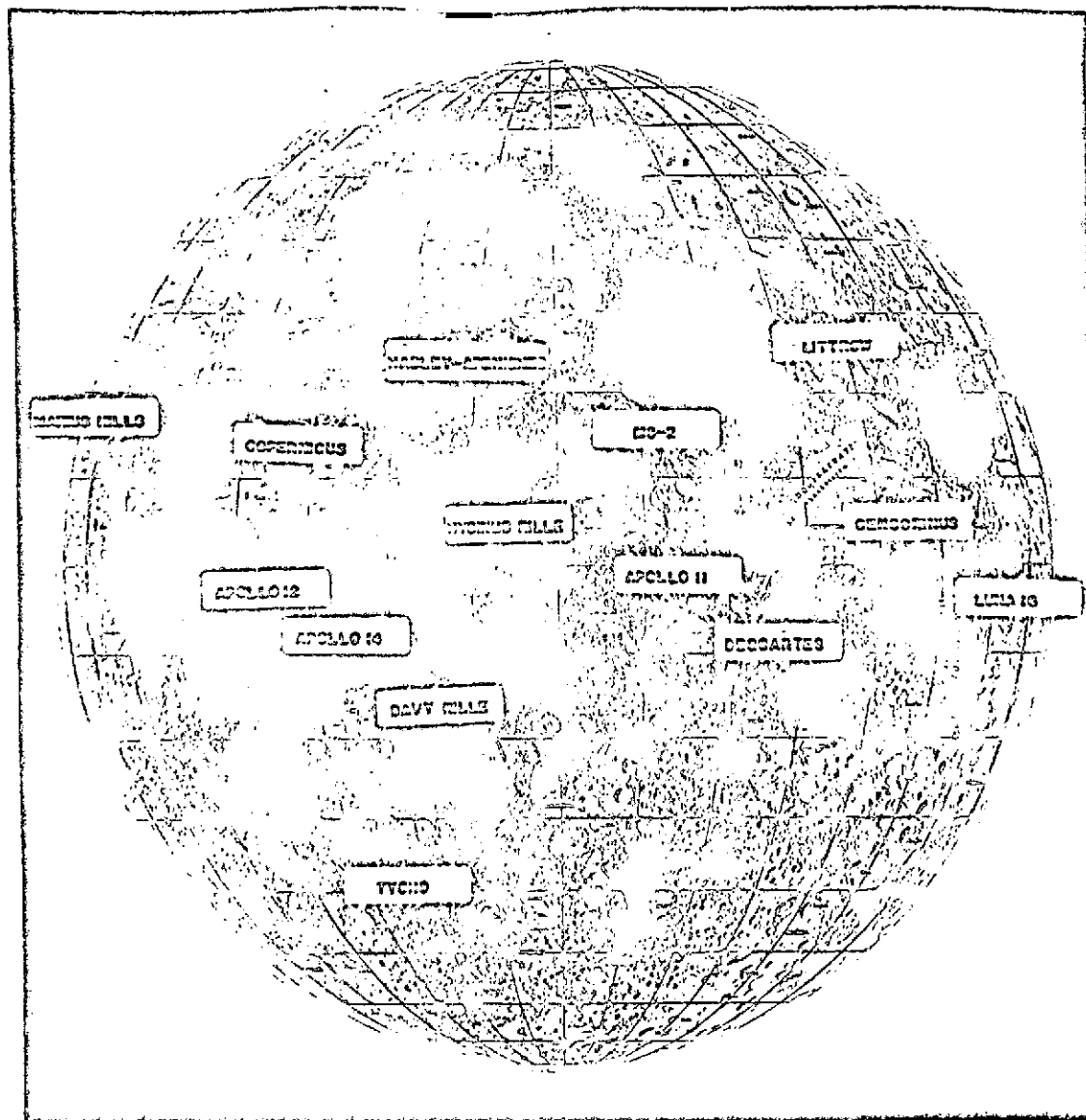
White, W.B. and Keester, K.L., Selection rules and assignments for the spectra of ferrous iron in pyroxenes. Amer. Mineralogist, 52, 1508-1514, 1967.

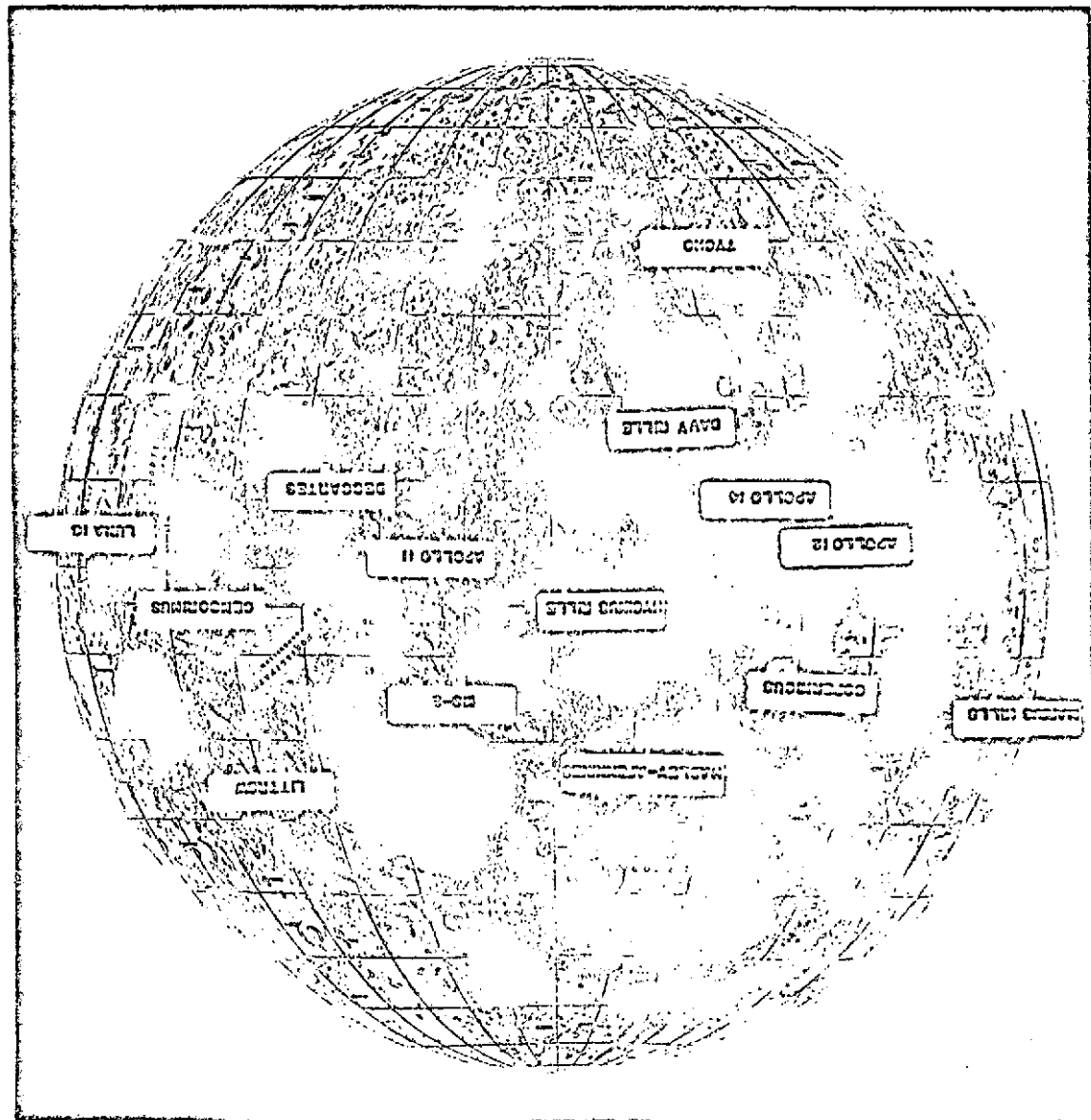
Zisk, S.H., et al., "Final report/radar studies of the moon" (NASA contract NAS 9-7830, M.I.T. Lincoln Laboratory, Lexington, 28 February 1970).

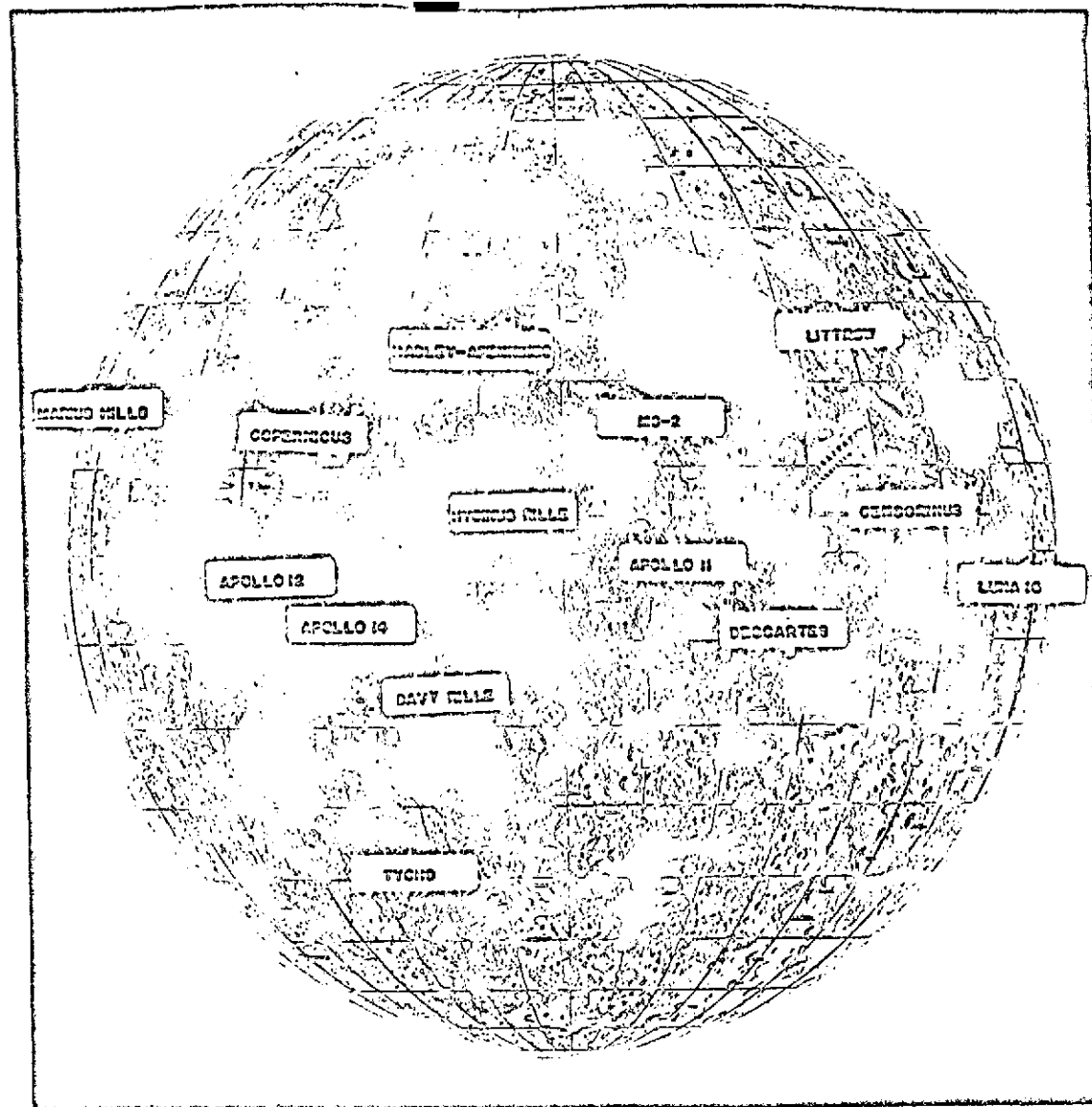
Zisk, S.H., Carr, M.H., Masursky, H., Shorthill, R.W., and Thompson, T.W., Lunar Apennine-Hadley region: Geological implications of earth-based radar and infrared measurements. Science, 173, 808-811, 1971.











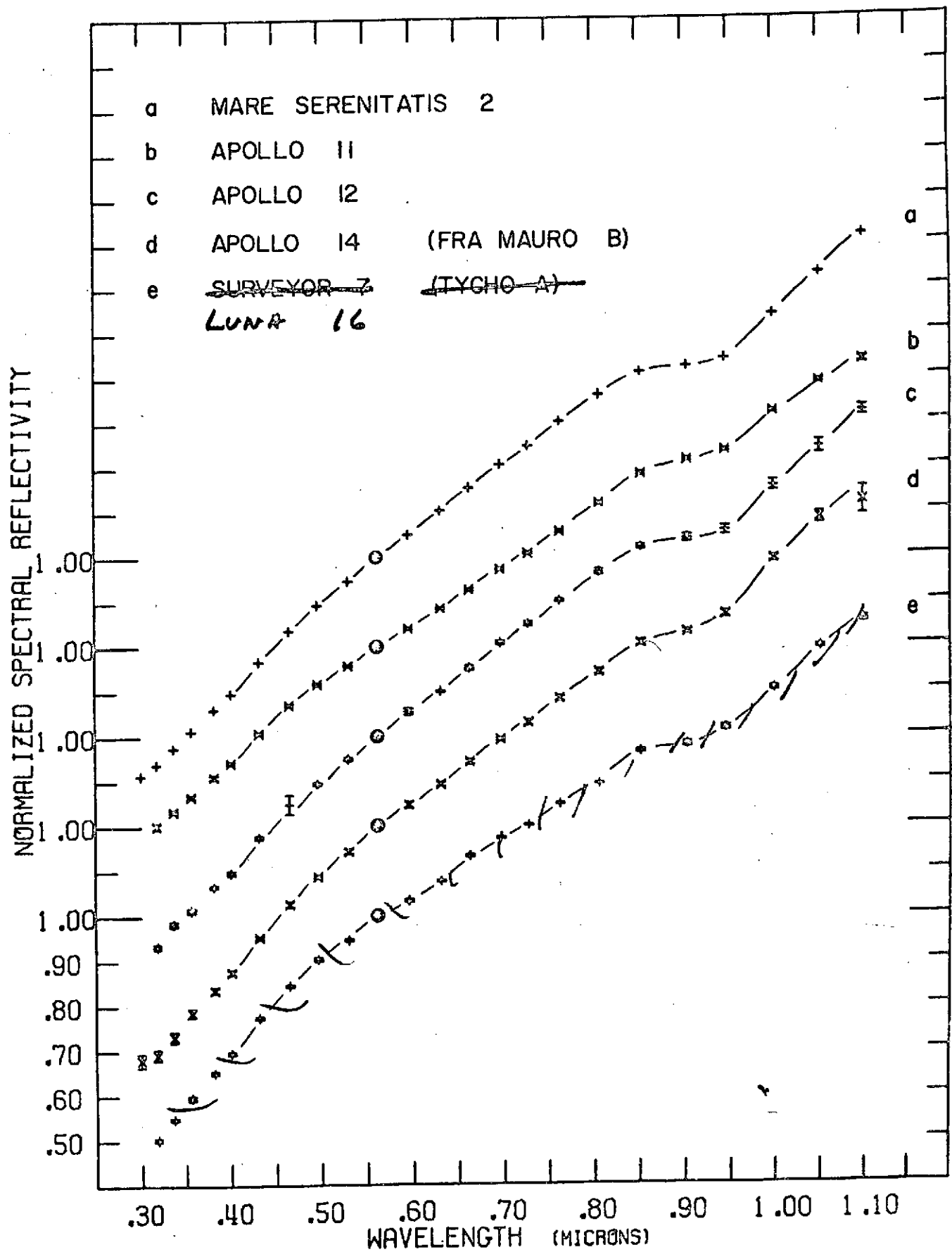
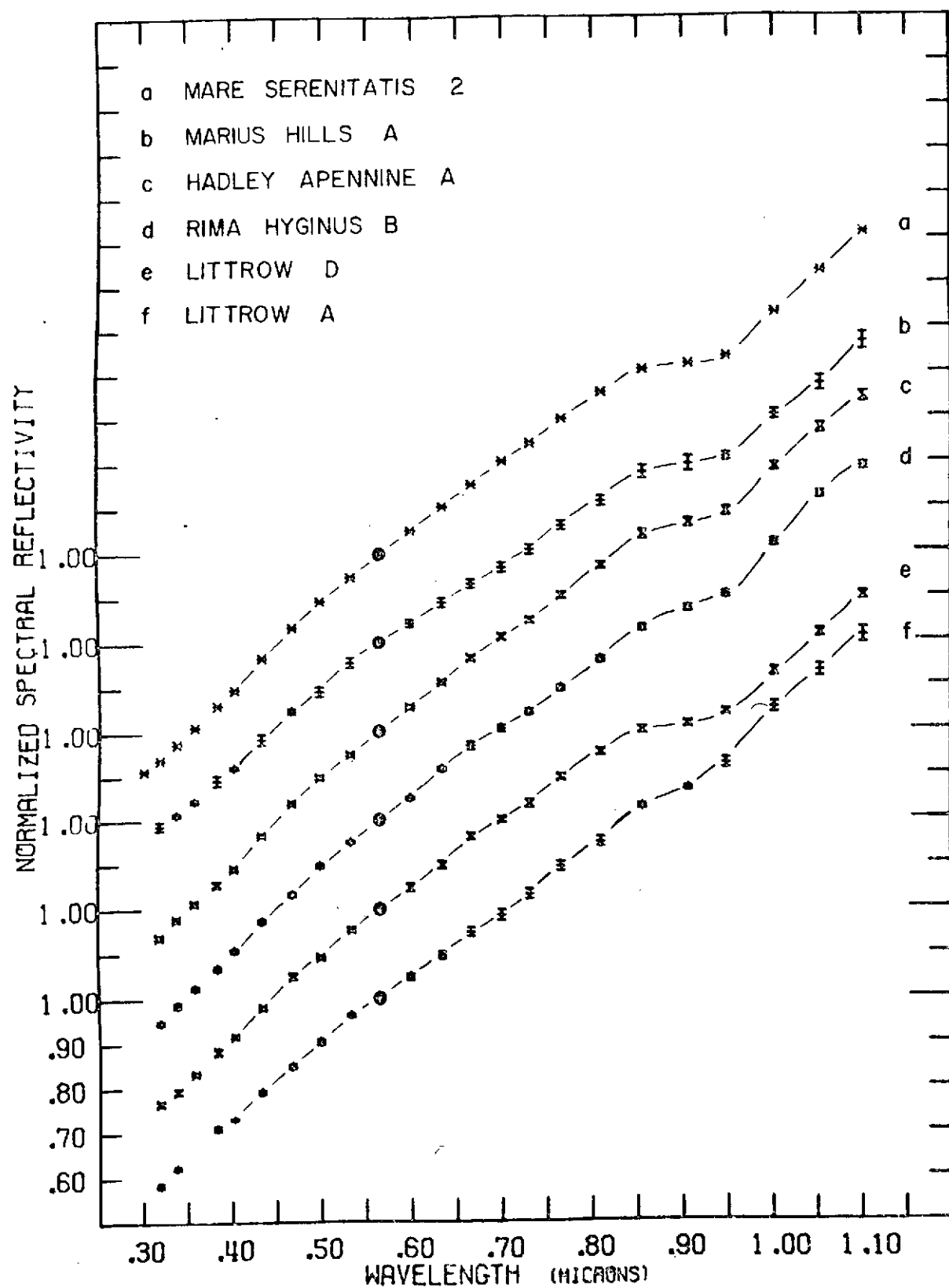
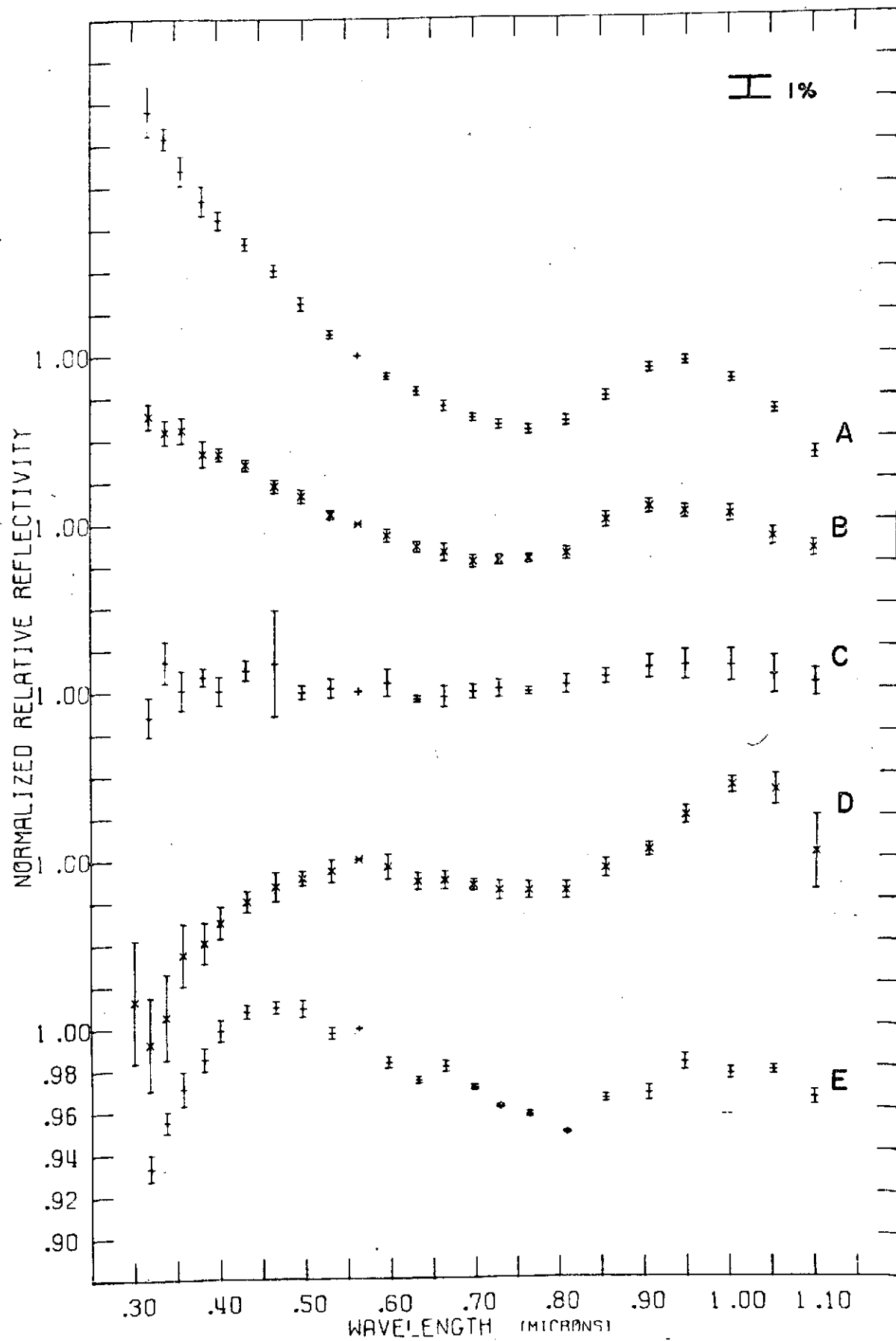
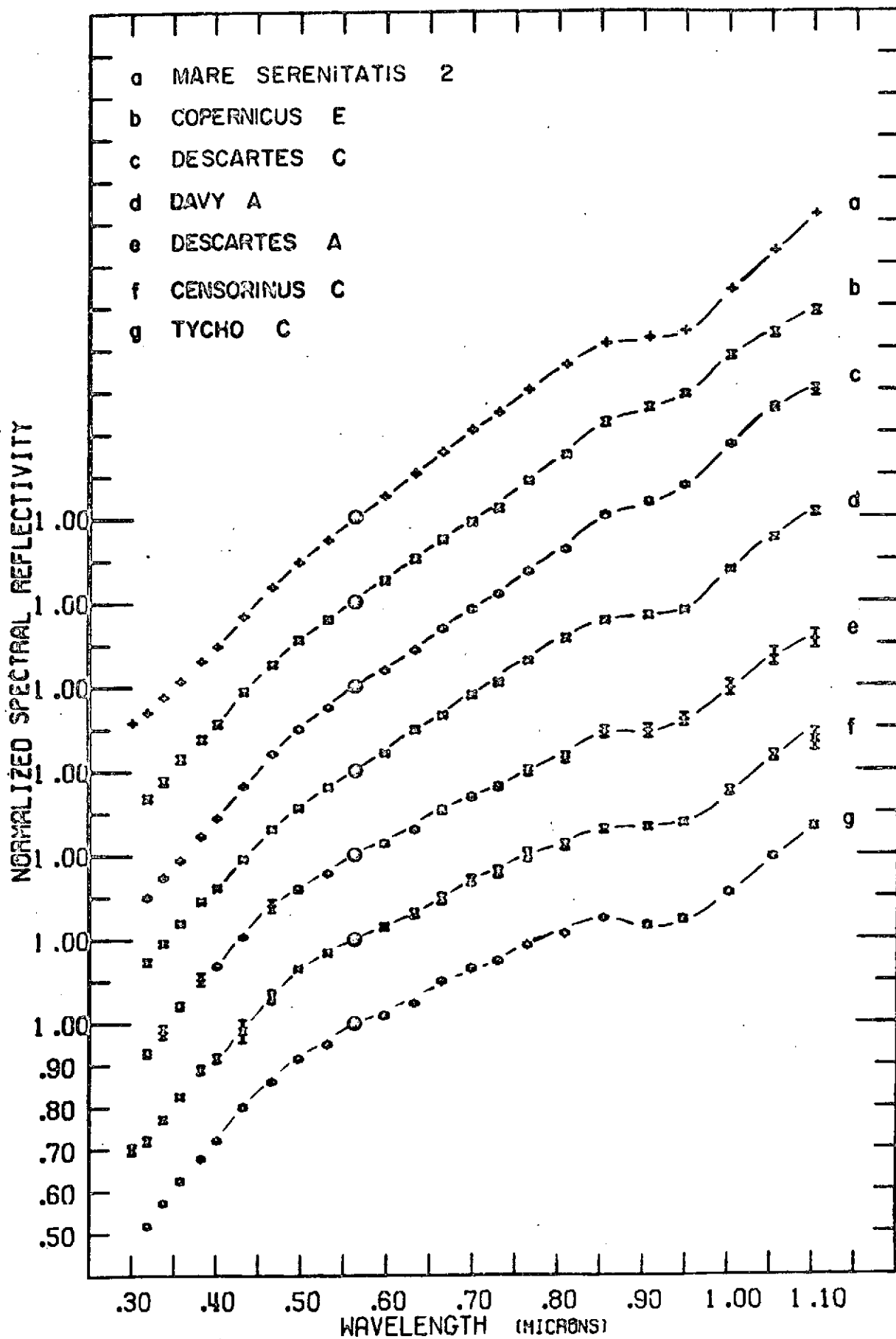
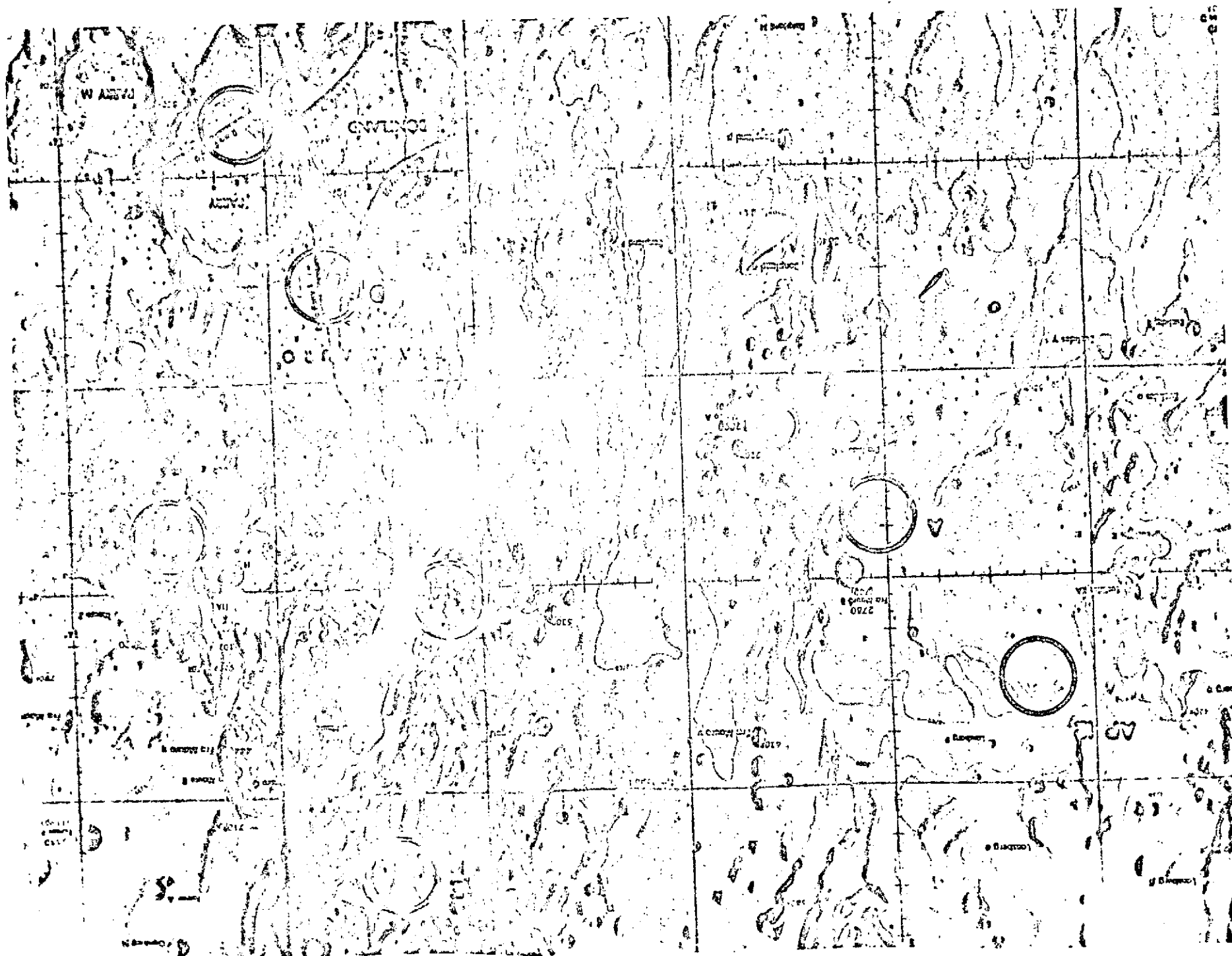


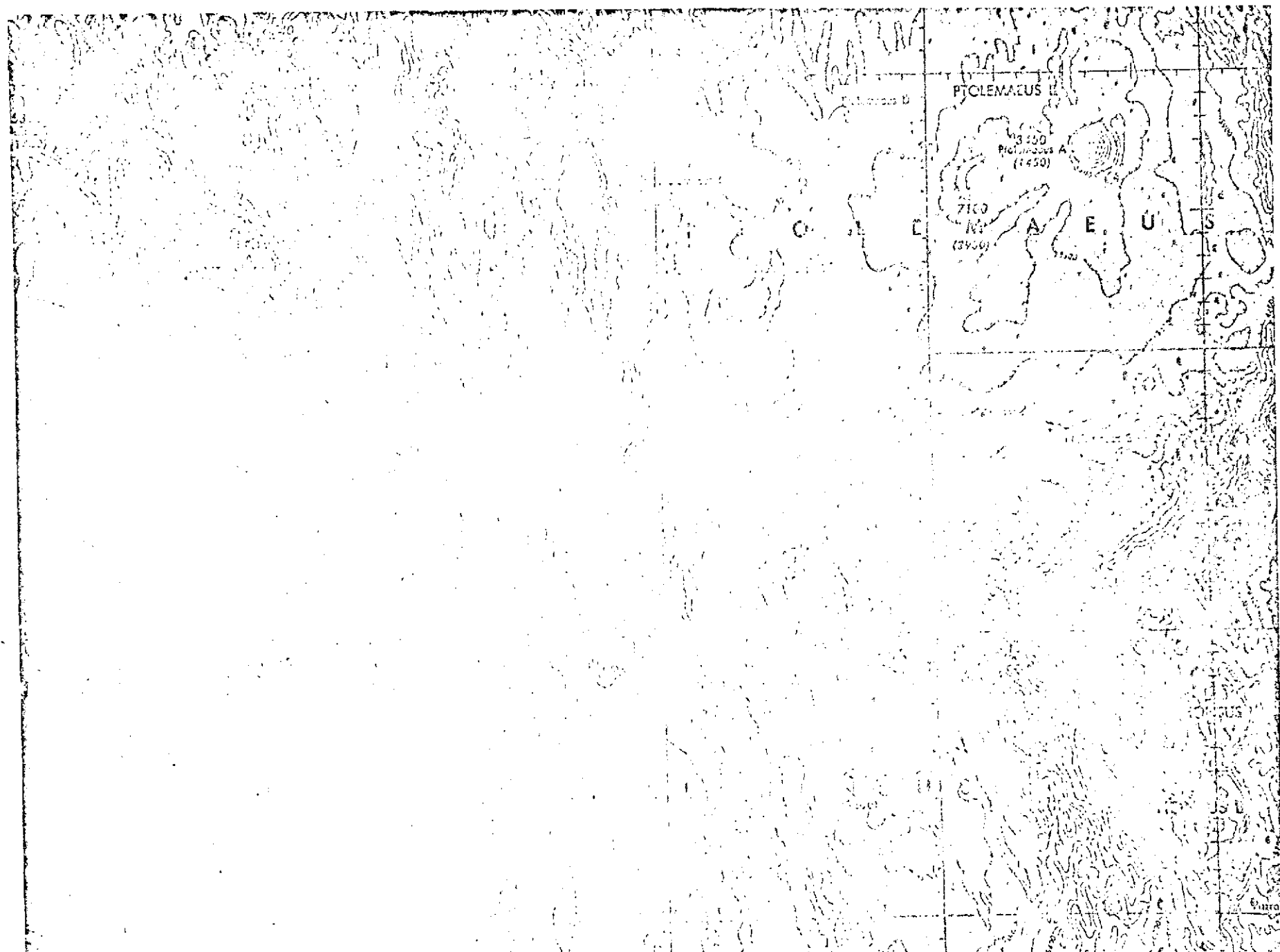
Fig 2











ATTACHMENT B

Proposal
to the
National Aeronautics and Space Administration
for
financial support of a spectral study
of suggested Apollo sites
for the one year period
1 November 1969--1 November 1970
in the
Department of Earth and Planetary Sciences
Massachusetts Institute of Technology
Cambridge, Massachusetts 02139
Thomas B. McCord, Principal Investigator

Thomas B. McCord, Assistant Professor
Planetary Physics

Frank Press, Head, Department of Earth
and Planetary Sciences

R.A. Albery, Dean, School of Science

S.H. Cowen, Director, D.S.R.

I. INTRODUCTION

This is a proposal for support of a program to study from the Earth the spectral reflection properties of possible Apollo landing sites on the lunar surface. Spectral reflectivity differences across the lunar surface seem to indicate compositional and/or mineralogical differences. A knowledge of compositional and mineralogical differences between proposed Apollo sites would be very helpful in helping to determine any one particular site which would be scientifically most interesting for study on one particular lunar Apollo flight. It is suggested that the spectral reflectivity of somewhere between 25 to 50 suggested Apollo sites be observed telescopically in the spectral region of 0.30 to 2.50 microns using the techniques developed by the principal investigator.

II. BACKGROUND

In 1967 the principal investigator began making observations of the spectral reflectance of various regions of the surface of the moon and Mars. These observations have continued up to the present (see references). Independently, Dr. John Adams at the same time began to study in the laboratory the reflectance of properties of common terrestrial minerals and rocks. Dr. Adams also has continued in his work (see references). The principal investigator and Dr. Adams began communicating soon after their

work was begun and they have been coordinating their work up to the present time. At the telescope observations have been made in the spectral region 0.40 to 1.10 microns of many lunar areas. A few observations from 1.0 to 2.50 have been acquired. All these measurements are relative to a standard lunar area. The calibration of a standard lunar area with a standard flux source and the sun from 0.30 to 2.50 microns has been completed and is currently being applied to the relative data. Current efforts are being made to acquire more infrared measurements and to refine the absolute calibration.

From the data obtained, reduced and interpreted to present it has been established that: 1) there exists structure including absorption bands in the spectral reflectivity curves for various areas of the lunar surfaces. 2) These spectral features differ from place to place and seem to correlate with morphology. 3) The spectral feature differences apparently indicate compositional and/or mineralogical differences. 4) There exists structure including absorption bands in the spectral reflectivity curve for powdered samples of terrestrial minerals and rocks measured in the laboratory. 5) The spectral features measured in the laboratory differed in a unique way among many minerals and rocks. 6) The spectral features differences measured in the laboratory indicate mineralogical differences. 7) The spectral features observed on the Moon and Mars are very similar to those observed

in certain terrestrial minerals and rocks in the laboratory. These results indicate that compositional and/or mineralogical differences can be mapped across the surface of the planets by mapping spectral reflectivity differences.

III. PROPOSED RESEARCH

It is proposed that the techniques and procedures developed by the principal investigator for general study of the lunar and martian surfaces be applied specifically to the study of suggested Apollo landing sites. The spectral reflectivity 0.30 to 2.50 microns of 25 to 50 suggested Apollo landing sites would be determined. The spectral reflectivity curves would be interpreted in terms of our past results. A comprehensive report would be prepared describing the spectral reflectance of the sites studied and interpretation of these reflectances in light of our previous work. Recommendation would be made as to which sites should be visited in order to uncover compositional differences on the lunar surface.

IV. PROCEDURES

The proposed spectral reflectivity observations would be made using the double-beam photometer technique developed earlier (see references). Telescopes at Mt. Wilson, California, Cerro Tololo, Chile and, possibly, Mona Kea, Hawaii, would be used to make the observations. Many of the sites to be studied are very small in areal extent, and, thus, large telescopes giving a large image at the focal plane are required. Thus the proposed study

will require somewhat more effort and care than our previous studies. The data will be reduced using computer techniques already developed.

V. BUDGET

Salaries

Principal Investigator	1,500
Research Staff (25%)	2,000
Secretary, part-time	3,000
Technician, part-time (25%)	<u>2,400</u>

Subtotal A	8,900
------------	-------

Graduate Research Assistant (100%)	6,300
---------------------------------------	-------

Undergraduate Assistants (Hrly)	<u>300</u>
---------------------------------	------------

Subtotal B	15,500
------------	--------

<u>Employee Benefits</u> at 14.2% of Subtotal A	1,264
--	-------

<u>Indirect Costs</u> At 46% of Subtotal B	7,130
---	-------

<u>Permanent Equipment</u>	5,500
----------------------------	-------

<u>Materials & Services</u>	4,000
---------------------------------	-------

<u>Other Costs</u> Computation	2,000
-----------------------------------	-------

Travel (including equipment freight costs)	
---	--

Domestic (including mostly	3,900
----------------------------	-------

travel to & from Mt. Wilson
& Palomar Observatories, Cal.,
and Hawaii to use the telescopes
located there.

Foreign (travel to & from the AURA telescope site, Cerro Tololo, Chile)	900
---	-----

Publications	<u>1,000</u>
--------------	--------------

Total Other Costs	7,800
-------------------	-------

TOTAL COST

~~42,000~~

41,200

VI. References

- Adams, J.B., Lunar and martian surfaces: petrologic significance of absorption bands in the near-infrared, Science, 159, 1453, 1968.
- Adams, J.B., Petrologic significance of absorption bands in the spectral reflectance of common silicate minerals, in preparation, 1969.
- Adams, J.B. and A.L. Filice, Spectral reflectance 0.4 to 2.0 microns of silicate rock powders, J. Geophys. Res., 72, 5705, 1967.
- Adams, J.B. and T.B. McCord, Mars: Interpretation of spectral reflectivity of light and dark regions, J. Geophys. Res., 74, No. 20, 1969.
- Duke, M. and L.T. Silver, Petrology of eucrites, howardites, and mesosiderites, Geochim. Cosmochim. Acta., 31, 1637, 1967.
- McCord, T.B., A double beam astronomical photometer, Applied Optics, 7, 475, 1968.
- McCord, T.B., Color differences on the lunar surface, Doctoral Dissertation, California Institute of Technology, January, 1968.

McCord, T.B., Comparison of the reflectivity and color of bright and dark regions on the surface of Mars, Ap. J., 156, 79, 1969.

McCord, T.B., Color differences on the lunar surface, J. Geophys. Res., 74, 12, 1969.

McCord, T.B., Time dependence of lunar differential color, Astron. J., 74, 273, 1969.

McCord, T.B. and J.B. Adams, Spectral reflectivity of Mars, Science, 163, 1058, 1969.

McCord, T.B. and T. Johnson, Relative spectral reflectivity 0.4--1.1 of selected areas of the lunar surface. J. Geophys. Res., 74, 4395, 1969.

McCord, T.B., T. Johnson and H.H. Kieffer, Differences between proposed Apollo sites: II, Visible and near-infrared reflectivity evidence, J. Geophys. Res., 74, 4385, 1969.

Murray, B.C., A.F.H. Goetz, H.H. Kieffer, and T.B. McCord, Differences between proposed Apollo sites: I, Synthesis of evidence, J. Geophys. Res., 74, 4385, 1969.

VII. QUALIFICATIONS

Thomas B. McCord received his B.S. in Physics from Pennsylvania State University in 1964, his M.S. in Geology and Geophysics in 1966 and his Ph.D. in Planetary Sciences and in Astronomy in 1968 from California Institute of Technology. From January to July 1968 he was a Research Fellow in Planetary Sciences at Caltech. In July 1968 he was appointed Assistant Professor of Planetary Physics at the Massachusetts Institute of Technology, a position he now holds. In April 1969 he was appointed visiting Associate in Planetary Science at the California Institute of Technology.

Dr. McCord is a member of the American Geophysical Union, American Astronomical Society (and also the Planetary Astronomy Special Section) and is a Fellow of the American Association for the Advancement of Science. He is a member of Sigma Xi.

Dr. McCord has performed research and has contributed to the literature in the area of solid state physics, celestial dynamics, astronomical instrumentation, observational astronomy of solar system objects and interpretation of these and other measurements. He is currently a coinvestigator on the Mariner Mars 1971 Television Experiment, and he is chairman of the committee to develop a local astrophysical observatory for M.I.T.

ATTACHMENT C


Proposal
to
National Aeronautics and Space Administration
for
financial support of a spectral study
of suggested Apollo sites
(extension)


Thomas B. McCord, Principal Investigator
Department of Earth and Planetary Sciences
Massachusetts Institute of Technology
Cambridge, Massachusetts 02139

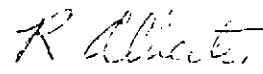
Period: 1 April, 1971 -
31 March, 1972

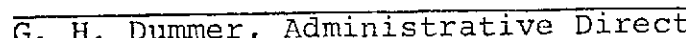
Amount: \$5000.00

Extension of Grant #NGR-22-009-496


Thomas B. McCord, Assistant Professor


Frank Press, Head, Department of Earth
and Planetary Sciences


R. A. Alberty, Dean, School of Science


G. H. Dummer, Administrative Director,
Division of Sponsored Research

This is a request for an extension of NASA Grant NGR-22-009-496 for a period of one year at a cost to NASA of \$5000. The project, "Spectral Reflection Properties of Proposed Apollo Landing Sites," has been completed in its major aspects and a report describing the results is being prepared and is scheduled to be available in approximately one month. However, there are several interesting items which we would like to follow up before we finish this study. First of all, some of the proposed landing areas have been moved since our observations were made. We would like to work at MSC with the mapping science group to fix these new sites and then measure them. Secondly, we would like to transfer our new data to the MSC data bank so it could be used by other scientists.

A budget to cover the work is given below:

Salary

P. I. part time	1500
--------------------	------

Indirect Costs

53% of P.I. Salary	800
--------------------	-----

Benefits

15% of P.I. Salary	200
--------------------	-----

Travel

6 trips, Boston to MSC	<u>2500</u>
------------------------	-------------

TOTAL	5000
-------	------

ATTACHMENT D

SPECTROPHOTOMETRY (0.3 to 1.1 μ) OF VISITED AND PROPOSED APOLLO LUNAR LANDING SITES

THOMAS B. McCORD, MICHAEL P. CHARETTE,
TORRENCE V. JOHNSON, LARRY A. LEBOWSKY, and CARLE PIETERS

*Planetary Astronomy Laboratory, Dept. of Earth and Planetary Sciences,
Massachusetts Institute of Technology, Cambridge, Mass., U.S.A.*

1. Introduction

The color of the lunar surface has been a topic of study since the beginning of the century (for a review of early studies, see McCord, 1968a). Only in the past few years, however, have the spectral reflectance properties of small regions of the lunar surface been determined throughout the spectral region where reflected solar radiation is important, i.e., from 0.3 μ to 2.5 μ .

Sufficient spectral resolution and intensity precision has now been achieved in the 0.3–2.5 μ region to detect absorption bands in the lunar reflection spectrum. Of equal importance is the appearance in the reflection spectrum of differences in both the continuum shapes and absorption band strengths from place to place on the lunar surface (McCord, 1968a, 1969a, b; McCord and Johnson, 1969, 1970; McCord *et al.*, 1972). These effects are important to our understanding of the Moon, since according to laboratory studies, the reflection spectrum of solids is controlled primarily by mineralogy and composition. Although only provisional predictions were available before the Apollo 11 samples were returned (Adams, 1968; McCord, 1968a), studies of the lunar samples supported and greatly extended these early results (Adams and Jones, 1970; Adams and McCord, 1970, 1971a, b; Conel, 1970; Conel and Nash, 1970).

The basis for the interpretation of absorption bands in the spectra of silicates between 0.3 μ and 2.5 μ was developed through the application of crystal field theory to mineralogy (Burns, 1965; White and Keester, 1966). Transmission spectra of oriented single crystals, using polarized light, led to later refinements in band assignments (Burns and Fyfe, 1967; Bancroft and Burns, 1967; White and Keester, 1967; Burns, 1970).

Absorption bands have also been studied in diffuse reflectance spectra of minerals and their powders (White and Keester, 1967; Adams and Filice, 1967), thus establishing a foundation upon which planetary surface composition can be determined (Adams, 1968).

This report discusses a study of the spectral reflectance of regions of the lunar surface containing most of the proposed Apollo landing sites. Using these measurements, information regarding surface properties such as composition and mineralogy can be obtained. Specifically (1) the presence of pyroxenes which cause an absorption band near 0.95 μ in the lunar reflection spectrum; (2) the proportion of crystalline to glassy material present in the soil which is derived from the slope of the reflectivity curve between 0.4 μ and 0.7 μ and strength of the 0.95 μ absorption band; (3) the presence of

Ti³⁺ ions in the glasses on the lunar surface which effects the reflection spectrum at blue and ultraviolet wavelengths.

The study uses information gained by analysis of the spectral properties of lunar samples in the laboratory and telescope spectra of over 100 lunar areas to provide information regarding the composition and mineralogy of each proposed lunar landing site. The reader is referred to McCord *et al.* (1972) and Adams and McCord (1971a, b) for background information which will be useful in understanding this report.

2. Observation and Data Presentation

Several areas of the lunar surface, approximately 18 km in diameter, were studied in the regions of the visited and proposed Apollo landing sites (see Figure 1 for region

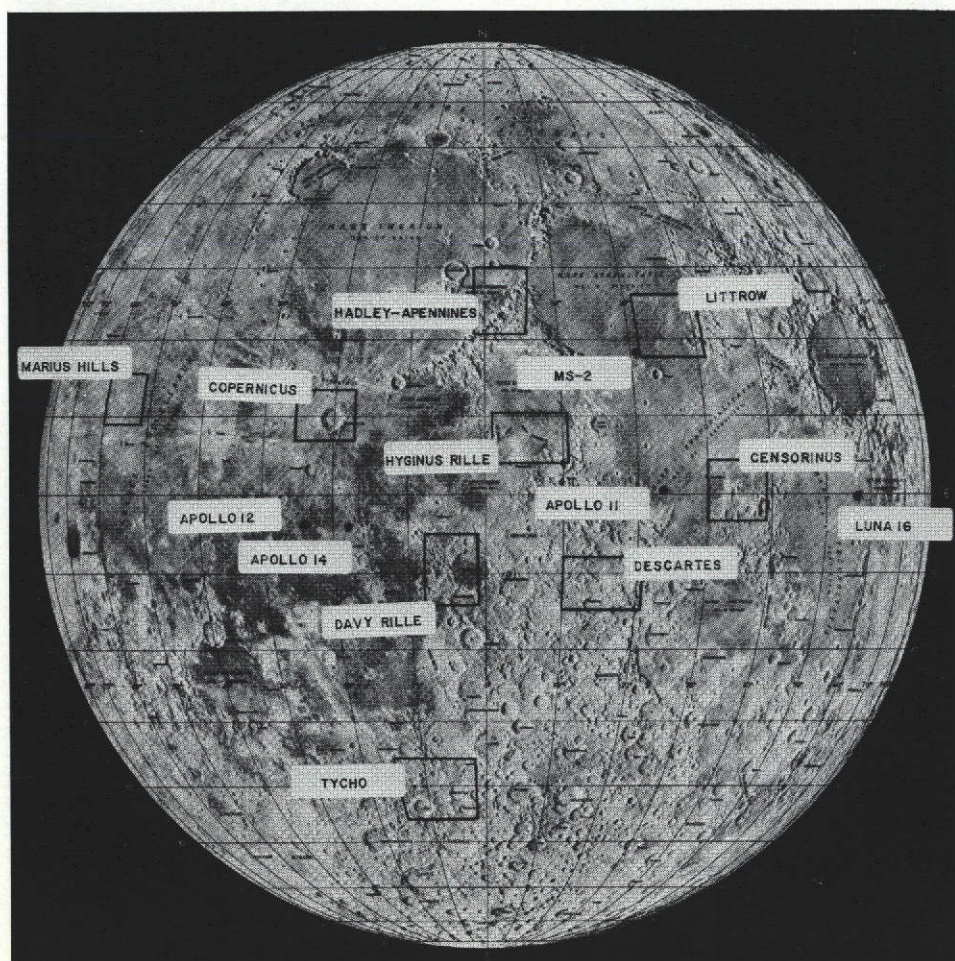


Fig. 1. ACIC map of the Moon showing the visited and proposed Apollo landing sites.

locations). The 24-in. (61 cm) and 60-in. (152 cm) telescopes on Mt. Wilson, California were used with a double beam, filter photometer (McCord, 1968b) to obtain the data. The spectral reflectivity of each area was measured in the spectral region from 0.3μ to 1.1μ , using 24 narrow-band interference filters. A detailed description of the equipment and technique used in this study is given in McCord *et al.* (1972).

The data are discussed in two sections. The measurements of sites from which samples have been returned to Earth and analyzed are discussed first. Laboratory analyses of the spectral properties and mineralogy of returned samples allow detailed interpretation of the telescopic spectral reflectivity curves. Much of this work has been published earlier and is reviewed for completeness.

The telescopic data for the proposed Apollo landing sites are discussed in the following section. The format for each site consists of a topographic map showing the locations of the areas observed, a description of the local geology, a set of *relative* spectral reflectivity curves for the observed areas, and a discussion of the results. The spectral reflectivity measurements are discussed in a separate section.

The topographic maps are taken from the *Lunar Atlas Chart* (LAC) series published by the U.S.A.F. Aeronautical Chart and Information Center. The geological descriptions have been derived from the U.S. Geological Survey's *Geologic Atlas of the Moon* and inspection of Lunar Orbiter and Apollo photographs.

The reflectivity data are presented in two forms. First, two graphs of the normalized *relative* spectral reflectivity, scaled to unity at 0.564μ , are given. These plots are obtained by dividing the reflectivity of a given area by the reflectivity of a standard area. The standard for the first plot is the Mare Serenitatis 2 standard area, while the standard for the second plot is a selected area within the investigated region. This use of relative reflectivities reveals important compositional information, since the relative data are sensitive to the small differences which exist in the spectrum of the various lunar areas.

Secondly, graphs of the normalized spectral reflectivity scaled to unity at 0.56μ are plotted in a separate section. The normalized spectral reflectivity is proportional to the ratio of light energy reflected from the lunar surface to the incident solar flux.

The *precision* of the spectral reflectivity measurements discussed in this report is usually less than 1%, as indicated by the error bars. The *accuracy* of the measurements is dependent on several variables. A variation of 2–3% is caused by changes in the phase angle of the Moon, depending on when observations were made. The lack of complete knowledge of the solar and stellar fluxes introduces a possible error of 4% in the curves from 0.3μ to 0.4μ , 1–2% from 0.4μ to 0.9μ , and 2–3% from 0.9μ to 1.1μ . It should be noted, however, that the relative spectral reflectivity curve shapes are not affected by the inaccuracies cited here.

3. Analysis of Lunar Samples from Visited Apollo Landing Sites

A. INTRODUCTION

The study of samples returned from the Moon has greatly increased our knowledge of the landing sites and their immediate surroundings. However, our understanding

of the vast areas beyond these sites is dependent, in large part, on remote measurements. Therefore, it is important that the returned samples be studied as ground truth for observations of proposed landing sites. The extension of the knowledge gained from these sample analyses to lunar areas not yet visited allows future landing sites of exceptional interest to be chosen. It also allows the study of large regions of the Moon for which the cost of *in situ* study would be prohibitive.

B. OBSERVATIONS AND RESULTS

Telescopic measurements of the spectral reflectivity for areas 18 km in diameter containing the Apollo 11, 12, 14 and Luna 16 landing sites and for the standard reference area in Mare Serenitatis (21.4E, 18.7N) are shown in Figure 2. All curves are scaled to unity at 0.564 μ to make the shapes directly comparable with each other.

The spectral reflectivity for all areas shown in Figure 2 increases steadily toward the red end of the spectrum. An absorption band appears near 0.95 μ in all curves. The curves are characteristic of most lunar areas which have been studied to date (McCord and Johnson, 1970; McCord *et al.*, 1972).

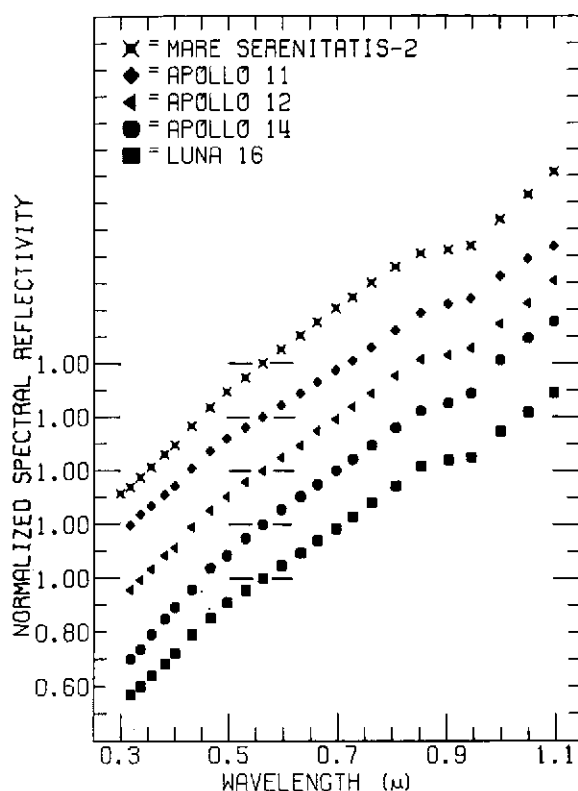


Fig. 2. Normalized spectral reflectivity of visited Apollo landing sites, scaled to unity at 0.56 μ .

There are small but significant differences between the curves shown in Figure 2, but they are difficult to analyze as plotted. Therefore, the *relative* spectral reflectivity curves (as described earlier) for the areas shown in Figure 2 are plotted in Figure 3 to resolve these subtle differences. Thus, the top curve in Figure 3 is the ratio of the fourth curve to the top curve in Figure 2. Note the expanded scale in Figure 3 as opposed to Figure 2.

It has been found (McCord, 1968a, 1969; McCord and Johnson, 1969; McCord *et al.*, 1972) that the shapes of the *relative* reflectivity curves can be used to identify several types of lunar material. Basically, all upland regions except bright craters and a few other anomalously bright areas have a single curve-type. Upland bright craters have curve-types which grade into upland material curves with increasing crater age. Mare regions illustrate a suite of curves within one general class. Mare bright craters have a distinct curve-type which grades into mare curves with increasing crater age.

Discussion of the above curve-types and lunar material identification is given in

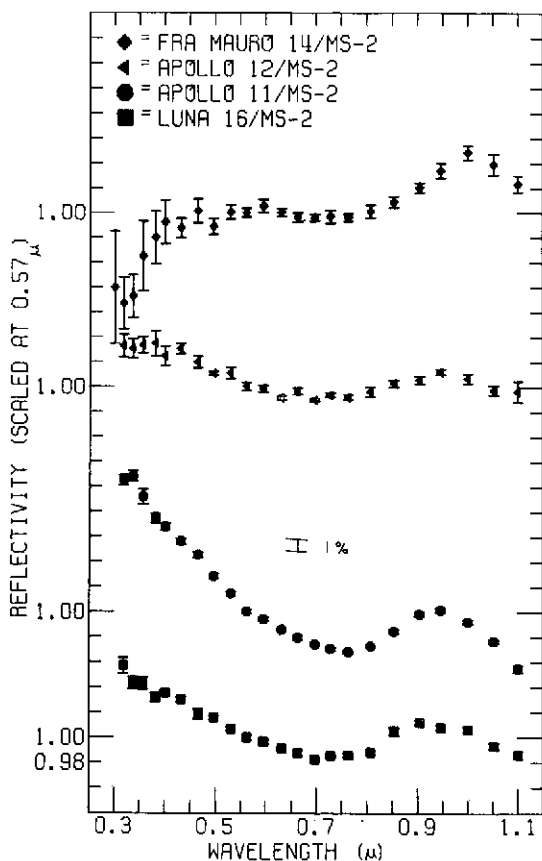


Fig. 3. Normalized relative spectral reflectivity of visited Apollo landing sites relative to Mare Serenitatis 2 standard.

McCord *et al.* (1972). According to this spectral type classification, the Apollo 11, 12 and Luna 16 curves all have mare-types curves. The Apollo 11 curve is near the 'blue' end member of the mare curve series, while the Apollo 12 curve falls near the 'red' end member of the series. The Luna 16 landing site curve is intermediate between the two aforementioned curves. The Apollo 14 curve is a typical upland curve.

C. INTERPRETATION

Apollo 11: Laboratory reflectivity curves of Apollo 11 rock, breccia, and soil samples have been compared with Earth-based telescopic measurements of the landing site and with petrologic analysis of the samples (Adams and McCord, 1970a, b; Birkebak *et al.*, 1970; Conel and Nash, 1970; McCord and Johnson, 1970). The telescopic curve for the Apollo 11 site agrees very closely with the laboratory curve for the bulk surface fines. From these data, it was concluded that: (1) the surface fines at Apollo 11 site are representative of the lunar surface material within ten or more kilometers of the landing area; (2) Lunar fines produce much weaker absorption bands than the rocks; (3) Exposed, crystalline rocks are not sufficiently abundant at the landing site to significantly influence the reflectivity curve of the site; (4) The single, weak band at 0.95 μ in the telescope curve is due mainly to clinopyroxene, with a minor influence of olivine on the band position; (5) The low albedo of the lunar soil can be attributed to the presence of iron and titanium ions on the glass present in the lunar soil.

Apollo 12: The telescopic spectral reflectivity curve for the Apollo 12 landing site (Figure 2) shows an absorption band at 0.95 μ , as does the Apollo 11 curve. Also, the Apollo 12 curve continuum is similar to the Apollo 11 continuum. As in the Apollo 11 curve, these data would indicate that the clinopyroxene and dark glass in the Apollo 12 soil strongly influence the reflectivity curves. Laboratory analysis of the Apollo 12 samples confirm these interpretations (Adams and McCord, 1971a, b).

The intensity of the absorption band and the slope of the telescopic reflectivity curve continuum for the 18 km region containing the Apollo 12 site differ slightly from those of the Apollo 12 soil samples. Laboratory analysis of surface and subsurface soil samples, and of mineral separates from these samples, indicate that these differences are due to variations in the relative proportion of crystalline to glassy material in the soil. These same studies (Adams and McCord, 1971a, b; Conel and Nash, 1970) demonstrated that vitrification of lunar crystalline material changes the spectral properties of the material. These changes are observed when reviewing the range of telescopic curves from bright craters (more crystalline material, less glass) to mare surface-material (less crystalline material, more glass) (McCord *et al.*, 1972).

Further studies of the Apollo 12 samples (Adams and McCord 1971a, b) have revealed that the spectral region from 0.3 μ to 0.6 μ is affected by the amount of Ti^{3+} ions present in the lunar glass. Ti^{3+} ions in the glassy material have been found to produce a relative increase in reflectivity in the ultraviolet. Ti^{3+} ions are also found in ilmenite, but the mineral is so opaque that almost no light which enters the crystal is scattered back into space. Thus, titanium in ilmenite has little effect on the spectral reflectivity curves.

Laboratory studies of titanium-rich lunar minerals and glasses, and of artificially generated glasses (Conel, 1970; Adams and McCord, 1970a, b, 1971a, b) show that the amount of titanium present in the lunar glasses can be measured using spectral reflectivity curves. This information was used to predict the lower titanium content in the Apollo 12 samples over the Apollo 11 samples (Johnson and Soderblom, 1969).

Luna 16: The spectral reflectivity curve for the Luna 16 landing (Figure 2) has a $0.95\ \mu$ absorption band and a positively sloping curve similar to those for the Apollo 11 and Apollo 12 landing site curves.

The Luna 16 relative spectral reflectivity curve (Figure 3) is a mare-type curve which is intermediate between the Apollo 11 and Apollo 12 curves (McCord *et al.*, 1972). The absorption band is similar to that found in the Apollo 11 curve, but the continuum is more similar to the Apollo 12 continuum. It can be inferred from these data that the crystal-to-glass ratio of the Luna 16 soil is similar to that of Apollo 11, but the titanium content is more similar to the Apollo 12 content. The Luna 16 sample analyses available to date bear out these interpretations.

Apollo 14: The spectral reflectivity curve for the Apollo 14 landing site has an absorption band near $0.95\ \mu$ but it is much shallower than in any landing site curve previously discussed. The overall curve shape suggests the presence of glasses but the much higher albedo of this upland area over the mare regions implies that a lower amount of Ti^{3+} and Fe^{2+} exists in the glasses of the region, i.e. less dark glass is present. The absorption band position again indicates pyroxenes as a major mineral present in the soil.

The relative spectral reflectivity curve (Figure 3) is a typical example of an upland curve (McCord *et al.*, 1972). The shallowness of the absorption band at $0.95\ \mu$ can be clearly seen. The decrease in slope toward the ultraviolet indicates a much lower titanium content at the site than in the maria, especially the Apollo 11 site.

A preliminary study of the Apollo 14 fines reveals a good correlation between the laboratory and the telescopic spectral reflectivity curves. The detailed interpretation of the spectral properties of these samples is not yet available.

4. Analysis of Proposed Landing Sites

Most of the lunar areas suggested as landing sites for the Apollo program are discussed in this section. The selection of areas to study was made more than one year ago. The changing nature of the Apollo program has made some of these sites at least temporarily uninteresting. In the meantime several sites not included here have been suggested seriously. The large amount of work inherent in a study of this nature requires production methods be adopted. Thus we were unable to keep up with the changing Apollo program and had to freeze our site selection early.

However, the information contained here will allow some extrapolation to other areas without direct measurements. A careful reader of this report and the referenced material will develop a feel for the spectral analysis and he will be better able to judge other sites.

Presented in this section are maps showing observation area locations and size, plots of relative spectral reflectivity for each area and a discussion both of the site and its spectral properties. We have attempted to discuss only the properties of each site. We are not attempting to 'sell' one site over another. Here are the data, do as you please with them.

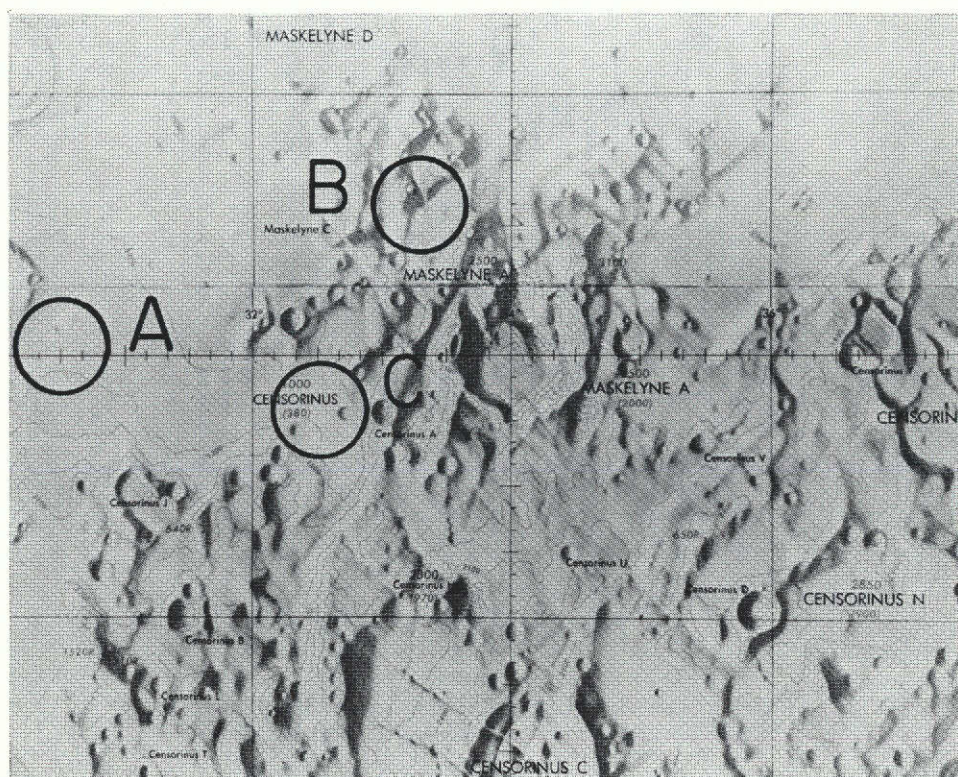


Fig. 4a. ACIC topographic map of the Censorinus area.

CENSORINUS

Spot	Lat.	Long.	Date	Runs	Phase	Unit	Curve Type
A	0°05'N	30°30'E	10/17/70	3	+35°	Em	Mare
B	1°10'N	33°15'E	10/17/70	3	+35°	IpIt	Uplands
C	0°25'S	32°30'E	10/17/70	3	+35°	Cs	Uplands Bright crater

Censorinus A: Mare material, with moderate albedo and high crater density; regolith similar to Apollo 11 site.

Censorinus B: Rough, hummocky material with low crater density and deep regolith.

Censorinus C: Crater with steep slopes, sharp rim, and high albedo ray material radiating outward; boulders extensive and deep regolith.

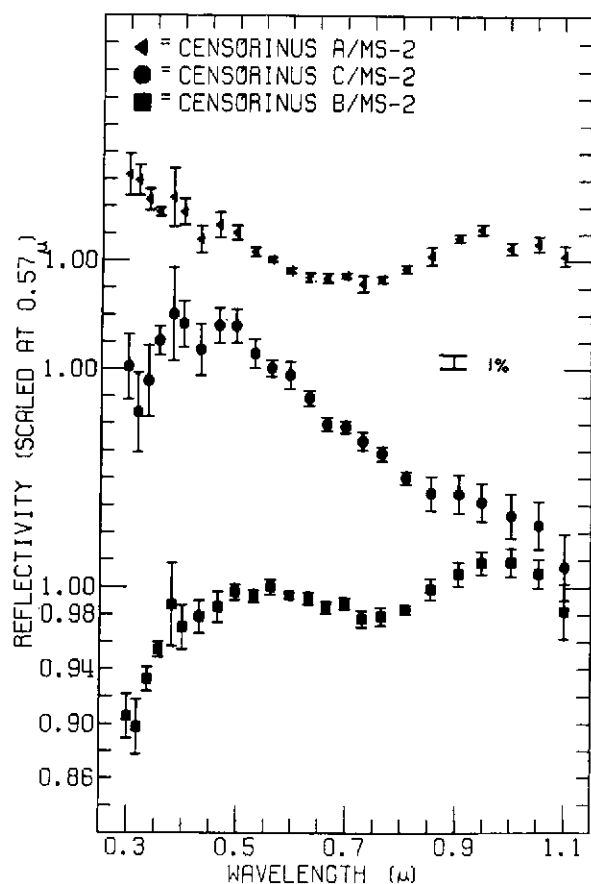


Fig. 4b. Normalized relative spectral reflectivity of Censorinus spots relative to Mare Serenitatis 2 standard.

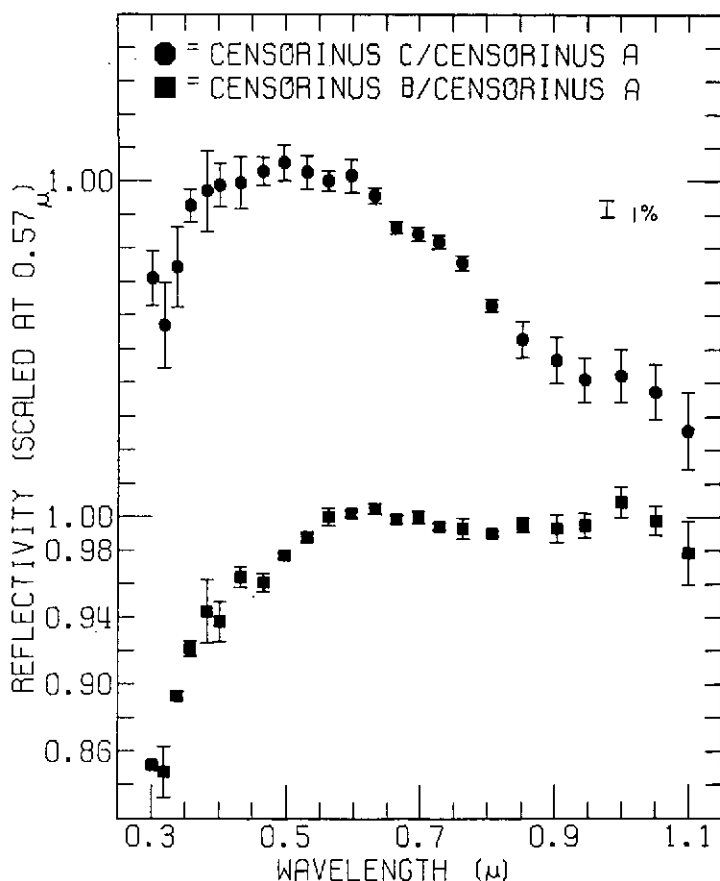


Fig. 4c. Normalized relative spectral reflectivity of Censorinus spots relative to Censorinus A.

Discussion

We find that CENSORINUS A probably has a bulk surface soil composition which is very similar to that found at the Luna 16 landing site. CENSORINUS B seems to have a composition similar to the Apollo 14 landing site. CENSORINUS C is typical of areas where freshly-exposed rock and breccia is predominant.

Our results indicate that soil with a higher ratio crystalline to glassy material and exposed rock and/or breccia exists within the region of Censorinus crater. Radar (Zisk *et al.*, 1970) and thermal (Shorthill, 1970) studies also confirm the existence of exposed rock in the region. The sampling of a locale where freshly exposed material of greater than usual amounts of crystalline material predominates has not occurred to date (except possibly at Cone Crater) and could provide baseline data for interpretation of the aforementioned spectral curve series.

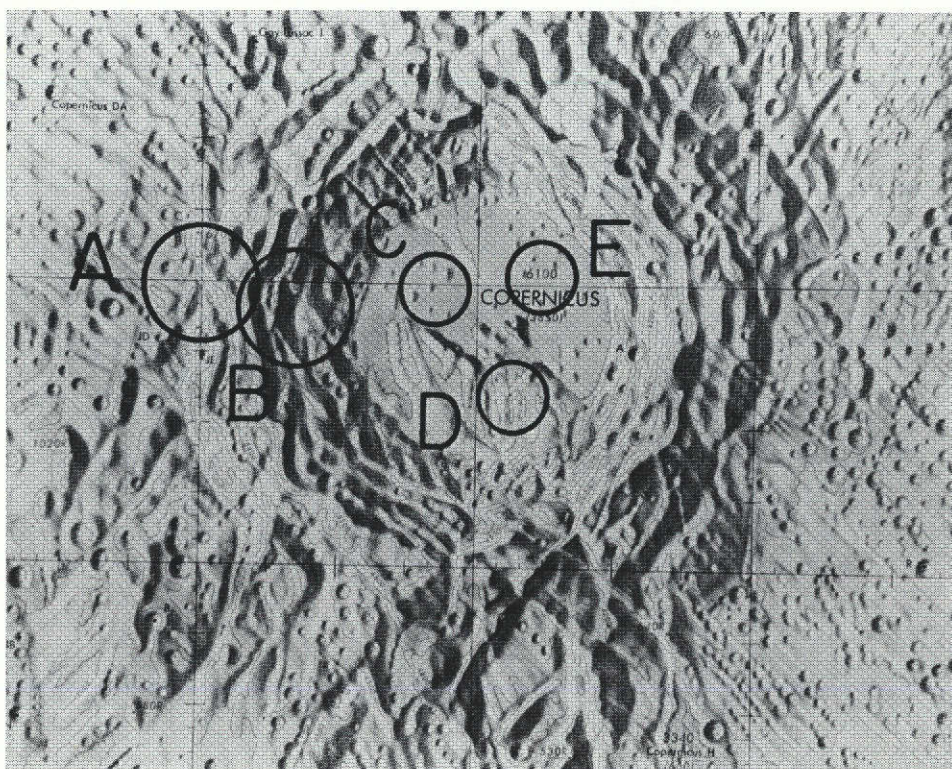


Fig. 5a. ACIC topographic map of the Copernicus area.

COPERNICUS

Spot	Lat.	Long.	Date	Runs	Phase	Unit	Curve type
A	10°00'N	22°00'W	1/9/71	2	-27°	Ccrh	Uplands
B	9°50'N	21°20'W	1/9/71	5	-27°	Cs	Uplands
C	10°00'N	20°20'W	1/9/71	6	-27°	Ccfs	Uplands
D	9°15'N	19°45'W	1/9/71	4	-27°	Ccfh	Uplands
E	10°05'N	19°35'W	1/9/71	5	-27°	Ccfh	Uplands

Copernicus A: High, local relief with discontinuous hills and valleys concentric to Copernicus; high crater density and shallow regolith.

Copernicus B: Terraced walls on slopes of Copernicus, with extensive hummock features subdued, deep regolith and talus.

Copernicus C: Level terrain with domes having boulder on summits; large amount of faulting, high crater density and shallow regolith.

Copernicus D: Irregular hills, low crater density and deep regolith.

Copernicus E: Irregular hills, with extensive faulting; domes with boulders on summits.

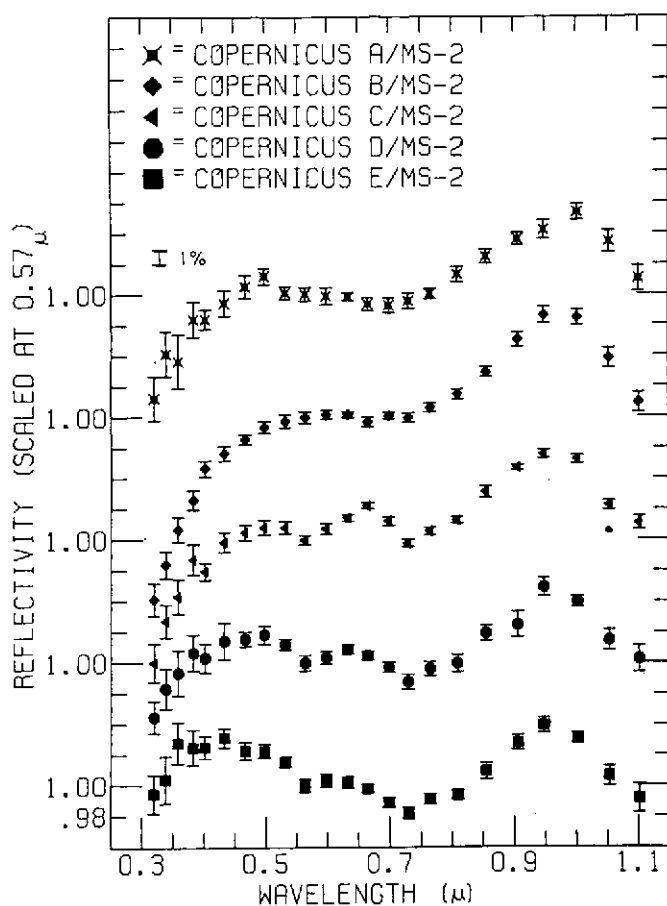


Fig. 5b. Normalized relative spectral reflectivity of Copernicus spots relative to Mare Serenitatis 2 standard.

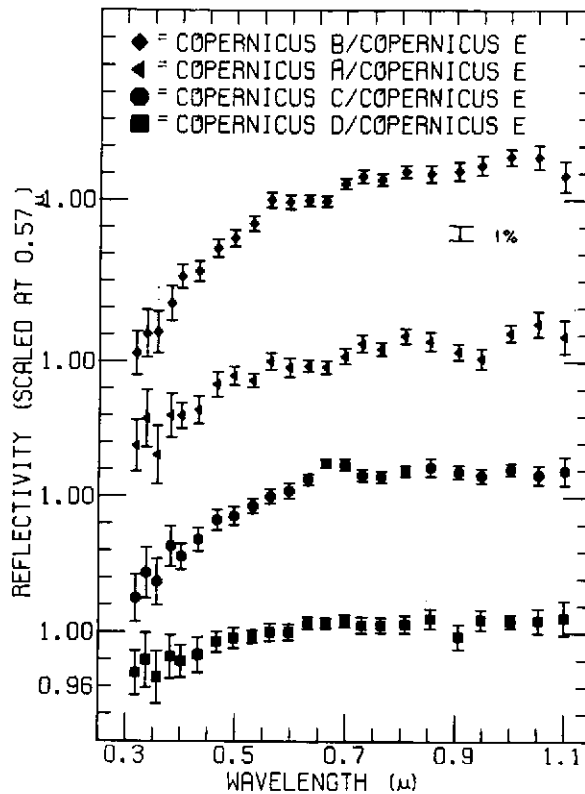


Fig. 5c. Normalized relative spectral reflectivity of Copernicus spots relative to Copernicus E.

Discussion

The bulk surface soil composition at COPERNICUS A and B are probably similar to that of the Apollo 14 landing site. The downturn in the ultraviolet at COPERNICUS B is perhaps a function of differing exposed material at the various levels on the Copernicus slopes. The composition of the soil at COPERNICUS C, D and E is probably similar to the Apollo 14 landing site material.

The Copernicus area has been shown to be an uplands region, and is quite similar to the Apollo 14 landing site in its spectral reflectivity. We believe that although Copernicus is situated in the mare, the event which formed the crater penetrated through the mare fill to the upland material (McCord *et al.*, 1972).

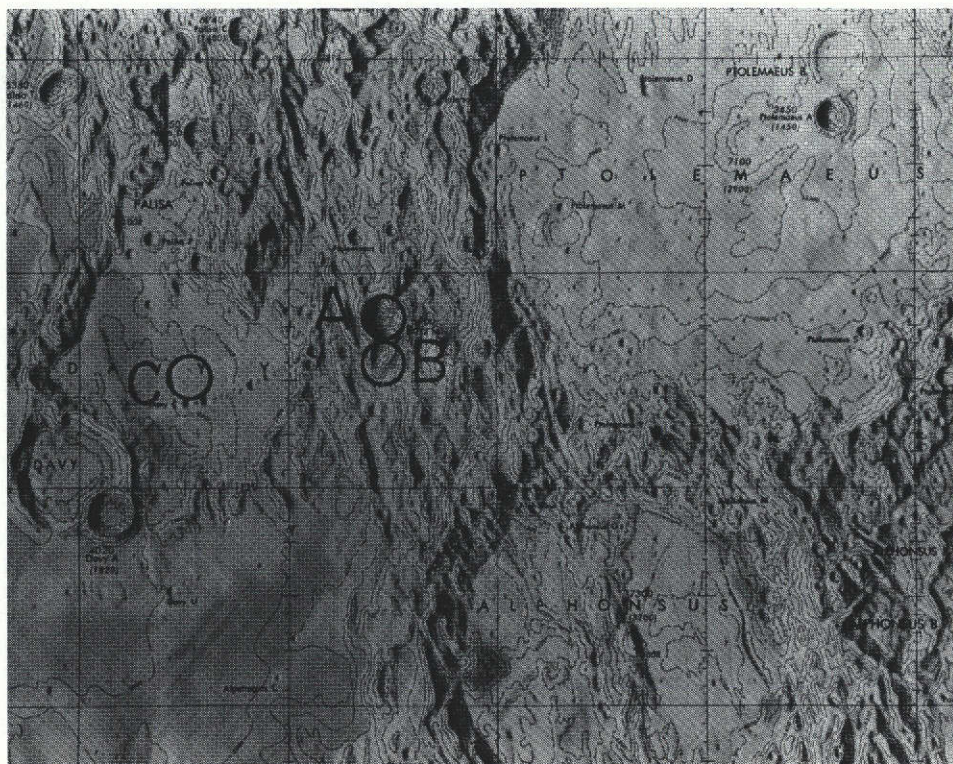


Fig. 6a. ACIC topographic map of the Davy Rille area.

DAVY RILLE

Spot	Lat.	Long.	Date	Runs	Phase	Unit	Curve type
A	10°25'S	5°05'W	1/11/71	4	-4°	CEch	Upland bright crater
B	10°50'S	5°05'W	1/11/71	4	-4°	CEch	Mare
C	13°00'S	6°55'W	1/11/71	4	-4°	Ica	Uplands bright crater?

Davy Rille A: Crater with high albedo, sharp rim, and very smooth, steep walls.

Davy Rille B: Region with both crater and uplands material; crater has sharp rim and steep walls.

Davy Rille C: Area of intermediate albedo and high crater density; numerous ghost craters and deep regolith.

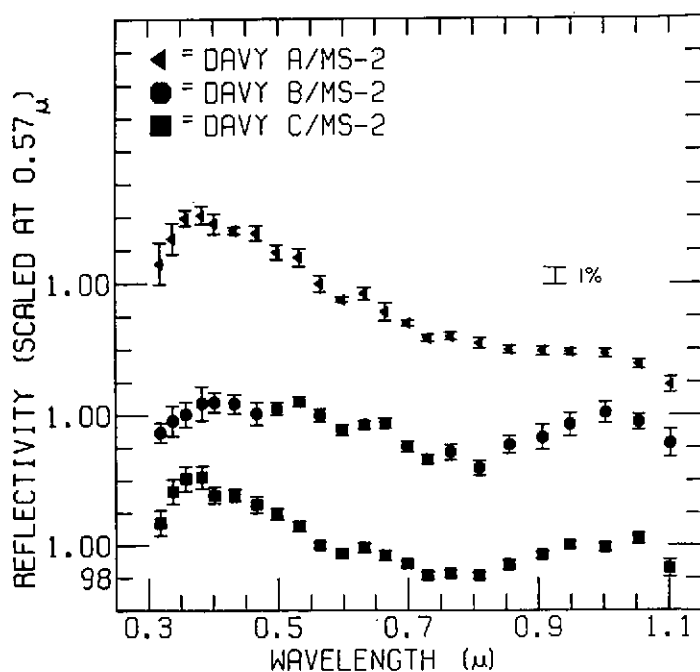


Fig. 6b. Normalized relative spectral reflectivity of Davy Rille spots relative to Mare Serenitatis 2 standard.

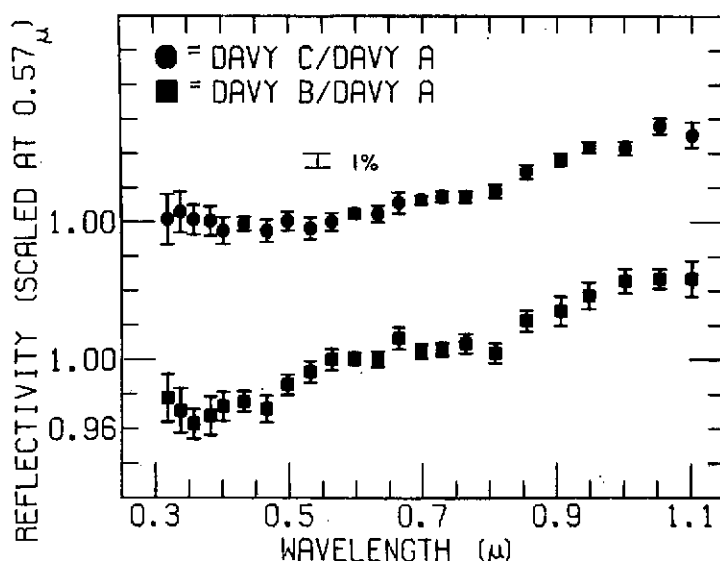


Fig. 6c. Normalized relative spectral reflectivity of Davy Rille spots relative to Davy Rille A.

Discussion

The DAVY RILLE A area probably contains some freshly exposed, high crystalline material. In the DAVY RILLE B region, the bulk soil composition is probably similar to that of a low-titanium uplands region. The DAVY RILLE C area probably contains uplands material in the form of Imbrium ejecta. It may also contain some freshly exposed, crystalline material which may be similar to that at DAVY RILLE A, or material which may have been ejected from the crater-chain. However, the spatial resolution of the data tends to make such an interpretation very tenuous at best.

The bulk surface soil composition in the observed areas is probably not substantially different from uplands material. However, sufficiently high spatial resolution data were not obtained to determine the characteristics of the crater chain itself. Therefore, the worth of detailed investigation of the crater chain cannot be determined from the study. These data do establish several areas where bright crater and uplands material interfaces probably exist. The interface between such areas would be extremely interesting to investigate.

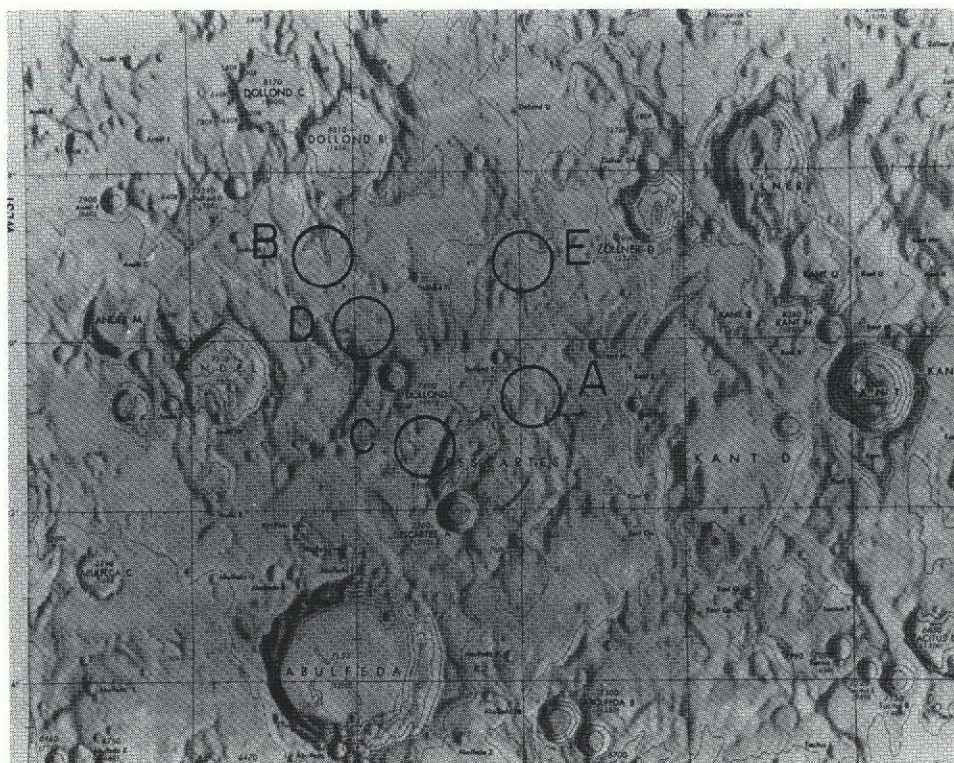


Fig. 7a. ACIC topographic map of the Descartes area.

DESCARTES

Spot	Lat.	Long.	Date	Runs	Phase	Unit	Curve type
A	10°40'S	15°05'E	10/17/70	3	+ 34°	CEhf	Upland bright crater
B	9°00'S	13°35'E	10/17/70	3	+ 34°	pII	Uplands
C	11°15'S	14°50'E	12/15/70	5	+ 33°	Ihf	Uplands
D	9°50'S	14°05'E	10/18/70	4	+ 46°	Ihf	Uplands
E	9°05'S	16°00'E	12/15/70	2	+ 33°	Ihf	Uplands

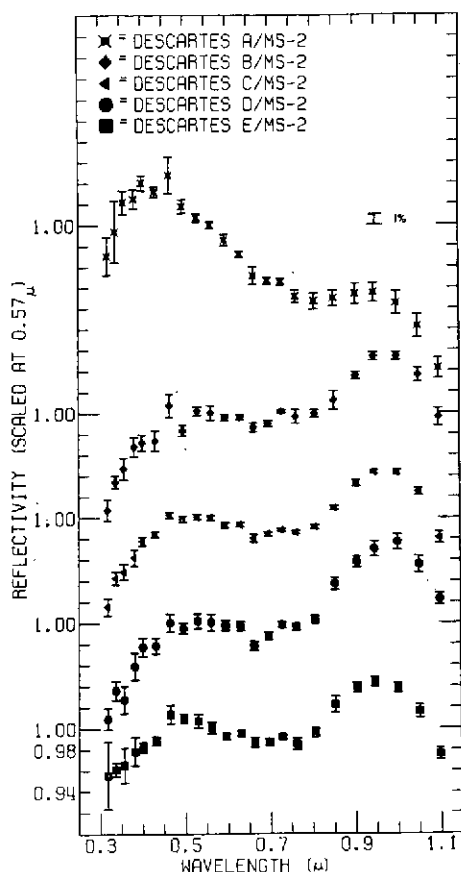
Descartes A: Hilly, furrowed region with an elevation which is higher than the surrounding terrain and a very high albedo.

Descartes B: An area of upraised material, with moderate albedo.

Descartes C: Hilly region, with subdued features and a moderate regolith.

Descartes D: An area of upraised material, with moderate albedo.

Descartes E: Hilly region, with subdued surface features and moderate regolith, crater density and albedo.



Discussion

It can be inferred from these data that DESCARTES B, C and E have bulk surface soil compositions which are similar to that at the Apollo 14 landing site. DESCARTES D may have less pyroxene and greater titanium content than the Apollo 14 landing site.

DESCARTES A is centered on the Kant Plateau, which has been described as volcanic in origin (Milton, 1968). The similarity of the DESCARTES A curve to that of TYCHO B and CENSORINUS C indicates that the surface material is highly crystalline, probably freshly exposed, and contains much less dark glass than the surrounding uplands material. Radar backscatter at 3.8 cm is greater in this area than surrounding regions (Zisk, 1970). Both results imply a (relatively) recent event, not obviously associated with any crater, exposed fresh material in this area.

Although most of the Descartes area is composed of upland material similar to the

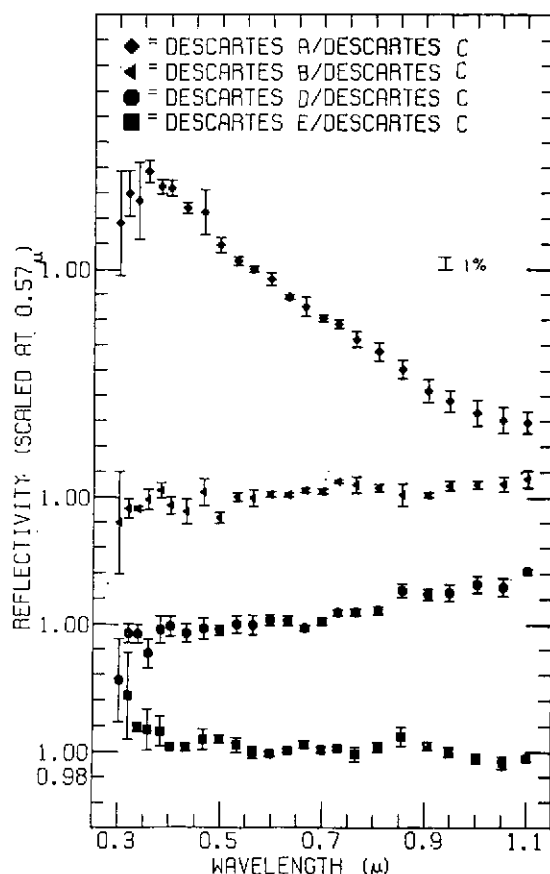


Fig. 7c. Normalized relative spectral reflectivity of Descartes spots relative to Descartes C.

Apollo 14 landing site, the Kant Plateau region is extraordinary in its exposure of fresh material. In view of the above data, it is important to sample the Kant Plateau region during a Descartes mission. We feel that such sampling will provide the best chance to study an area where processes other than cratering may have recently occurred. The contact between the Kant Plateau region and the surrounding uplands region, occupied by the so called Cayley Formation, could also yield important information on (1) the structural relations between these two regionally important upland units, (2) origin of the bright Descartes plateau material, (3) origin of the Cayley Formation and (4) the mixing of different lunar soils.

In our opinion, a mission to this region without strong emphasis on sampling Kant Plateau material would be unfortunate since the type of upland material which surrounds the Kant Plateau, i.e. the Cayley Formation and the more subdued appearing parts of the Descartes Formation, have probably been previously sampled.

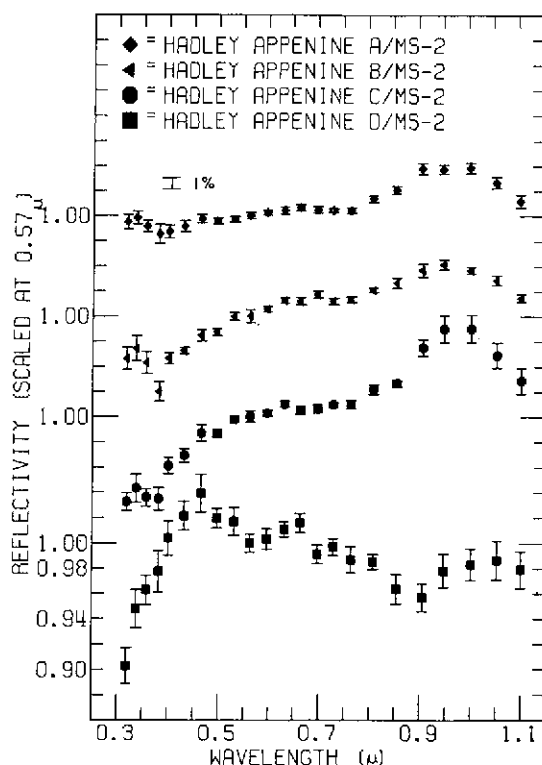


Fig. 8b. Normalized relative spectral reflectivity of Hadley-Apennines spots relative to Mare Serenitatis 2 standard.

Discussion

The HADLEY-APENNINE A area probably has a soil composition similar to the non-ray material (Adams and McCord, 1971a) found at the Apollo 12 landing site in the ratio of crystalline to glass in the soil. HADLEY-APENNINE B's soil composition is most likely similar to that found at HADLEY-APENNINE A except for a decrease in the titanium content. The HADLEY-APENNINE C region probably contains uplands material similar to that found at the Apollo 14 landing site. The HADLEY-APENNINE D area probably contains freshly exposed, higher-crystalline material. The exposure may have been the result of gravity-slumping on the slopes of the Apennine Front.

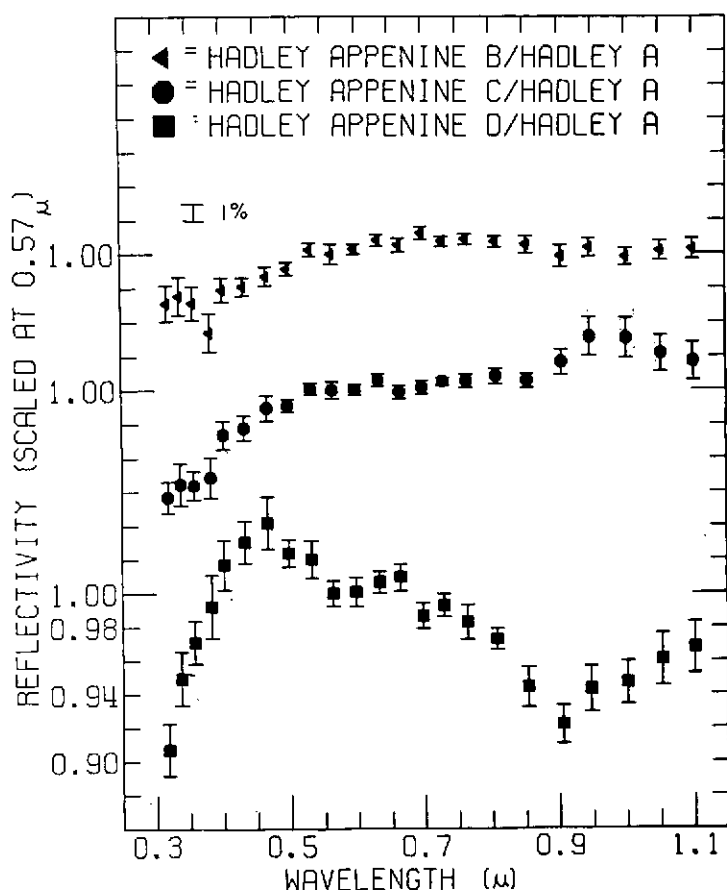


Fig. 8c. Normalized relative spectral reflectivity of Hadley-Apennines spots relative to Hadley-Apennines A.

The Hadley-Apennine region probably contains material which has been previously sampled during the mare and upland mission. However, it would be worthwhile to sample the area at the edge of Hadley Delta, since it could reveal important information regarding the interface between mare and uplands regions. Also, the similarity between the Hadley Delta and Apollo 14 landing site material, as seen in the telescopic spectra, could support the hypothesis of a common Imbrium event producing Fra Mauro Formation material.

The difference between the reflectivities of HADLEY-APPENINE C and D cannot be explained at present, and radar measurements offer no clue (Zisk *et al.*, 1971), since both features are strongly enhanced.

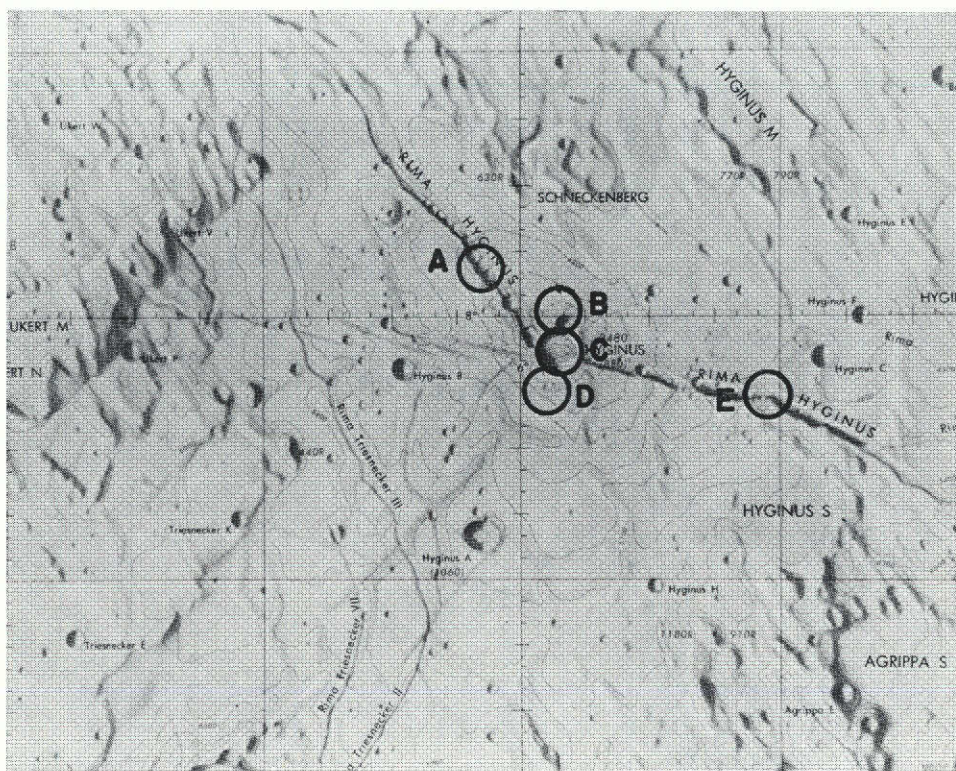


Fig. 9a. ACIC topographic map of the Hyginus Rille area.

HYGINUS RILLE

Spot	Lat.	Long.	Date	Runs	Phase	Unit	Curve type
A	8°20'N	5°40'E	1/10/71	4	-15°	CEch	Mare
B	8°05'N	5°15'E	1/10/71	5	-15°	Cld	Mare
C	7°45'N	6°15'E	1/10/71	5	-15°	CEch	Mare
D	7°25'N	6°10'E	1/10/71	4	-15°	Cld	Mare
E	7°25'N	7°55'E	1/10/71	4	-15°	CEch	Mare

Hyginus Rille A: Crater chain material, with extensive talus of high albedo on floor of craters; exposed, stratified layers on walls.

Hyginus Rille B: Flat, mare material with very low albedo, high crater density and subdued features.

Hyginus Rille C: Crater with low albedo, steep slopes and large talus blocks; high crater density and subdued features on floor.

Hyginus Rille D: Flat, mare material, similar to Hyginus Rille B.

Hyginus Rille E: Very high albedo crater chain material, similar to Hyginus Rille A.

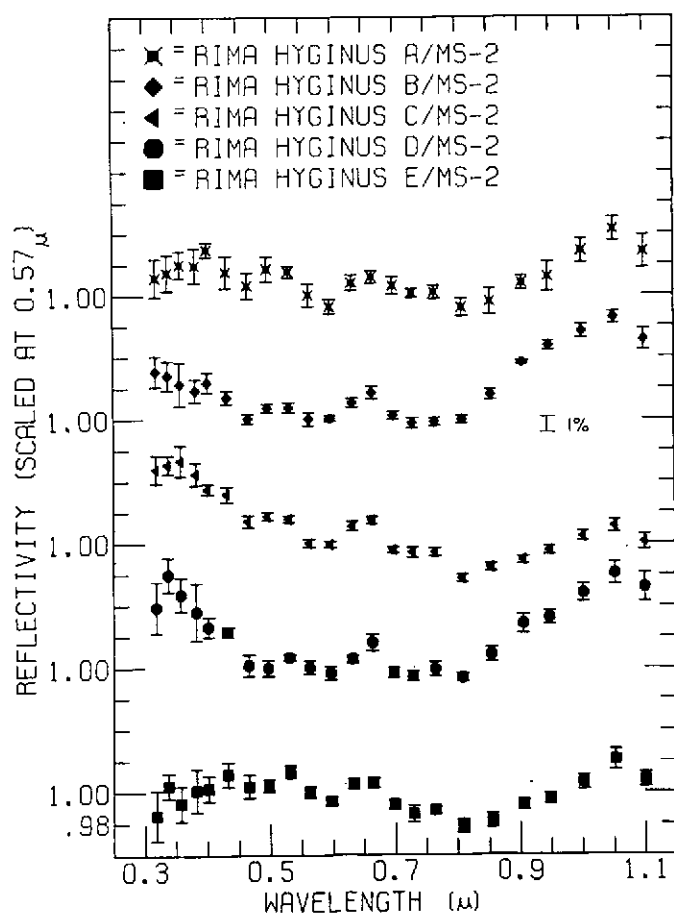


Fig. 9b. Normalized relative spectral reflectivity of Hyginus Rille spots relative to Mare Serenitatis 2 standard.

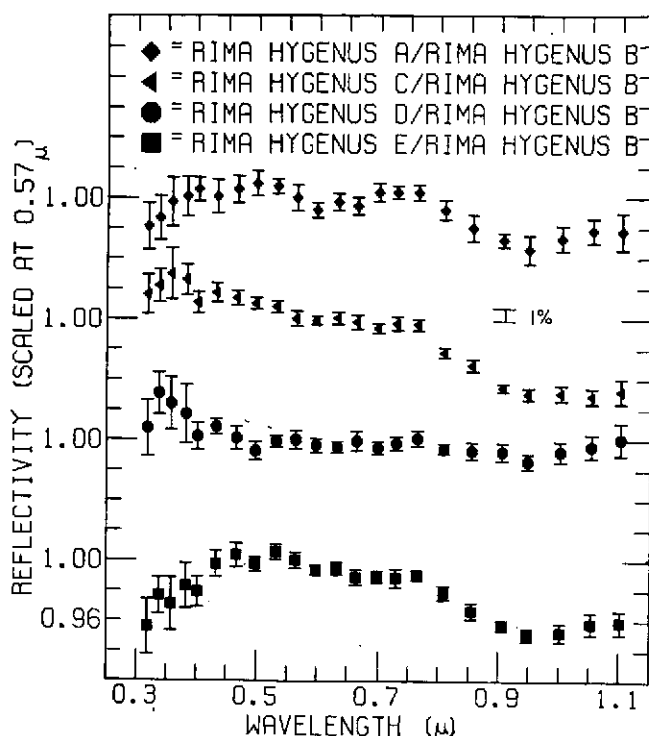


Fig. 9c. Normalized relative spectral reflectivity of Hyginus Rille spots relative to Hyginus Rille B.

Discussion

The HYGINUS A, C and E areas probably contain mare material that has been previously sampled during the Apollo 12 mission and perhaps will be sampled during the Apollo 15 mission. The HYGINUS RILLE B and D regions' surface soil composition probably is the same as HYGINUS A, C and E except for a marked increase in the dark glass content.

Although most of the material in the Hyginus Rille region probably has been previously sampled, the dark material at HYGINUS B and D are anomalous in their relatively high reflectivity in the ultraviolet and the near-infrared, and in their low depolarized radar backscatter values (Zisk *et al.*, 1970). This material is part of a dark mare series whose end member is LITTROW A, and whose origin may be relatively recent (see Littrow analysis).

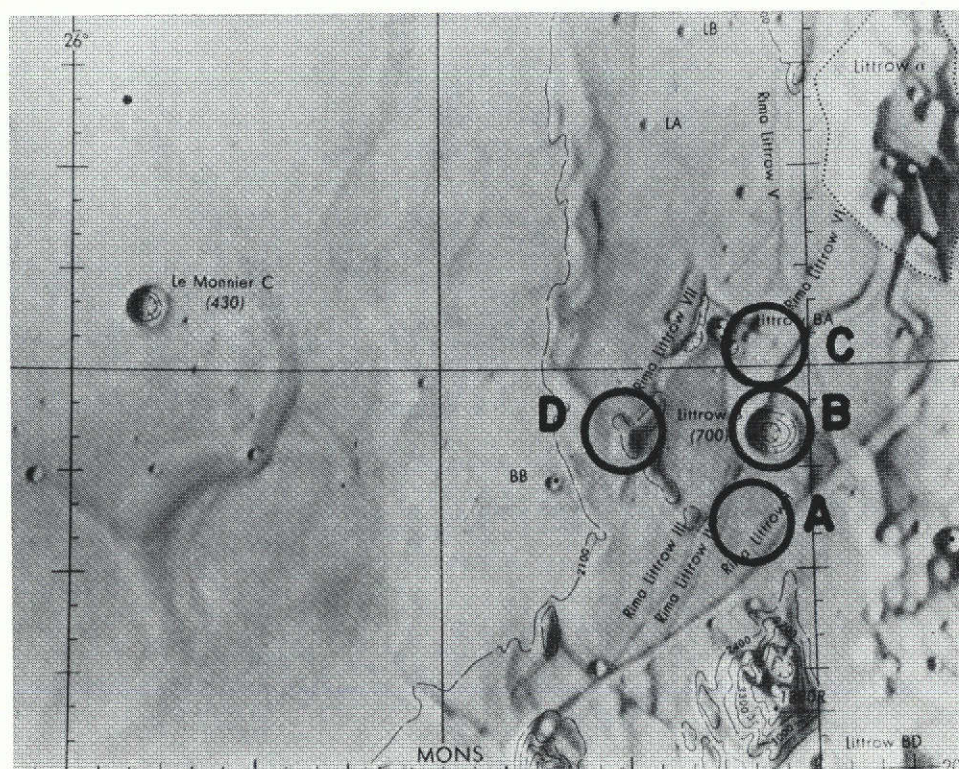


Fig. 10a. ACIC topographic map of the Littrow area.

LITTROW

Spot	Lat.	Long.	Date	Runs	Phase	Unit	Curve type
A	21°15'N	29°40'E	1/11/71	4	-3°	CId	Dark mare
B	21°40'N	29°45'E	1/11/71	3	-3°	Cc	Mare
C	22°05'N	29°45'E	1/11/71	3	-3°	Cc	Mare
D	21°40'N	29°00'E	1/11/71	3	-3°	Im	Mare

Littrow A: Level topography with very low albedo (0.05), subdued craters and thick regolith.

Littrow B: Sharp-rimmed crater with slumping of walls; surrounding terrain hummocky, with thick regolith and high albedo.

Littrow C: Sharp-rimmed crater with rocky floor; similar to Littrow B.

Littrow D: Relatively smooth topography and low ridges, with moderately low albedo and high crater density.

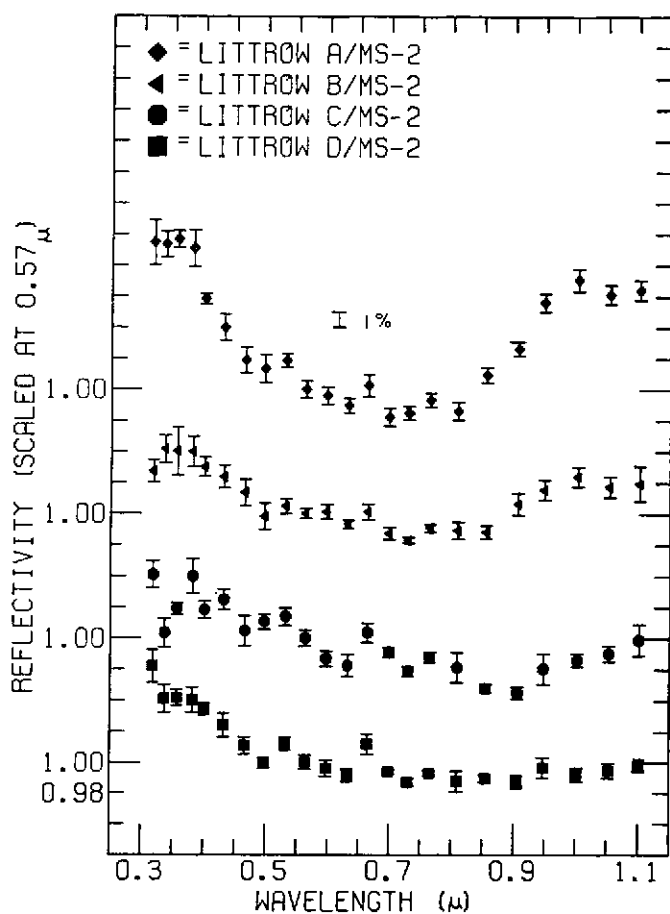


Fig. 10b. Normalized relative spectral reflectivity of Littrow spots relative to Mare Serenitatis 2 standard.

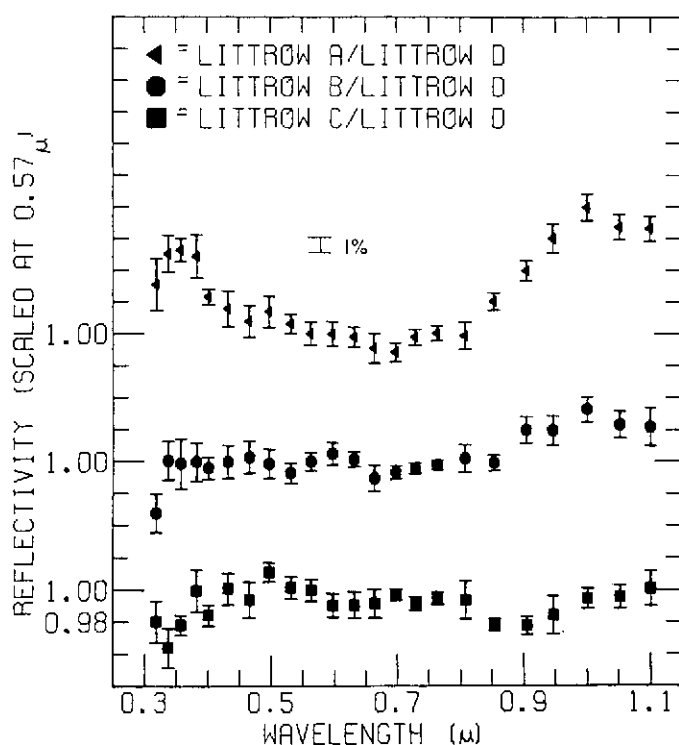


Fig. 10c. Normalized relative spectral reflectivity of Littrow spots relative to Littrow D.

Discussion

The LITROW A relative reflectivity curve is similar to the Apollo 11 curve in some ways. However, this region is quite anomalous to most of the Moon because of its low albedo, high ultraviolet and near-infrared reflectivity, and very low depolarized radar backscatter values (Zisk *et al.*, 1970). The non-crystalline nature of the surface soil is indicated by the shape of the 0.95 μ feature, which indicates a distinct scarcity of pyroxene in the soil. This effect could not have been produced by impact vitrification, since the anomaly is localized. Some form of local event, such as volcanism, could have produced such a rockfree surface.

The curves for LITROW B and C do not fit either the mare or upland crater series of relative reflectivity curves (McCord *et al.*, 1972). The surface soil at these areas is probably a mixture from nearby areas. LITROW D exhibits a typical mare curve which is similar to the Apollo 12 curve, although this area probably has more titanium in the soil.

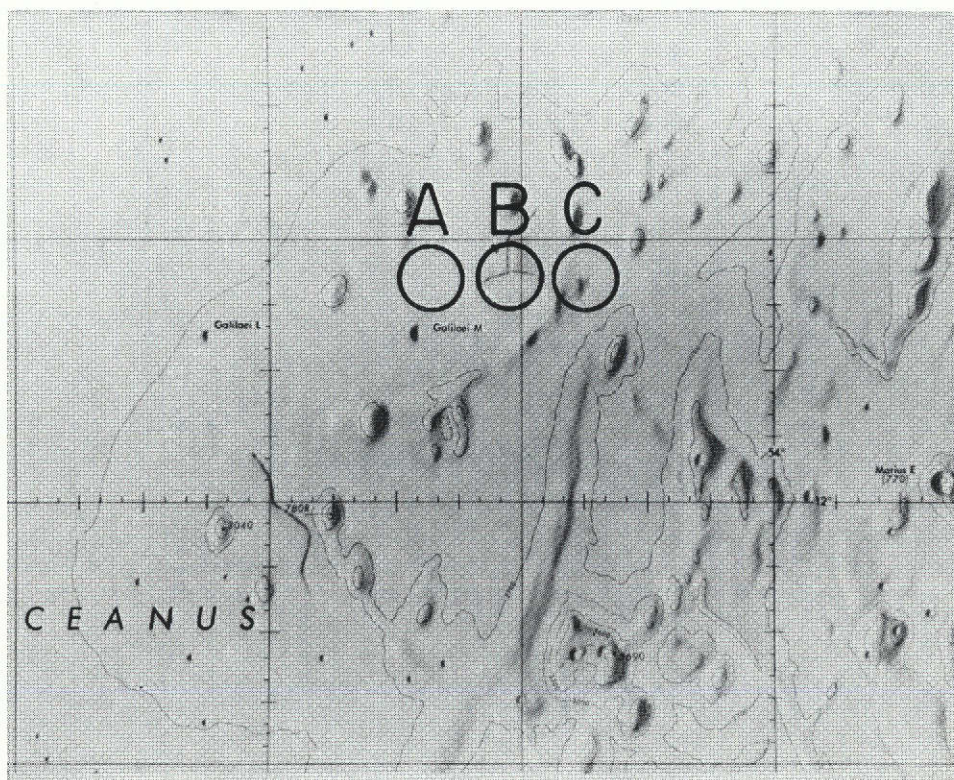


Fig. 11a. ACIC topographic map of the Marius Hills area.

MARIUS HILLS

Spot	Lat.	Long.	Date	Runs	Phase	Unit	Curve type
A	13°45'N	56°45'W	1/15/70	3	+44°	Emp	Mare
B	13°45'N	56°05'W	1/15/70	3	+44°	Emp	Mare
C	13°45'N	55°30'W	1/15/70	2	+44°	Emp	Mare

Marius Hills A: Smooth, undulating material with low domes and subdued features.

Marius Hills B: Region of wrinkle ridges and domes, with deep regolith.

Marius Hills C: Flat, mare material with a high crater density.

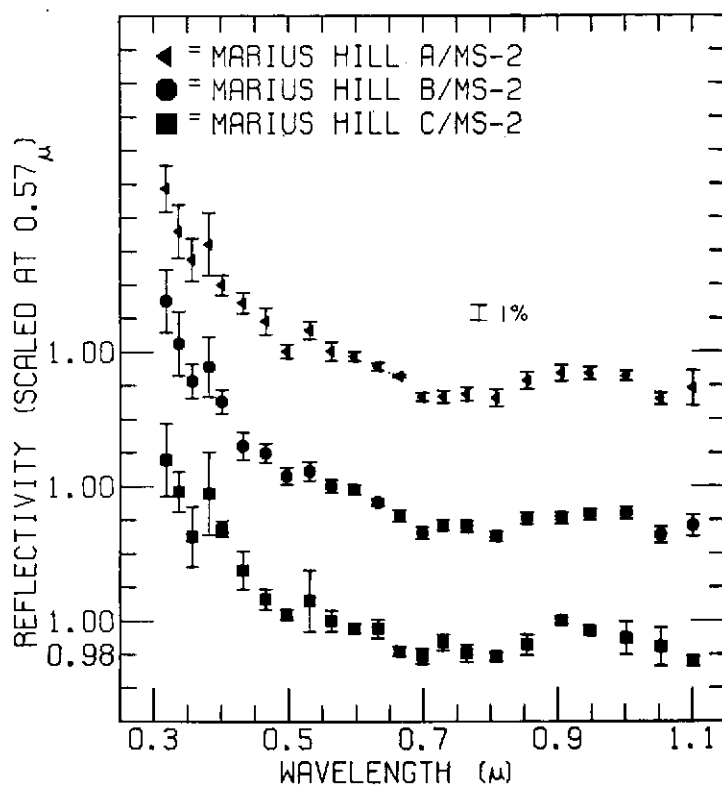


Fig. 11b. Normalized relative spectral reflectivity of Marius Hills spots relative to Mare Serenitatis 2 standard.

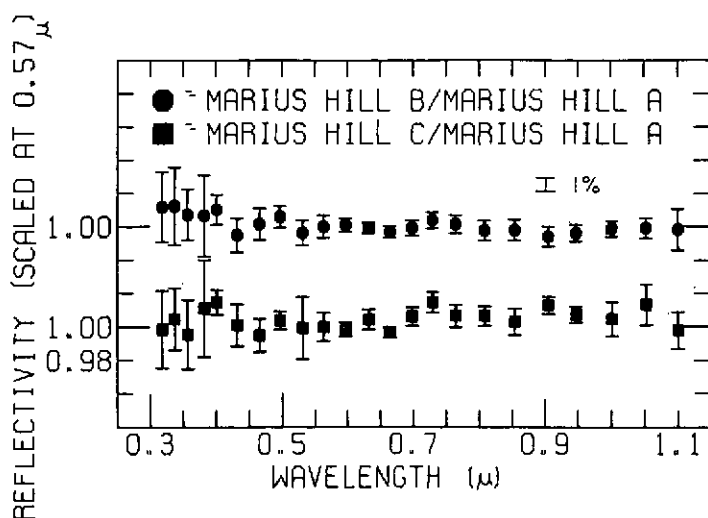


Fig. 11c. Normalized relative spectral reflectivity of Marius Hills spots relative to Marius Hills A.

Discussion

It can be inferred from these data that Marius Hills site is intermediate in bulk soil composition between the Luna 16 and Apollo 11 landing site. The composition is probably closer to the Apollo 11 site but with perhaps less titanium. These spectral reflectivities are also similar to other areas in Oceanus Procellarum (McCord, 1968).

As with Davy Rille, high spatial resolution measurements of suspected volcanic features were not performed, and the possibility of small, localized areas of very different material exists. On the basis of these spectral reflectivity measurements, it is recommended that the Marius Hills region be placed as low-priority for a manned mission, as it is similar to previously sampled material in bulk soil composition and the surrounding mare.

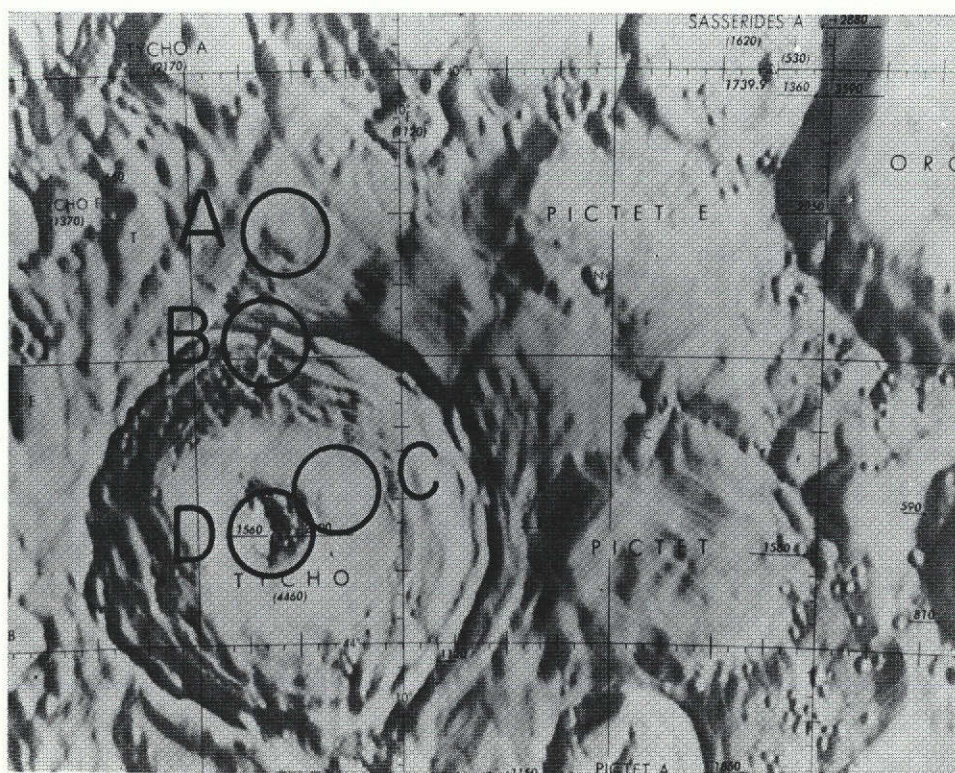


Fig. 12a. ACIC topographic map of the Tycho area.

TYCHO

Spot	Lat.	Long.	Date	Runs	Phase	Unit	Curve type
A	41°05'S	11°05'W	11/11/70	3	-26°	Cerr	Uplands
B	41°55'S	11°20'W	11/11/70	3	-26°	Ccw	Uplands bright crater
C	42°55'S	10°40'W	11/11/70	3	-26°	Ccfh	Uplands bright crater
D	43°15'S	11°20'W	11/11/70	2	-26°	Ccp	Uplands bright crater

Tycho A: Area of lower albedo than surrounding terrain, containing Surveyor 7 landing site; hummocky material radial to Tycho.

Tycho B: Region of rough, angular hummocks on a terraced wall, with high albedo; lineation radial to Tycho and many exposed boulders.

Tycho C: Area containing extremely rough, non-directional hummock and ridge system; numerous fissures and high albedo.

Tycho D: Region of angular peaks and ridges with fairly smooth, steep slopes and high albedo.

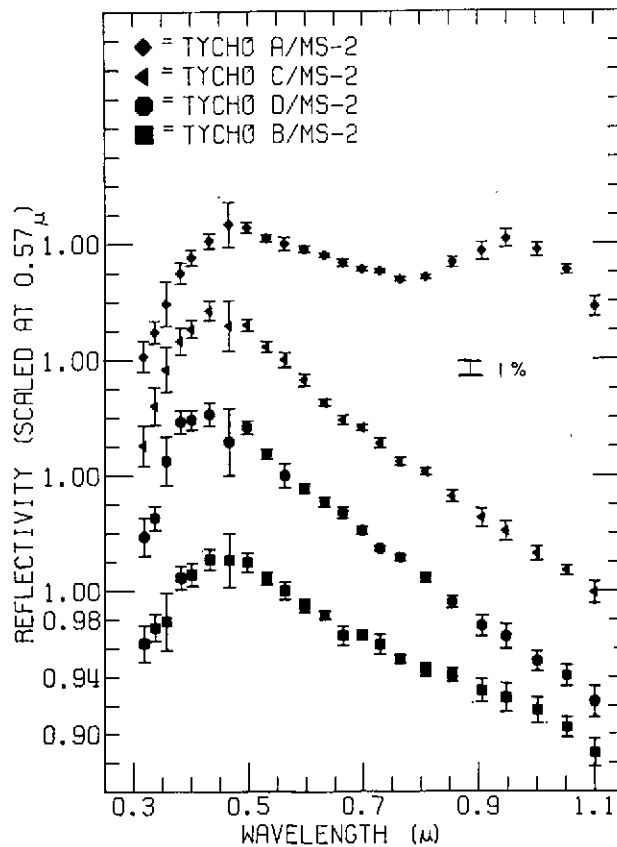


Fig. 12b. Normalized relative spectral reflectivity of Tycho spots relative to Mare Serentatis 2 standard.

Discussion

The Tycho region is extremely interesting since it contains a large amount of higher crystalline material over a vast surface area. This region should be sampled, inasmuch as an area where such high crystalline rocks predominate has yet to be visited. Such a manned mission would yield samples which could establish a baseline for this 'end member' of the bright crater series, and thus allow interpretation of bright crater spectra for other areas of the Moon.

The TYCHO A area, which contains material of the dark 'halo ring', is quite anomalous to the Tycho region. The processes that cause this area to appear as uplands material cannot be explained at this time.

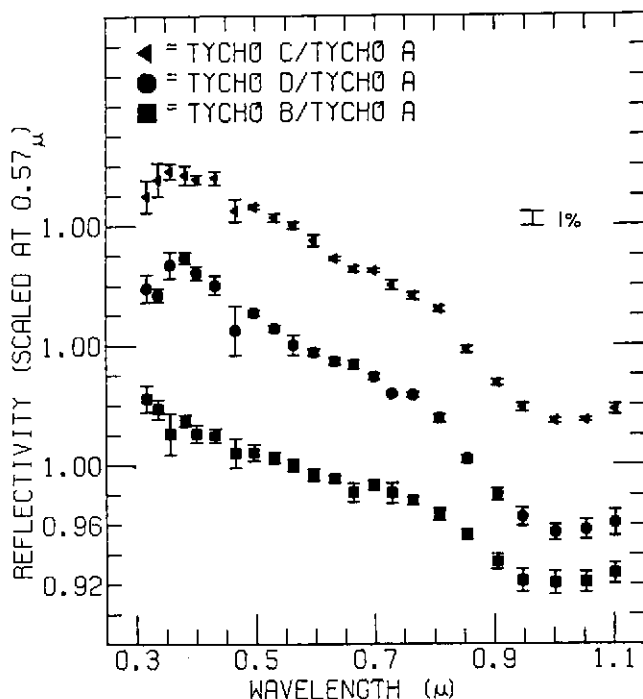


Fig. 12c. Normalized relative spectral reflectivity of Tycho spots relative to Tycho A.

It should be noted that a manned mission to the contact between the dark 'halo ring' and the bright, exposed material at the rim probably would have the potential for a maximum scientific return.

The TYCHO A area probably contains some form of uplands material which is similar to the Apollo 14 landing site soil. The TYCHO B area contains more crystalline, exposed material. The variation of the 0.95 μ band relative to TYCHO C and D is perhaps a function of different material in the exposed layers on the slopes of Tycho, although contamination by TYCHO A material within the observed area cannot be ruled out. Both TYCHO C and D have similar curves, thus indicating that the surfaces of the floor and central peaks have the same amount of crystalline material.

5. Spectral Reflectivity Measurements

A. INTRODUCTION

In the last section the relative spectral reflectivities of several areas near each of the proposed landing areas were discussed. These relative curves are derived by dividing the reflectivity of the area of interest by that of a standard area. Two standard areas were used for each region studied: (1) The area in Mare Serenitatis was used for all regions, and (2) an area within the region studied. The spectral reflectivity curve for the Mare Serenitatis standard area is given in Figure 2. The spectral reflectivity curves for the regional standard areas are given in this section.

B. OBSERVATIONS AND RESULTS

The spectral reflectivity curves scaled to unity at 0.56μ and one area from within each lunar region studies are given in Figure 13. As can be seen in Figures 2 and 14, the curve for almost all lunar areas are quite similar and one must resort to the

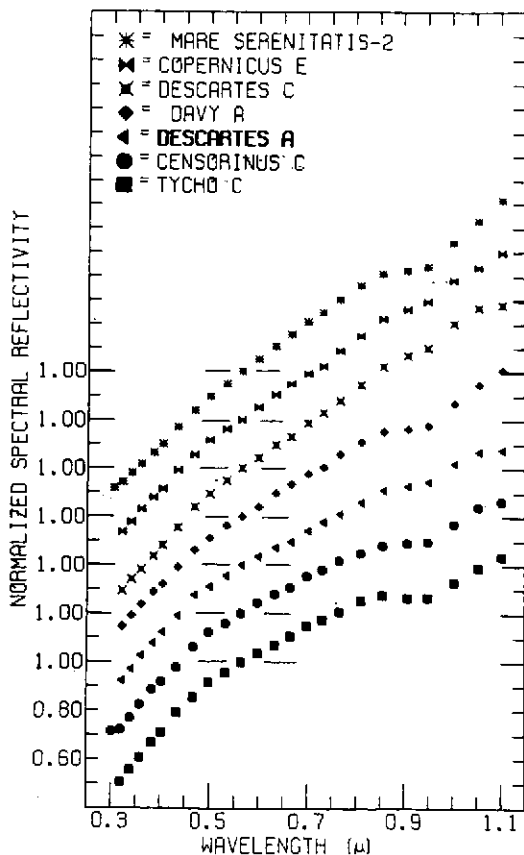


Fig. 13a.

relative curves to show the small but significant differences between the spectral properties of different lunar areas. All curves have a positive slope toward the red spectral region and show the absorption band near 0.95 μ .

C. INTERPRETATION

The overall curve slopes (the red color) for all areas is an expression of the colored glass content of the lunar soil (Adams and McCord, 1970, 1971a, b; Conel, 1970; Conel and Nash, 1970). The curve slopes less (less red color) and becomes less linear as the proportion of glass to crystalline material in the soil becomes smaller. The depth of the absorption band also follows this parameter to some extent (more glass, less band). From this and the curves in Figure 13 it is apparent that colored glass is a significant component of the soil everywhere we observed. Bright crater material is more crystalline than other regions.

The absorption band near 0.95 μ is an expression of the pyroxenes in the soil. The

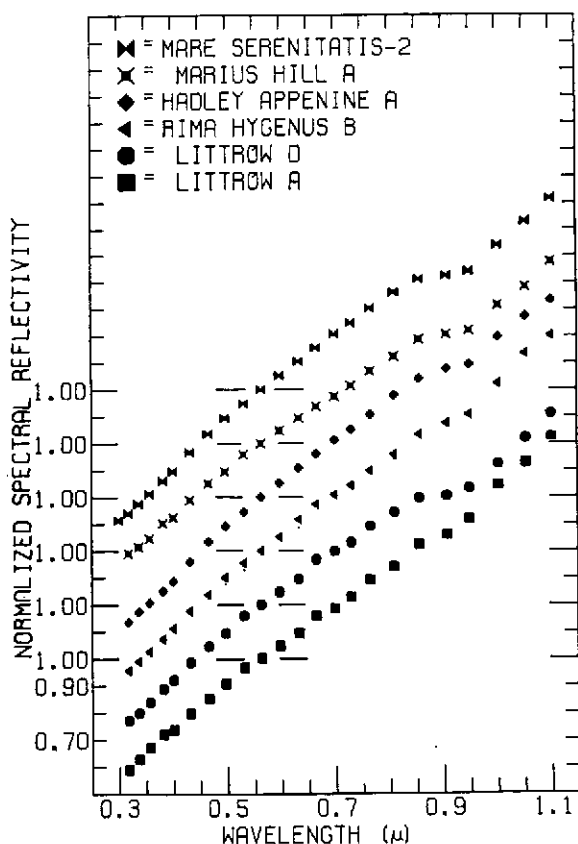


Fig. 13b.

Figs. 13a-b. Normalized spectral reflectivity of Mare Serenitatis 2 standard and proposed Apollo landing sites, scaled to unity at 0.56.

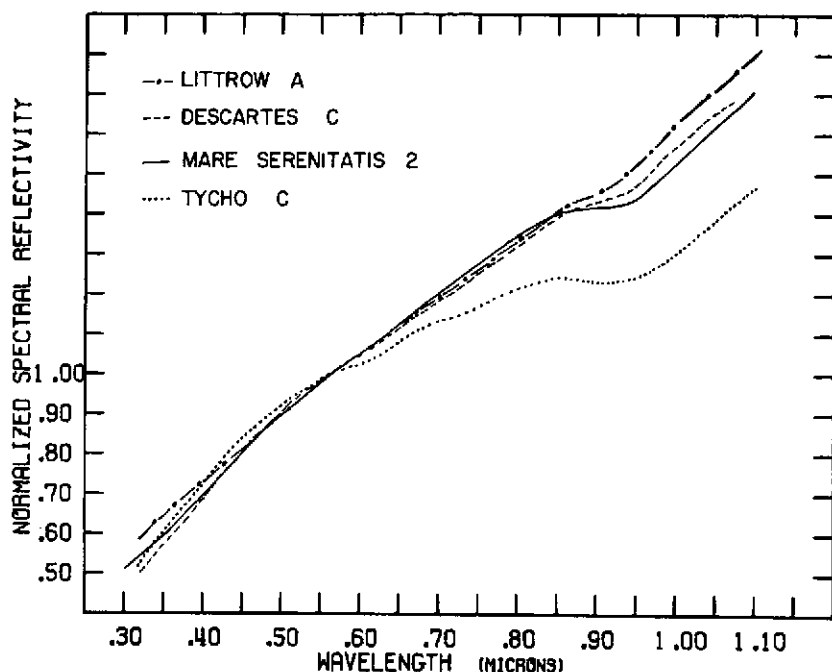


Fig. 14. Normalized spectral reflectivity of several proposed Apollo landing sites and Mare Serenitatis 2 standard scaled to unity at 0.56μ , showing differences in curve slopes.

band appears at about the same wavelength position with varying strengths in all curves. Pyroxenes must have a major influence on the lunar soil spectrum almost everywhere.

Acknowledgements

We wish to thank Dr John B. Adams of the College of the Virgin Islands and Dr Thomas R. McGetchin of M.I.T. for many useful discussions. Mr Laurence Bass of MIT assisted with data handling.

This research was carried out under NASA Grant NGR-22-009-496 and NGL 22-009-350.

References

- Adams, J. B.: 1968, *Science* **159**, 1453-1455.
- Adams, J. B. and Filice, A. L.: 1967, *J. Geophys. Res.* **72**, 5705-5715.
- Adams, J. B. and Jones, R. L.: 1970, *Science* **167**, 737-739.
- Adams, J. B. and McCord, T. B.: 1970, *Proceedings of the Apollo 11 Lunar Science Conference (Suppl. 1, Geochim. Cosmochim. Acta)* **3**, 1937-1945.
- Adams, J. B. and McCord, T. B.: 1971a, *Science* **171**, 567-571.
- Adams, J. B. and McCord, T. B.: 1971b, *Proceedings of the Apollo 12 Lunar Science Conference (Suppl. 2, Geochim. Cosmochim. Acta)* **3**, 2183-2195.
- Bancroft, G. M. and Burns, R. G.: 1967, *Am. Mineral.* **52**, 1278-1287.
- Birkebak, R. C., Cremers, C. J., and Dawson, J. P.: 1970, *Proceedings of the Apollo 11 Lunar Science Conference (Suppl., Geochim. Cosmochim. Acta)* **3**, 1993-2000.

- Burns, R. G.: 1965, 'Electronic Spectra of Silicate Materials: Application of Crystal-Field Theory to Aspects of Geochemistry', Ph.D. Dissertation, University of California, Berkeley.
- Burns, R. G.: 1970, *Mineralogical Applications of Crystal-Field Theory*, Cambridge University Press, Cambridge.
- Burns, R. G. and Fyfe, W. S.: 1967, in *Researches in Geochemistry* (ed. by P. H. Abelson), Vol. 2, 259-285.
- Conel, J. E.: 1970, Jet Propulsion Laboratory Space Programs Summary 3, 26-31; 37-62.
- Conel, J. E. and Nash, D. B.: 1970, *Proceedings of the Apollo 11 Lunar Science Conference (Suppl. 1, Geochim. Cosmochim. Acta)* 3, 2013-2023.
- Johnson, T. V. and Soderblom, L. A.: 1969, *J. Geophys. Res.* **74**, 6046-6048.
- McCord, T. B.: 1968a, 'Color Differences in the Lunar Surface', Ph.D. Dissertation, California Institute of Technology, Pasadena.
- McCord, T. B.: 1968b, *Appl. Opt.* **7**, 475.
- McCord, T. B.: 1969, *Astron. J.* **74**, 273-278.
- McCord, T. B. and Johnson, T. V.: 1969, *J. Geophys. Res.* **74**, 4395-4401.
- McCord, T. B. and Johnson, T. V.: 1970, *Science* **169**, 855-858.
- McCord, T. B., Charette, M. P., Johnson, T. V., Lebofsky, L. A., Pieters, C., and Adams, J. B.: 1972, *J. Geophys. Res.* **77**, 1349-1359.
- Milton, D. J.: 1968, in U.S.G.S. Geologic Atlas of the Moon, I-546.
- Shorthill, R. H.: 1970, 'Brief Description of Apollo Landing Sites in Terms of Earth-Based Infrared Observations', Boeing, Technical Note 016, April 1970.
- Soderblom, L. A.: 1970, 'The Distribution and Ages of Regional Lithologies in the Lunar Maria', Ph.D. Dissertation, California Institute of Technology.
- White, W. B. and Keester, K. L.: 1966, *Am. Mineral.* **51**, 774-491.
- White, W. B. and Keester, K. L.: 1967, *Am. Mineral.* **52**, 1508-1514.
- Zisk, S. H. et al.: 1970, 'Final Report/Radar Studies of the Moon', (NASA contract NAS 9-7830, M.I.T. Lincoln Laboratory, Lexington, 28 February 1970).
- Zisk, S. H., Carr, M. H., Masursky, H., Shorthill, R. W., and Thompson, T. W.: 1971, *Science* **173**, 808-811.

ATTACHMENT E

ELECTRONIC SPECTRA OF PYROXENES AND INTERPRETATION OF
TELESCOPIC SPECTRAL REFLECTIVITY CURVES OF THE MOON

John B. Adams*

Caribbean Research Institute, College of the Virgin Islands
St. Croix, Virgin Islands 00820

and

Thomas B. McCord

Planetary Astronomy Laboratory, Department of Earth and
Planetary Sciences, Massachusetts Institute of Technology,
Cambridge, Massachusetts 02139

25 February 1972

Submitted to: Proceedings Third
Lunar Science Conference

*Present address: West Indies Laboratory, Fairleigh Dickinson
University, St. Croix, Virgin Islands 00820

Abstract -- Data are presented that relate the wavelength positions of the major Fe^{2+} optical absorption bands in pyroxenes to overall pyroxene composition. The bands appear in reflectivity spectra of rock and soil samples from Apollos 11, 12, 14 and 15, and can be used to determine average pyroxene composition in the multiphase assemblages. Differences in average pyroxene content between rocks and soils at the four Apollo sites imply that the mare and highland soils have been cross-contaminated by one another. Spectral curves of lunar soil samples agree very closely with telescopic measurements of ⁸⁻_A 18 km-diameter areas which include the landing sites. The characteristic telescopic spectral curve types for (a) background mare, (b) mare bright craters, (c) background uplands, and (d) upland bright craters are reproduced in the laboratory with the mare and upland samples. Based on lunar sample data it is now possible to make semiquantitative estimates for the telescopically observable areas of the moon of (a) the crystal:glass ratio, (b) the Ti content of the glass in the soil, and (c) the average pyroxene composition.

INTRODUCTION

In previous papers on the optical properties of Apollo samples (ADAMS and JONES, 1970; ADAMS and McCORD, 1970, 1971a, 1971b) we pointed out that the principal absorption bands in visible and near-infrared reflectance spectra of lunar rocks and soils arise from the mineral pyroxene. The wavelength positions of the bands, furthermore, are related to the pyroxene composition. In this paper we present new data on the optical spectra of pyroxenes which relate band positions to composition. We then discuss the classification of lunar rocks and soils in terms of average pyroxene composition. Finally, the laboratory data are compared with spectra of the moon obtained using earth-based telescopes.

PYROXENE SPECTRA

The electronic spectra of pyroxenes have been studied by several workers during the last seven years. For recent reviews see BURNS et al., 1971 and LEWIS and WHITE, 1972. Polarized absorption measurements of single crystals have yielded spectra of high resolution, and at present there is reasonable agreement about the assignments of the major bands.

In pyroxenes the strongest absorptions arise from electronic transitions in Fe^{2+} . Only one spin-allowed transition is possible for the Fe^{2+} ion in octahedral coordination and this results in the band near $1\ \mu\text{m}$ that is common to several minerals. In the pyroxene structure, however, the oxygen polyhedra around the cations are strongly distorted from

octahedral symmetry so that additional energy levels are resolved and additional spin-allowed transitions arise. This splitting of the crystal field leads to two intense bands, one near 1 μm and another near 2 μm . These bands are polarization-dependent in terms of intensity and wavelength position. Figure 1 shows the spectra of a single grain of zoned augite-pigeonite from sample 12063. The measurements are through the courtesy of Dr. Peter Bell of the Geophysical Laboratory.

In diffuse reflected light the two main Fe^{2+} bands are easily resolved. Powdered samples (representing all possible crystallographic orientations) yield bands that are some average of the different absorptions seen in the single-crystal polarized spectra. The band positions in the reflectance spectra, however, still preserve evidence of the crystal structure and composition of the pyroxene. For example, as several authors have noted, the magnesian orthopyroxenes have intense bands near 0.9 μm and 1.8 μm whereas high-calcium pyroxenes exhibit bands near 1.0 μm and 2.3 μm . Figure 2 illustrates the reflectance curves for an enstatite and for the augite-pigeonite 12063 (also shown in Figure 1).

The relationship between the wavelength positions of the two main bands and the pyroxene composition is shown in Figure 3 (lower curve). The figure is a plot of the position of the short wavelength band (vertical axis) against the position of the longer wavelength band (horizontal axis). The points in Figure 3 (lower curve) are derived from diffuse reflectance spectra of essentially pure pyroxene phases, although some of

the pigeonites are zoned or intergrown with augite. Chemical analyses are completed for most of the pyroxenes shown. A more detailed discussion of these and other data is being prepared for separate publication. We are concerned here with the major compositional groupings.

Figure 3 (lower curve) shows a rather well-defined curving trend of points extending from the shorter to the longer wavelengths. All pyroxenes fall along the trend. The orthopyroxenes (open circles) occupy the short wavelength positions. In general, the orthopyroxene bands shift to longer wavelengths as the Fe:Mg ratio increases. The two orthopyroxene points near $0.935\ \mu\text{m}$ and $2.05\ \mu\text{m}$ have Fe:Mg $>80\%$. The filled circles are pigeonites and subcalcic augites. In general, the bands in this group shift to longer wavelengths with increasing calcium content of the pyroxene. The filled triangles represent the calcic augites and the members of the diopside-hedenbergite series. These pyroxenes cluster at the long wavelength end of the diagram.

Figure 3 (lower curve) is useful for determining the approximate composition of an unknown pyroxene from its diffuse reflection spectrum, providing that the two main bands are clearly developed. The figure cannot be used to identify unknowns when the two bands are absent or indistinct, as in some pyroxenes containing important amounts of trivalent ions (Al^{3+} , Ti^{3+} , Fe^{3+}). Mixtures of pyroxene and other minerals having bands within the given wavelength region fall off the trend line. For example the addition of olivine to a low-

calcium pyroxene has the effect of moving the pyroxene point vertically on the diagram. The addition of mafic glass (bands near $1.0\ \mu\text{m}$ and $1.9\ \mu\text{m}$) would move the point of the mixture above and/or to the left of the curve.

LUNAR SAMPLE SPECTRA

The lunar pyroxenes have two intense and clearly developed absorption bands (Figures 1 and 2) and lie on the trend in Figure 3. The low abundance of trivalent ions, especially of Fe^{3+} , allows the Fe^{2+} bands to be well resolved. Single-crystal polarized spectra of lunar pyroxenes have been measured by BURNS (1971, 1972) and BELL (1972). ADAMS and McCORD (1971b) discussed the diffuse reflection spectrum of a pyroxene separate from rock 12063. They showed, furthermore, that the main Fe^{2+} bands in the pyroxene account for the two strong bands in the spectrum of the whole rock. The presence of plagioclase, ilmenite, glass and minor amounts of other phases does not affect the wavelength positions of the pyroxene bands, which persist in the spectra of rocks, breccias and soils.

If the two strong pyroxene bands survive unaltered in wavelength in the spectra of lunar bulk rocks and soils, then the bulk materials should plot on the pyroxene compositional trend of Figure 3. This is indeed the case as is shown in the middle curve of Figure 3.

It is also evident from Figure 3 (middle curve) that the Apollo samples spread along the pyroxene compositional trend, implying that there are significant differences in average

pyroxene composition among the lunar materials. Apollo 14 samples (open squares) cluster toward the low-calcium end of the compositional trend. This is in good agreement with published analyses, which indicate a preponderance of pigeonite and orthopyroxene in the Apollo 14 materials (LSPET, 1971). The Apollo 11 and 12 mare samples, on the other hand, have more calcic pyroxenes ranging from pigeonite to subcalcic augite and augite. These materials (solid triangles) have longer wavelength bands in the reflectance spectra and plot separately from the Apollo 14 rocks and soils. The one exception is a sample of anorthosite that was separated from the Apollo 11 bulk soil. The anorthosite has a low-calcium pyroxene (WOOD et al. 1970) which accounts for the lone solid triangle at 0.92 μm and 1.95 μm .

Five samples of Apollo 15 soil are shown on Figure 3. In general, the Apollo 15 samples are intermediate between the Apollo 14 materials and those from the Apollo 11 and 12 mare sites. As end-members of the Apollo 15 sample suite (Apennine front and mare materials) are approached, the points in Figure 3 plot with the appropriate upland or mare group. The Apollo 15 point at 0.95 μm and 2.10 μm , for example, is a pyroxene-rich soil from the mare site 9a. Only partial results of our Apollo 15 measurements are presented here. A more detailed account will be published at a later date.

It is of interest to note that the Apollo 11 and 12 samples extend into an unoccupied part of the pyroxene compositional trend that lies between the pigeonites and the calcic-augites and diopsides. The gap apparently arises because the

two main pyroxene bands are not clearly developed in the common terrestrial augites that would otherwise be expected to occupy this part of the diagram. Augites typically contain Fe^{3+} and other trivalent ions (Ti^{3+} , Al^{3+}). Their reflectivity curves show strong absorption throughout the short wavelength end of the spectrum, the result mainly of Fe^{3+} - Fe^{2+} charge transfers. The spin-allowed Fe^{2+} bands are only weakly developed and are superposed on a steeply sloping continuum, making it difficult to assign band positions from the diffuse reflection spectra.

In contrast, the lunar augites contain little or no Fe^{3+} (Hafner *et al.* 1971). The strong absorption at short wavelengths is absent, and the spin-allowed Fe^{2+} bands are clearly developed. It appears, therefore, that pyroxenes with well developed bands near $0.97\ \mu\text{m}$ and $2.15\ \mu\text{m}$ are strongly reduced. Natural pyroxenes of this type may effectively be restricted to extraterrestrial sources.

SOILS

From the data in Figure 3 (middle curve) it is apparent that the band positions in spectra of soils from a given site do not necessarily match those for the associated rocks and breccias. It thus appears that the average pyroxene compositions of most soils differ slightly from the average pyroxene compositions of the bedrock from which the soils were at least in part derived.

The top curve in Figure 3 shows the Apollo sample points labeled according to (a) soils and (b) rocks and breccias. The Apollo 12 surface soils are at the short-wavelength end of

the group of points that represent the ^{mare} rocks and breccias. The exact position of the Apollo 11 soil is uncertain, however, owing to the indistinct band near 2 μ m. The average pyroxene of these mare soils appears to be less calcic than for the mare basalts. We interpret this to mean that the Apollo 12 soils (and possibly the Apollo 11 soils) contain a component of low-calcium pyroxene which moves the bands of the averaged pyroxene spectrum to shorter wavelengths. This foreign pyroxene component probably is accounted for by the presence of anorthositic and KREEP rock fragments, both of which contain low-calcium pyroxenes. (For reference, the bands for the anorthositic separate from the Apollo 11 soil are represented by the inverted triangular symbol on the same figure. KREEP materials are represented by several of the Apollo 14 breccia points.)

Several investigators have identified contaminant phases in the lunar soils. In the Apollo 11 soil (1-5 mm range) WOOD et al. 1970 found 5.9% crystalline anorthositic material which typically contains low-calcium clinopyroxene. Although pyroxene is only a minor mineral (<10%) in the anorthositic fragments, it contributes strong optical absorption bands (ADAMS and McCORD 1971b, NASH and CONEL 1972). Using analyses of glass in the Apollo 11 fines REID et al. (1972) also report the presence of 6% anorthositic material.

The most abundant contaminant in the Apollo 12 soil is KREEP (Meyer et al. 1971) which, including crystalline and glassy material, comprises approximately 30% to 50% of the soils and a larger proportion of some breccias. KREEP rock

is dominated by plagioclase and orthopyroxene. MARVIN et al. (1971) report that crystalline norite-anorthosite comprises from 8% to 19% of the 0.6-3 mm size fraction of the various Apollo 12 soils. REID et al. (1972) report 29% Fra Mauro basalt (=KREEP =norite) and 3% anorthositic material in the Apollo 12 fines, based on calculations from glass analyses. Using MARVIN et al.'s (1971) figure of 16% norite-anorthosite (crystalline) for soil 12070 and assuming that orthopyroxene makes up 50% of the rock we estimate that approximately 8% of the Apollo 12 soil shown on Figure 3 may consist of orthopyroxene.

The Apollo 14 soils shown in Figure 3, ^(top curve) as filled squares fall at the high-calcium end of the cluster of Apollo 14 breccias and rocks. The three filled squares that lie farthest to the right represent surface and near-surface bulk soils. The lower left solid square represents soil from the edge of Cone Crater (sample 14141). The Cone Crater soil shows a close affinity to the Apollo 14 breccias, from which it has been largely derived as evidenced by the abundance of breccia fragments (40-60 percent) even in the small-size fractions (62.5 μ m) (LSPET 1971).

On the basis of the inferred average pyroxene composition from Figure 3 the Apollo 14 bulk soils cannot have been derived entirely from the Apollo 14 breccias. It is suggested instead that the Apollo 14 soils are contaminated by a component of high-calcium pyroxene. The only known source at present for high-Ca pyroxene is the mare materials.

REID et al. (1972) estimate that there is approximately

11% mare-derived glass in the Apollo 14 soils. Chao et al. (1972) found titanium-rich ($\text{TiO}_2 = 7.8\%$) glasses, which they suggest are derived from a mare area. Glass (1972) also defines a category of mare-derived glasses in the Apollo 14 soils. The presence of mare-derived glasses implies that some amount of crystalline material (including high-calcium pyroxene) should be present also. STEELE and SMITH (1972) categorized igneous lithic fragments from the 1-2 mm fines. Their Type I high-alumina basalt (14310 type) has the highest-Ca pyroxenes (augite and pigeonite); however in Figure 3, 14310 plots just to the left of the Apollo 12 anorthosite, indicating that the optical properties of the pigeonite component are dominant in this rock. STEELE and SMITH also comment that there is little correspondence between the 1-2 mm lithic fragments and the glass composition types of REID et al. (1972). It thus appears that any high-Ca pyroxene contaminant must occur mainly in the <1 mm fraction of the soil. CARR and MEYER (1972) note that there is a maximum of 6% igneous (basalt) fragments (origin unspecified) in the <1 mm fines, whereas light and dark hornfels breccias are the dominant types of fragments. The task of finding mare contaminants is more difficult in the mature Fra Mauro soils, where the host rocks and the contaminants may have been homogenized through several generations of breccia formation. If our conclusions based on the pyroxene bands in Figure 3 are correct, there remain to be identified a few percent of mare pyroxene in the Apollo 14 soils.

Apollo 15 soil samples from the area of the LM and from the Apennine front have similar band positions. The points on Figure 3 lie between the Apollo 11 and 12 points and those for Apollo 14. The notable exception is the Apollo 15 soil sample from site 9a which is rich in calcic pyroxene (LSPET 1971b) and which expectably plots in the cluster of mare basalts. The main group of Apollo 15 soils has an average pyroxene composition intermediate between that of highland and mare materials. We conclude that the Apollo 15 surface soils are cross-contaminated, and that both the Apennine front (upland) materials and the mare soils have been partially blended over the area sampled.

APPLICATIONS OF PYROXENE SPECTRA

A principal objective of our investigation of the optical spectra of the pyroxenes is to strengthen interpretation of telescopic spectral reflectivity data. It is significant, for example, that the main bands in the spectra of lunar rocks fall along the pyroxene trend diagram (Figure 3). Remote spectra of rocky areas, such as fresh craters, therefore, should give information on the average pyroxene composition. Few telescopic data are available, however, in the $2\text{ }\mu\text{m}$ wavelength region owing to instrument-sensitivity limitations, although improved techniques are now being tested at the telescope. We presently rely on the wavelength position of the band near $1\text{ }\mu\text{m}$ for interpretation of the pyroxene composition. It is possible to measure the telescopic band near

1 μ (McCord et al. 1972) to within about 0.02 μ m, which would allow a distinction to be made, for example, between the Apollo 14 rocks (0.92 μ m) and the Apollo 11 and 12 rocks (0.96 μ m). As we have discussed already the absorption bands in the soils converge to similar values probably owing to contamination effects. The soils are not readily distinguished using the single band (see Figure 3); and because telescopes sense mainly soil material, similar band positions are seen for highland and mare areas.

On the other hand the convergence of band positions for the soils becomes an indicator for contamination; and since contamination is time-dependent, it should be possible to separate fresh from old craters in a given material by their pyroxene band positions. This can already be done on the basis of band depths and the overall shapes of the spectral curves, which are controlled by the crystal:glass ratio (ADAMS and McCORD 1971a, 1971b, 1972).

Cone Crater provides an example. The spectral reflectance curve of the Cone Crater soil (14141) shows deep (12%) pyroxene band structure which correlates with the very low (<10%) glass content of the soil. In contrast, the soil near the LM (14421, 14259) has 40-75% glass (LSPET, 1971b) and weak (6%) pyroxene bands. If an earth-based or satellite-borne telescope with adequate spatial resolution (better than 1 km) were available, it would be possible to identify Cone Crater as having a high crystal:glass ratio on the basis of the depth of the 0.91 μ m band alone. The second line of evidence would be the ratio of the Cone Crater curve to that of the surrounding soil. The

resulting "spectral type" (McCORD et al. 1972) also correlates with a high crystal:glass ratio (Figure 5). If we now add the evidence from the positions of the two pyroxene bands at $0.91 \mu\text{m}$ and $1.98 \mu\text{m}$ it would then be apparent that the Cone Crater material does not plot with the more mature soils on Figure 3, and therefore must be relatively uncontaminated.

There is additional and independent evidence that Cone Crater exposes fresh materials. BURNETT et al. (1972) report cosmic ray exposure ages of $24 \pm \frac{2}{1}$ m.y. for rocks from the flank of Cone Crater, and ages of 110 m.y. to 590 m.y. for typical rocks near the LM landing area. This is in close agreement with the results of CROZAZ et al. (1972), and is further supported by the work of DRAN et al. (1972).

COMPARISON OF TELESCOPIC AND LUNAR SAMPLE CURVES

In addition to the laboratory analysis of the spectral reflectivity of the lunar samples, we have been measuring the spectral reflectivity of many 10-to-18-km diameter areas of the moon from Earth using ground-based telescopes. In this way we hope to extrapolate from information gained at the Apollo sites to other unvisited areas of the front face of the moon.

The telescope measurements of the spectral reflectivity of 18-km diameter areas containing the Apollo 11 and Apollo 12 landing sites were compared to laboratory measurements of Apollo samples (ADAMS and McCORD 1970, 1971a, 1971b). Excellent agreement was found for the surface soil samples indicating that (1) the telescope measurements were accurate to a percent or so, (2) the telescope observations determine the soil properties but are little affected by rocks, (3) the surface soil

samples taken at Apollo sites are representative on a regional scale, and (4) the absorption bands in the telescope reflectivity curves are a measure of the pyroxene content of the soil. Since the $0.95\ \mu\text{m}$ absorption appears at nearly the same wavelength in all telescope curves measured so far (McCord et al. 1972), the soil must be of nearly uniform average pyroxene content over the entire front surface of the moon, a result in agreement with our hypothesis of the mixing of the lunar soil.

In Figure 4 telescope measurements of an 18-km and an 8-km diameter area, containing the Apollo 14 and Apollo 15 landing sites respectively, are compared to laboratory measurements of surface soil samples acquired at these sites. The agreement is excellent; the formal errors on the telescope measurements are about the size of the symbols (<1 percent). The conclusions from the earlier measurements of this type are confirmed.

The telescopic spectral reflectivity curves for all lunar areas are similar in their shape. However, small but very important differences exist among these curves (McCord et al. 1972). To better display these small differences we have developed what we call the relative spectral reflectivity. This quantity is calculated by dividing the spectral reflectivity curve for each area by that for a standard area; in our telescopic case, the standard area is a uniform area of Mare Serenitatis. These ratio curves show the differences between the spectral properties of two lunar areas much more clearly than do the spectral reflectivity curves themselves

(see McCORD et al. (1972) for detailed presentation).

We have measured and calculated relative spectral reflectivity curves for more than 150 lunar areas, always using the standard area in Mare Serenitatis as the denominator in these ratios. All the ^ucurves obtained can be arranged into four non-intersecting sets according to their shape. These four sets -- we call them spectral types -- are directly correlated with four morphological units: background maria, background uplands, mare bright craters, and upland bright craters (McCORD et al., 1972).

In an attempt to understand how these four distinct spectral curve types arise we have calculated relative spectral reflectivity curves for several of the lunar samples as measured in the laboratory. For these laboratory calculations the Apollo 12 soil sample curve was used as a standard by which all other sample curves were divided. This^e Apollo 12 soil sample has a spectral reflectivity very similar to that for the Mare Serenitatis standard area used for the telescope measurements.

Figure 5 shows the relative spectral reflectivity curve for the Apollo 11 soil (determined in the laboratory) along with the relative spectral reflectivity curve for the Apollo 11 site in Tranquillitatis. The similarity is clear; the Apollo 11 soil has a background-mare spectral type.

Figure 6 shows the relative spectral reflectivity curve for a powdered Apollo 12 basalt. Notice how well this spectral curve type matches those observed telescopically for fresh mare bright craters.

The soil from the Apollo 14 landing site yields a background uplands spectral curve type, as can be seen by comparing it with the telescopic background uplands spectral curve type shown in Figure 7.

And finally, the relative spectral curve type for upland bright craters is duplicated in the laboratory by soil from Cone Crater (Figure 8). Note that Aristarchus shows an upland bright crater curve even though it is located in a mare area. Apparently Aristarchus has punched through the mare fill, exposing relatively fresh upland-like material from below the mare (McCord et al., 1972).

We have demonstrated that the shapes of the relative spectral reflectivity curves measured using telescopes (observing relatively large lunar areas) can be duplicated using Apollo samples measured in the laboratory. In summary (1) the background mare spectral type corresponds to mature ^(glassy) mare soil, (2) the background upland spectral type corresponds to mature ^(glassy) upland soil, (3) the mare bright crater spectral type corresponds to powdered crystalline mare rock, and (4) the upland bright crater spectral type corresponds to immature ^(crystalline) soil formed in upland material.

From the comparison of telescope and laboratory measurements of lunar material several conclusions can be drawn:

(1) Telescope measurements are accurate.

(2) The lunar-spectral-type classification derived from telescope observations is strongly supported by laboratory measurements.

(3) The correlation of lunar spectral classifications with lithologic units is verified.

(4) The features in the relative spectral reflectivity curves, from which the lunar spectral type classification is made, can now be explained in terms of the specific mineralogy and composition of the lunar surface material.

(5) The uniformity of spectral properties to this high precision over the background mare and over the background upland regions is further support for the mixing hypothesis. However, the uplands and mare do have slightly different spectral characteristics, indicating that the mixing of the soils is not complete.

(6) With the explanations and confirmations of the telescope results we have obtained from the laboratory measurements of the samples, we can now proceed with meaningful geologic exploration of the front face of the moon down to about 1 km spatial resolution using groundbased telescopes. As before, we can map differences between units on the lunar surface. But it is now possible to interpret these differences in terms of the compositional and mineralogical properties of the surface material. It appears likely that we eventually can specify quantitatively several compositional and mineralogical properties of individual units on the lunar surface including (a) crystal to glass ratio, (b) amount of Ti in glass, and (c) the average pyroxene composition.

Acknowledgments -- We thank Dr. Peter Bell of the Geophysical Laboratory for providing us with an absorption spectrum of a pyroxene grain from our sample 12063. Mr. Michael Charette of M.I.T. assisted with laboratory measurements of terrestrial pyroxenes and lunar samples. *Dr. M. Mauterle (Orsay, France) kindly provided irradiation measurements of selected* This work was supported by NASA grants (NGR-22-009-350 and NGR 52-083-003).

REFERENCES

- ADAMS J.B. and JONES R.L. (1970) Spectral reflectivity of lunar samples. Science 167, 737-739.
- ADAMS J.B. and McCORD T.B. (1970) Remote sensing of lunar surface mineralogy: Implications from visible and near-infrared reflectivity of Apollo 11 samples. Proc. Apollo 11 Lunar Sci. Conf., Geochim. Cosmochim. Acta Suppl. 1, Vol. 3, pp. 1937-1945. Pergamon.
- ADAMS J.B. and McCORD T.B. (1971a) Alteration of lunar optical properties: Age and composition effects. Science 171, 567-571.
- ADAMS J.B. and McCORD T.B. (1971b) Optical properties of mineral separates, glass, and anorthositic fragments from Apollo mare samples. Proc. Second Lunar Sci. Conf., Geochim. Cosmochim. Acta Suppl. 2, Vol. 3, pp. 2183-2195. M.I.T. Press.
- ADAMS J.B. and McCORD T.B. (1972) Optical evidence for regional cross-contamination of highland and mare soils. Revised Abstr. Third Lunar Sci. Conf., pp. 1-3.
- BELL P.M. and MAO H.K. (1972) Initial findings of a study of chemical composition and crystal field spectra of selected grains from Apollo 14 and 15 rocks, glasses and fine fractions. Revised Abstr. Third Lunar Sci. Conf., pp. 55-57.

- BURNETT D.S., HUNEKE J.C., PODOSEK F.A., RUSS G.P., III, TURNER G., and WASSERBURG G.J. (1972) The irradiation history of lunar samples. Revised Abstr. Third Lunar Sci. Conf., pp. 105-107.
- BURNS R.G., HUGGINS F.E., and ABU-EID R. (1971) Polarized absorption spectra of single crystals of lunar pyroxenes and olivines. Conference on Lunar Geophysics, Lunar Sci. Inst.
- BURNS R.G., ABU-EID R., and HUGGINS F.E. (1972) Crystal field spectra of lunar silicates. Revised Abstr. of Third Lunar Sci. Conf. pp. 108-109.
- CHAO E.C.T., BOREMAN J.A., and MINKIN J.A. (1972) Apollo 14 glasses of impact origin. Revised Abstr. Third Lunar Sci. Conf., pp. 133-134.
- CARR M.H. and MEYER C.E. (1972) Petrologic and chemical characterization of soils from the Apollo 14 landing site. Revised Abstr. Third Lunar Sci. Conf., pp. 116-118.
- GLASS B.P. (1972) Apollo 14 glasses. Revised Abstr. Third Lunar Sci. Conf., pp. 312-314.
- HAFNER S.S., VIRGO D., and WARBURTON D. (1971) Cation distributions and cooling history of clinopyroxenes from Oceanus Procellarum. Proc. Second Lunar Sci. Conf., Geochim. Cosmochim. Acta Suppl. 2, Vol. 1, pp. 91-108. M.I.T. Press.
- LEWIS J.F. and WHITE W.B. (1972) Electronic spectra of iron in pyroxenes. Jour. Geophys. Res. in press.
- LSPET (Lunar Sample Preliminary Examination Team) (1971a) Preliminary examination of the lunar samples from Apollo 14, Science 173, 681-693.

LSPET (Lunar Sample Preliminary Examination Team) (1971b)
The Apollo 15 Lunar Samples: A Preliminary Description
~~Preliminary examination of the lunar samples from Apollo 15,~~
Science 175, 363-375.

MARVIN U.B., WOOD J.A., TAYLOR G.J., REID J.B., JR., POWELL B.N.,
 DICKEY J.S., JR., and BOWER J.F. (1971) Relative proportions
 and probable sources of rock fragments in the Apollo 12 soil
 samples. Proc. Second Lunar Sci. Conf., Geochim. Cosmochim.
Acta Suppl. 2, Vol. 1, pp. 679-699. M.I.T. Press.

MCCORD T.B., CHARETTE M., JOHNSON T.V., LEBOWSKY L., ~~and~~
and Adams J.B.
 PIETERS C. (1972) Lunar spectral types. Jour. Geophys. Res.
 in press.

MEYER C., JR., BRETT R., HUBBARD N.J., MORRISON D.A., MCKAY D.S.,
 AITKEN F.K., TAKEDA H., and SCHONFELD E. (1971) Mineralogy,
 chemistry, and origin of the KREEP component in soil samples
 from the Ocean of Storms. Proc. Second Lunar Sci. Conf.,
Geochim. Cosmochim. Acta Suppl. 2, Vol. 1, pp. 393-411.
 M.I.T. Press.

NASH D.B. and CONEL J.A. (1972) Further studies of the optical
 properties of lunar samples, synthetic glass and mineral
 mixtures. Revised Abstr. Third Lunar Sci. Conf., pp. 576-577.

REID A.M., RIDLEY W.I., WARNER J., HARMON R.S., BRETT R., JAKES
 P., and BROWN R.W. (1972) Chemistry of highland and mare
 basalts as inferred from glasses in the lunar soil. Revised
Abstr. Third Lunar Sci. Conf., pp. 640-642.

STEELE I.M. and SMITH J.V. (1972) Mineralogy, petrology, bulk
 electron-microprobe analyses from Apollo 14, 15 and Luna 16.
Revised Abstr. Third Lunar Sci. Conf., pp. 721-723.

WOOD J.A., DICKEY J.S., MARVIN U.B., and POWELL B.N. (1970)

Lunar anorthosites and a geophysical model of the moon.

Proc. Apollo 11 Lunar Sci. Conf., Geochim. Cosmochim. Acta

Suppl. 1, Vol. 1, pp. 965-988. Pergamon.

CROZAZ, G., DROZD, R., HOHENBERG, C. M., HOYT, H.P. Jr., RAGAN, D.,
WALKER, R.M., AND YUHAS, D. (1972) Solar flare and galactic cosmic
ray studies of Apollo 14 samples. Revised Abstr. Third Lunar
Sci. Conf., pp. 167 - 169.

DRAN J.C., DURAUD J.P., MAURETTE M., DURRIEU L., JOURET C. and
LEGRESSUS C. (1972) Track metamorphism in extraterrestrial breccias.
Proc. Third Lunar Sci. Conf., Geochim. Cosmochim. Acta.
Suppl. 3, Vol. 3.

CAPTIONS

- Figure 1. Polarized absorption spectrum of a single crystal of clinopyroxene from rock 12063,79. Bulk of crystal is pigeonite ($\text{Wo}_{20} \text{En}_{38} \text{Fs}_{42}$) but rim is augite ($\text{Wo}_{40} \text{En}_{31} \text{Fs}_{29}$). Optical and microprobe analyses by Dr. Peter Bell, Geophysical Laboratory.
- Figure 2. Diffuse reflection spectra of pyroxene powders illustrating change in band positions with composition. Pyroxene 12063,79 is the same one shown in Figure 1.
- Figure 3. Diagrams of absorption band positions in reflectance spectra for terrestrial pyroxenes and lunar samples. Pyroxene absorption band near $1 \mu\text{m}$ is shown on the vertical axis. Band near $2 \mu\text{m}$ is on the horizontal axis. Lower curve shows pure pyroxenes of different compositions. Middle curve has lunar samples superposed on pyroxene points. Upper curve compares lunar soil bands with bands in spectra of rocks and breccias.
- Figure 4. Comparison of laboratory curves of lunar soils from Apollo 14 and 15 with telescopic curves of 18-km and 8-km diameter areas at respective landing sites.
- Figures 5-8. Comparison of laboratory relative reflectivity curves (using Apollo 12 soil as standard) with telescopic relative curves. The main spectral types on the moon are represented.

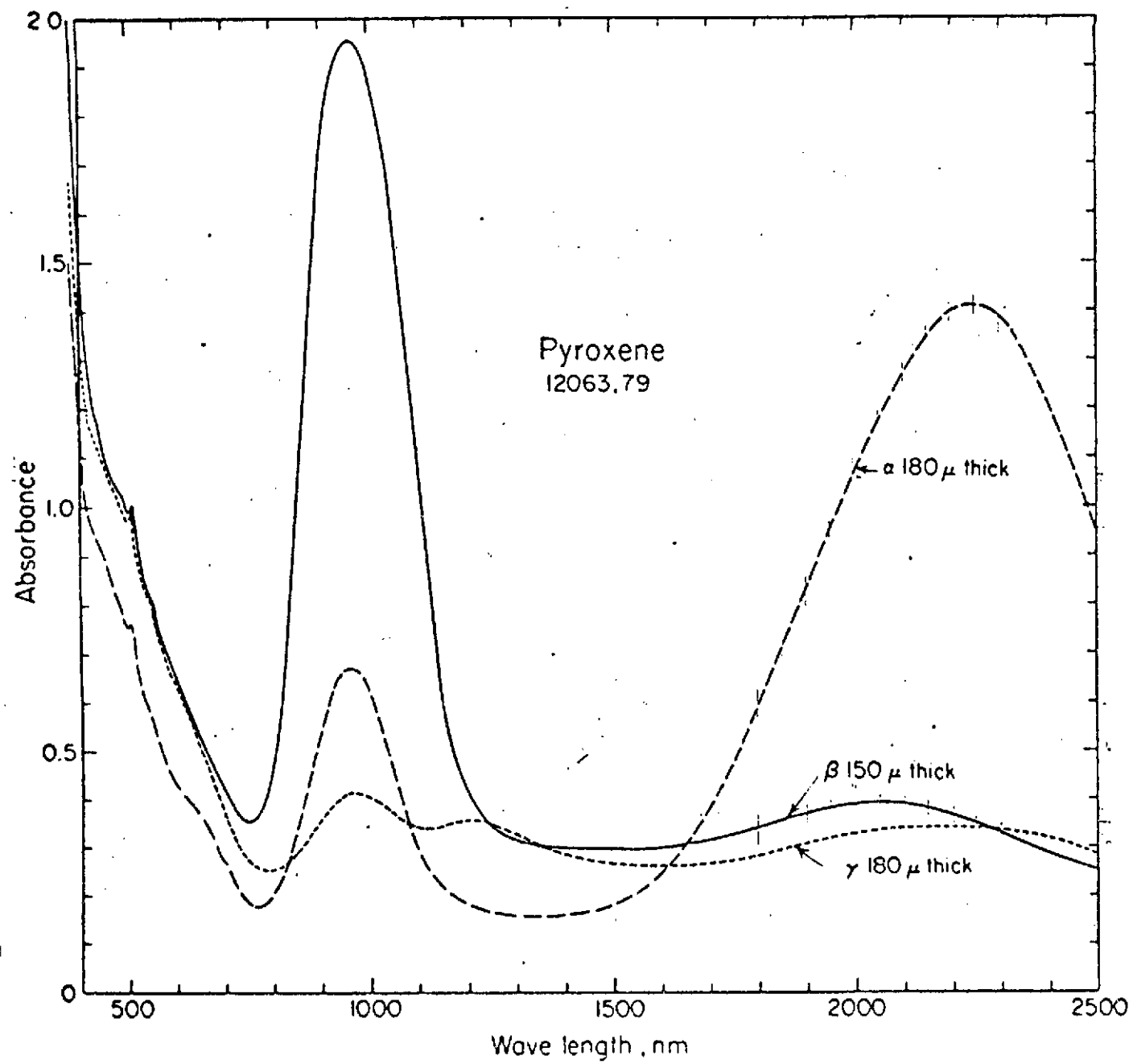
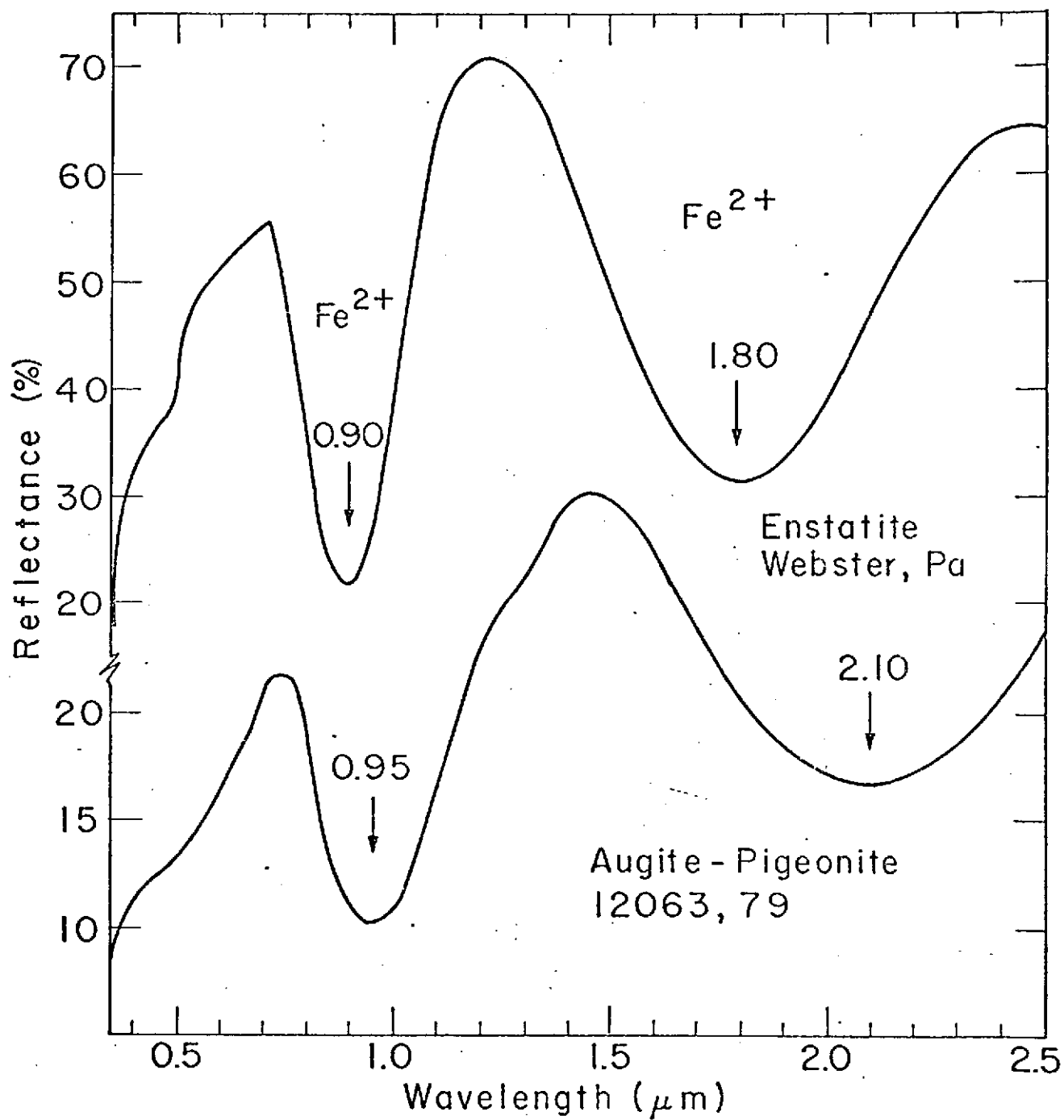
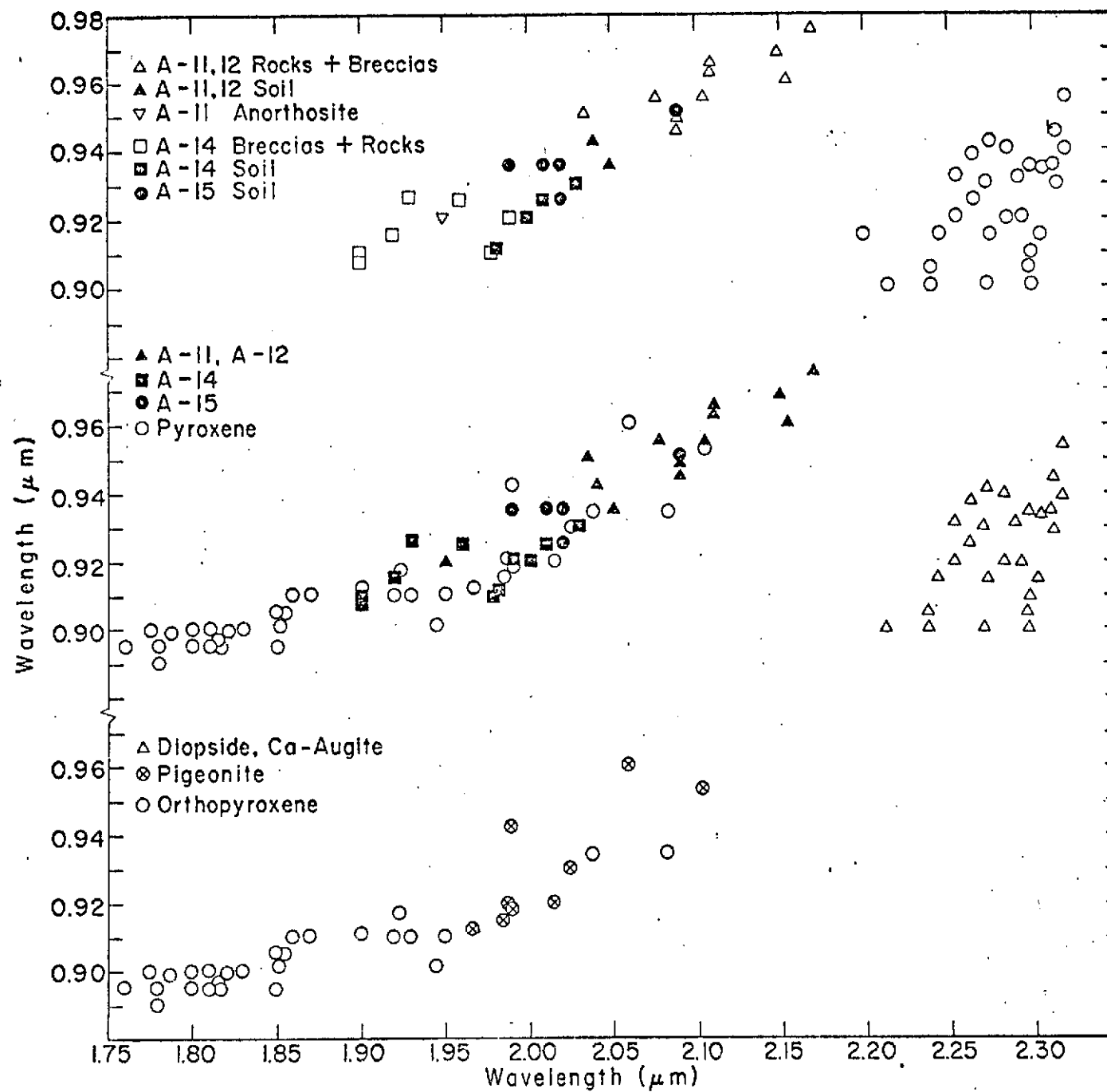
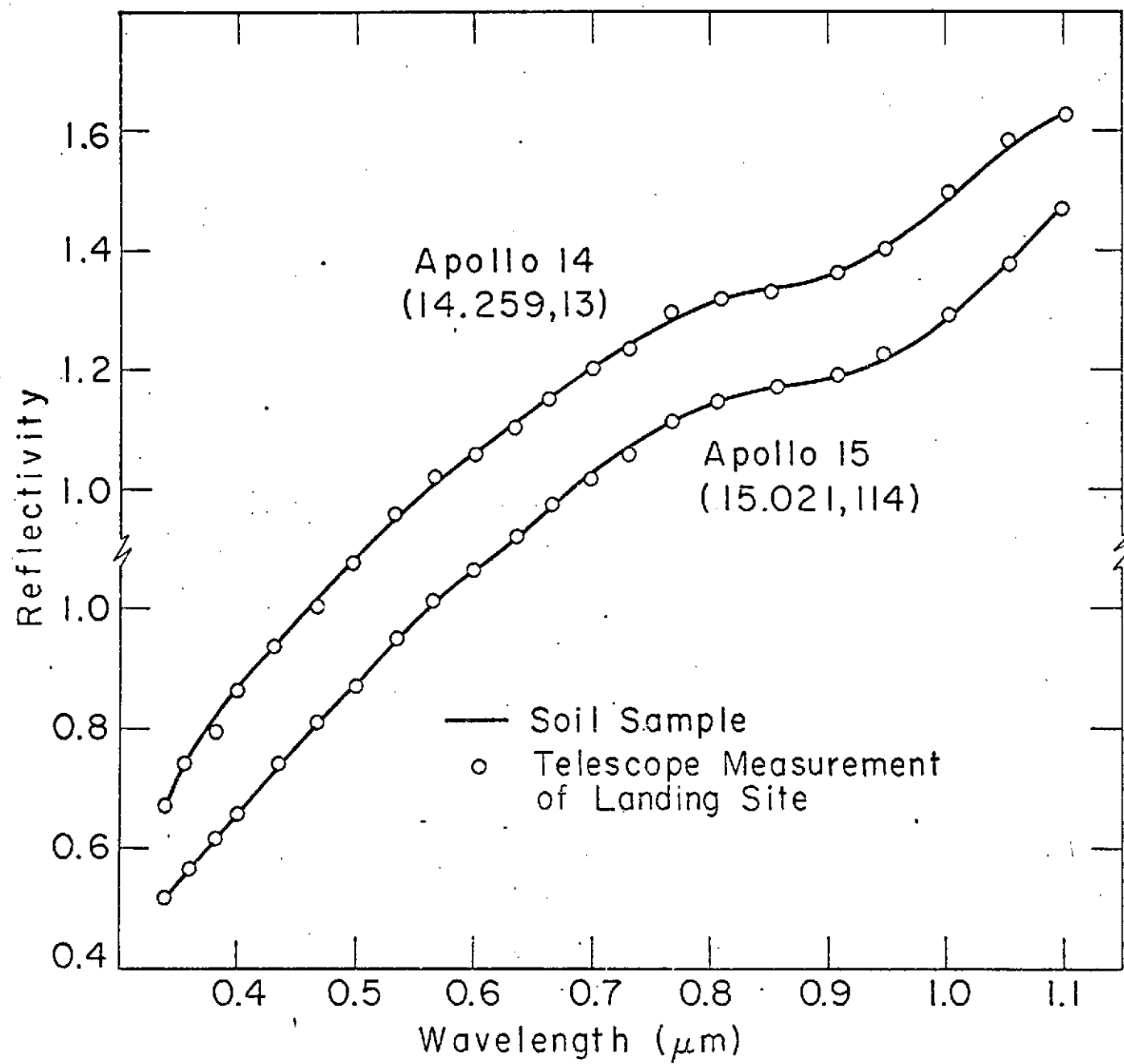


FIGURE 1

Fig. 2







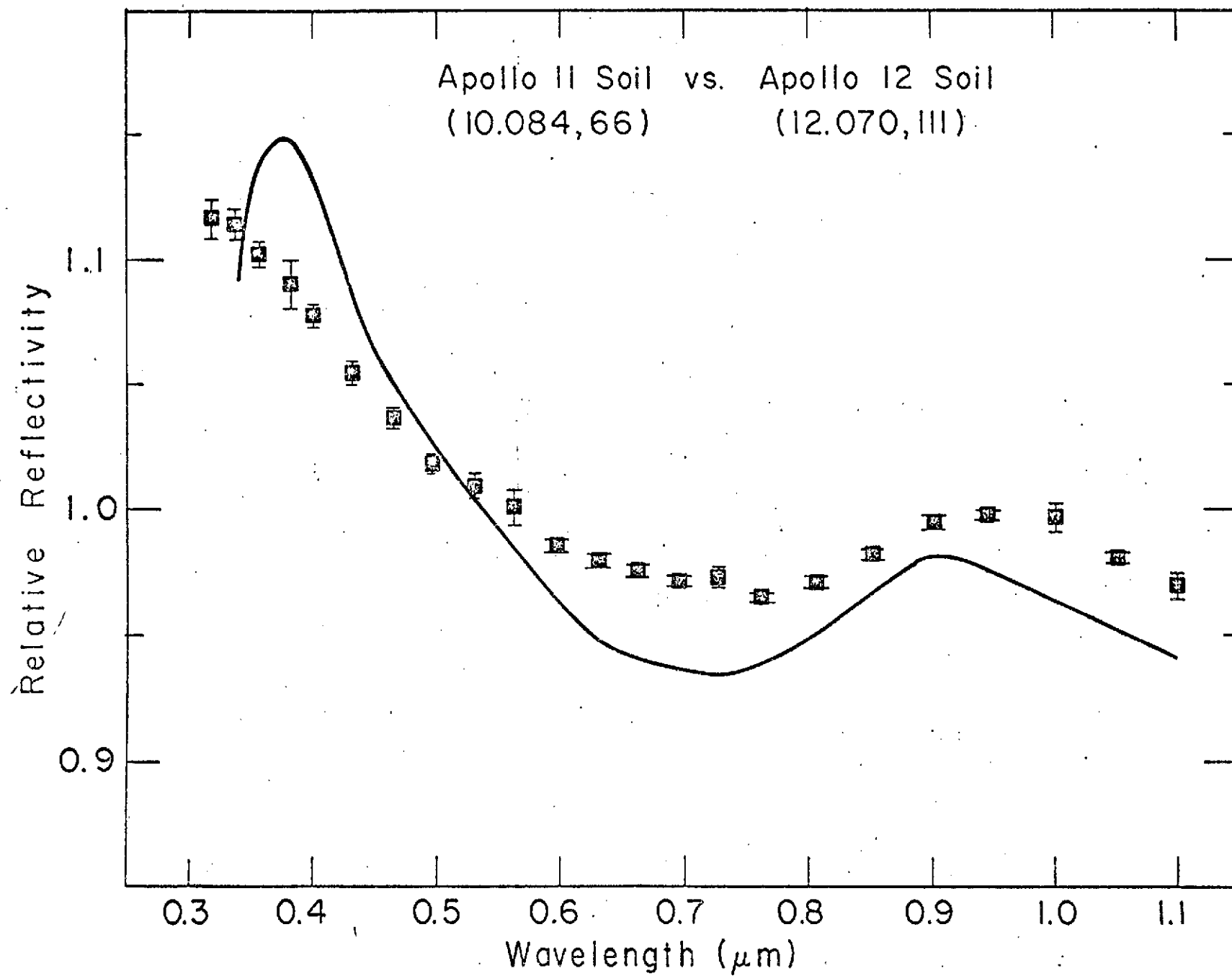
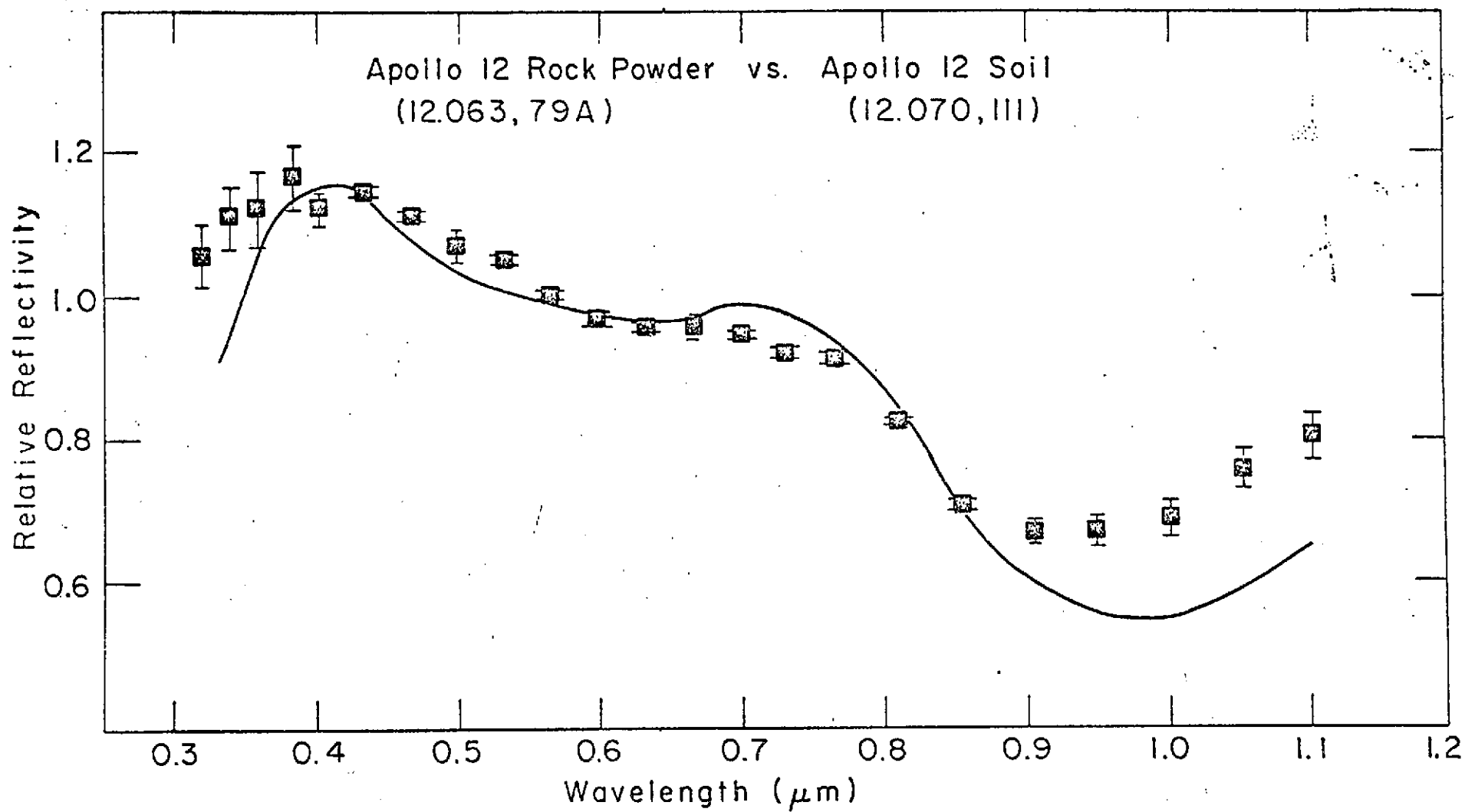
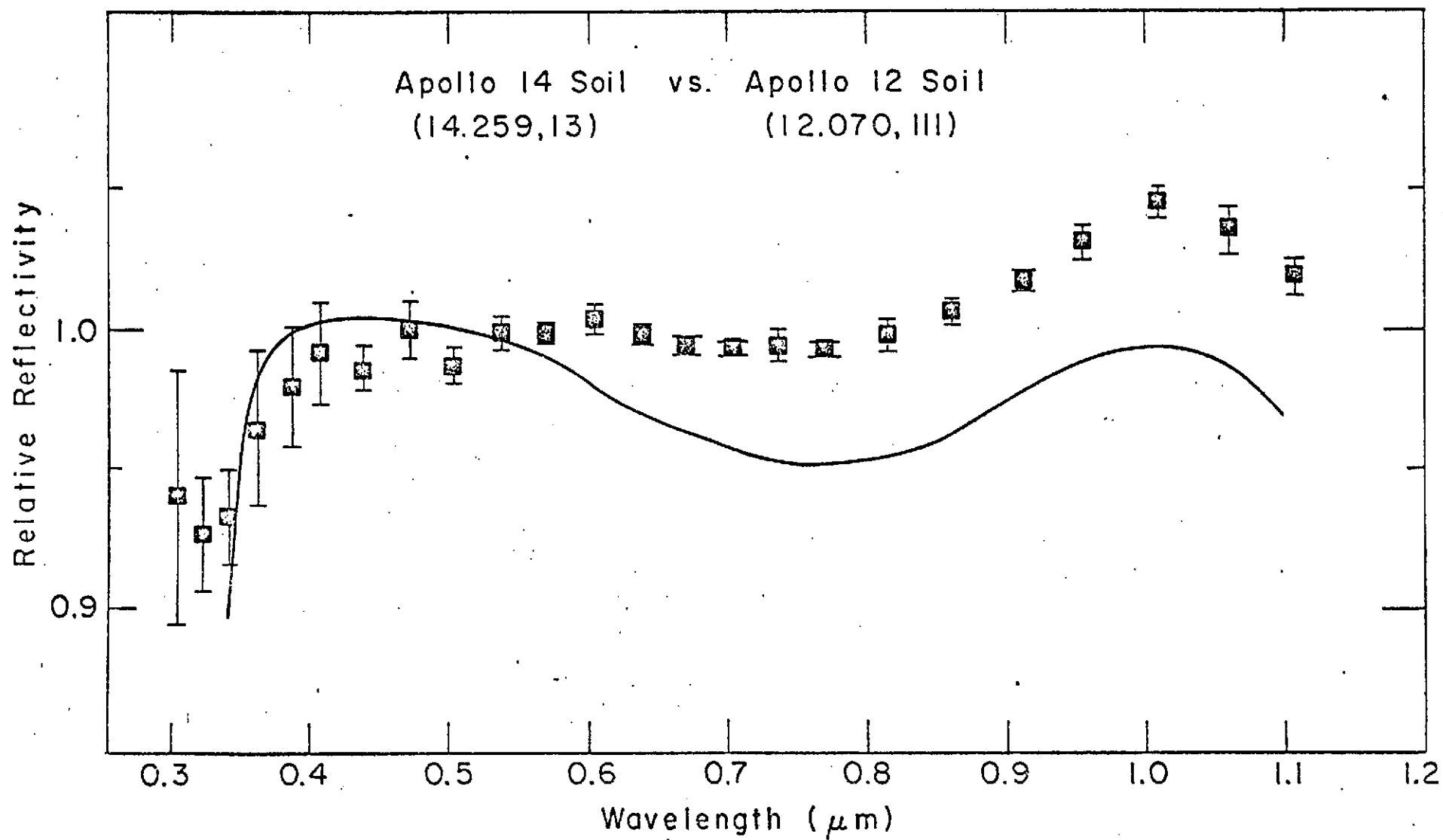


Fig 6.





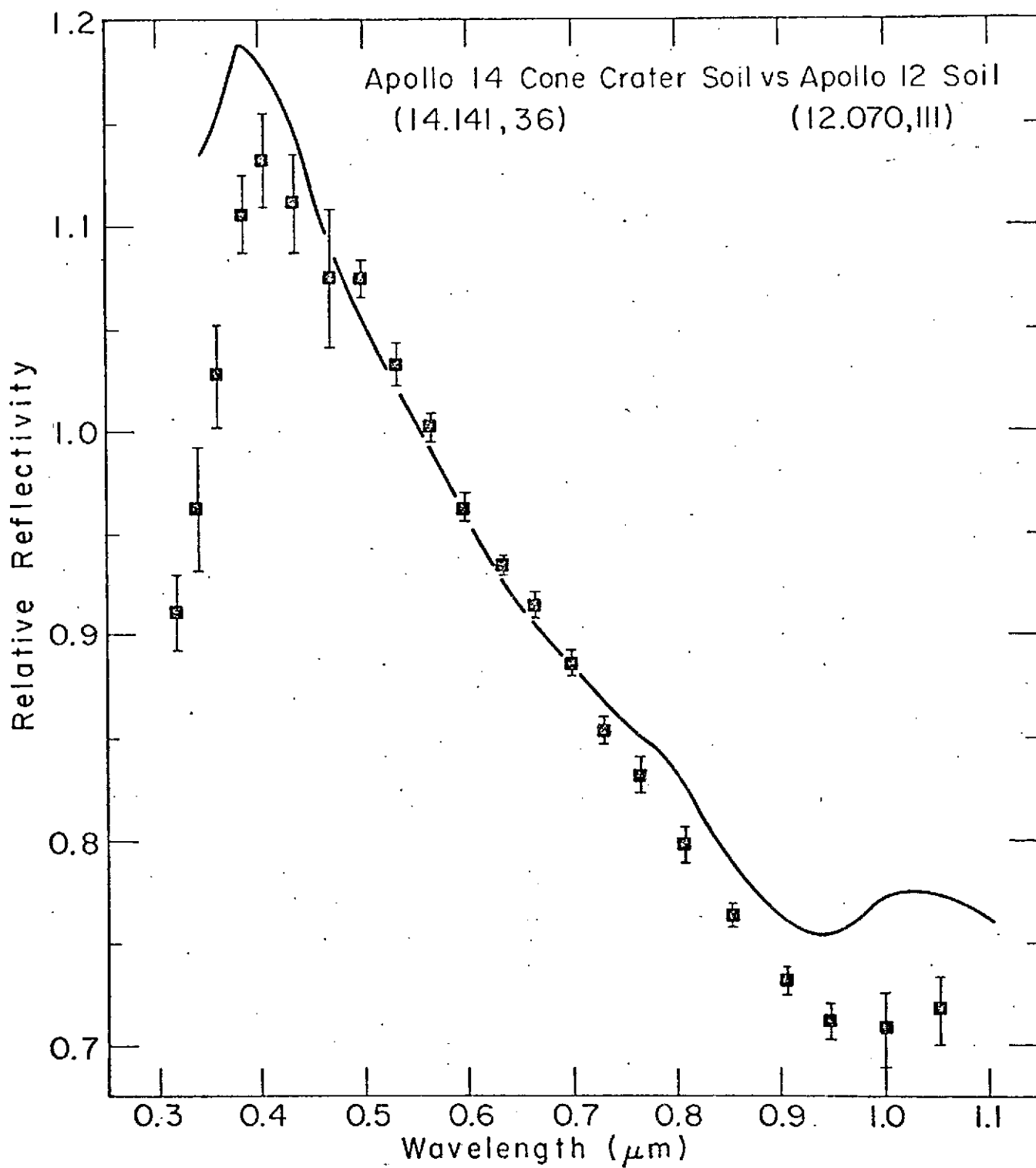


Fig 8

Other Reprints

Journal of Geophysical Research

VOLUME 77

MARCH 10, 1972

NUMBER 8

Lunar Spectral Types

THOMAS B. MCCORD, MICHAEL P. CHARETTE, TORRENCE V. JOHNSON,
LARRY A. LEBOWSKY, AND CARLE PIETERS

*Planetary Astronomy Laboratory, Department of Earth and Planetary Sciences
Massachusetts Institute of Technology, Cambridge, Massachusetts 02139*

JOHN B. ADAMS

*Caribbean Research Institute, College of The Virgin Islands
St. Croix, U.S. Virgin Islands 00820*

The spectral reflectance properties ($0.3\text{--}1.1\ \mu$) of a number of lunar mare, upland, and bright crater areas were observed with the use of ground-based telescopes. These new data are discussed in view of earlier studies in an attempt to provide a basis for more detailed interpretation. The spectral reflectivity curves ($0.3\text{--}1.1\ \mu$) for all lunar areas studied consist of a positive sloping continuum with a superimposed symmetric absorption band centered at $0.95\ \mu$. Upland, mare, and bright crater materials can be identified by their spectral curves. The curves for upland and mare regions show a range of shapes from fresh, bright craters to progressively darker background material that correlates with the apparent age of the surface features. The observed upland material has uniform spectral properties, but the mare material shows some variety, probably due to Ti^{2+} dispersed in lunar-soil glass. Copernicus and Aristarchus appear to have exposed upland material from beneath the mare but Kepler has not. This observation suggests that the mare is no deeper than about 15 km in the Copernicus area and about 6 km deep in the Aristarchus area, but in the Kepler area the mare must be at least about 5 km deep.

Study of samples returned from the moon and data from unmanned landers has greatly increased our knowledge of the landing sites visited. Our understanding of the vast areas beyond the landing areas is dependent in large part on remote measurements. In previous work [McCord, 1968a, 1969a, b; McCord and Johnson, 1969, 1970], it was shown that there are small but significant differences in spectral reflectance from place to place on the moon. The data were gathered by a telescopic technique [McCord, 1968b] used to measure the reflectance of small

(3–20 km) areas on the moon to a precision of less than a per cent.

The telescopic results were interpreted by using laboratory studies of the reflectance of silicate minerals [Adams and Filice, 1967; Adams, 1968]. The conclusions that lunar spectral reflectivity differences are controlled largely by mineralogy and that clinopyroxene is a major mafic mineral on the lunar surface have been verified since the return of lunar samples. Laboratory studies of returned samples [Adams and Jones, 1970; Adams and McCord, 1970, 1971a, b; Conel and Nash, 1970] have shown a close correlation between the optical properties

of lunar soil and the telescopic data; this close correlation implies that remote measurements can be interpreted for other parts of the surface of the moon.

This paper presents new telescopic observations of lunar spectral reflectivity and a discussion of the entire range of curve types that have been obtained to date. The importance of distinct classes of curves, based on shape, was recognized by McCord [1968a] and has been corroborated with work on Apollo 11 and 12 samples [Adams and McCord, 1971a, b]. The regular changes in spectral reflectivity that occur between mare and uplands and between bright craters and darker background material appear to indicate distinct differences in composition and age. Therefore an understanding of the lunar spectral types should be a valuable key to regional surface geology.

Telescope observations of the spectral reflectance at visible and near-infrared wavelengths of various areas of the lunar surface were discussed in several previous articles [McCord, 1968a, 1969a, b; McCord and Johnson, 1969, 1970]. It was shown that the reflectivity of all lunar areas studied increases continuously toward longer wavelengths to at least 2.5μ and that an absorption band is present in the spectrum of almost all lunar areas at about 0.95μ . There are small but significant differences in the reflection spectrum from place to place on the moon. The most important difference concerns the absorption-band depth and the continuum slope. These differences are correlated with the morphology of the lunar area observed.

A review of the literature on early studies of lunar spectral reflection telescope observations was given by McCord [1968a, also unpublished manuscript, 1972]. A more recent paper by Cruikshank [1969] was discussed by McCord and Johnson [1970]. Also, recent works by Soderblom [1970] and Goetz et al. [1971] that concern only a few spectral resolution elements but cover a large area of the lunar surface are of considerable importance toward the extension of the type of studies reported in the present article.

OBSERVATIONS

This report presents new observations of the spectral reflectivity in the spectral region 0.3–

1.1μ of lunar areas 18 km in diameter. These observations were obtained with the 24-in. and 60-in. (61 and 152 cm) telescopes on Mt. Wilson. A double-beam photometer was used in the single-beam mode. A set of twenty-four 1-in.-diameter narrow-band interference filters (see McCord and Westphal [1971] for characteristics), spaced every 200–500 Å between 0.3 and 1.1μ , was used to scan the spectrum. The filters were mounted in a wheel that was located immediately behind the focal plane aperture. An ITT FW-118 (S-1) photomultiplier tube was used (in a pulse-counting mode) as a detector. The pulses were counted and stored by a Fabri-tek instrument computer extensively modified by us for these observations. The filter wheel was continuously spun (4–6 rpm) behind the aperture while an area of the moon was guided on the aperture. The Fabri-tek gated the pulses so that certain memory locations were assigned for each area of the filter. When enough revolutions (1–4) of the filter wheel occurred to produce the desired ($\leq 1\%$) signal to noise ratio, the data were stored on digital magnetic tape for later computer reduction.

As in our previous work, a particular area in the Sea of Serenity (18.7°N , 21.4°E) was used as a calibration source. Generally, no more than 10–15 min elapsed between standard-area observations. On some nights, the standard area in the Sea of Serenity was measured alternately with a standard star. The positions and information about the observations of the lunar areas discussed in the article are given in Table 1. These observations were reduced to produce the intensity ratios $I_i(\lambda)/I_o(\lambda)$ and $I_o(\lambda)/I_s(\lambda)$, where I_i , I_o , and I_s are intensities for lunar area i , the standard lunar area, and the standard star. These ratios were scaled to unity at 0.564μ to remove the effects of albedo differences and to make curve comparisons easier. The first intensity ratio when scaled to unity at 0.564μ yields the normalized relative spectral reflectivity curve. This ratio is extremely sensitive to small differences in spectral reflectivity between lunar areas and can be measured very precisely. The second ratio when multiplied by the ratio $I_i(\lambda)/I_s(\lambda)$ yields the normalized spectral reflectivity curve for the standard lunar area. The product of the relative spectral reflectivity for the lunar area i and the

TABLE 1. Position, Description, and Observational Information on the Lunar Sites

Spot Name	Centered Coordinates	Run Date	Normal Albedo*	Phase Angle	No. of Runs	Description
Alphonsus 2	13°30'S, 4°10'W	Oct. 17, 1970	0.127 to 0.134	35°	3	Upland
Aristarchus	23°45'N, 47°30'W	Nov. 12, 1970	0.169 to 0.180	-13°	4	Large bright mare crater
Censorinus 2	0°25'S, 32°30'E	Dec. 7, 1970	0.192 to 0.206	-70°	3	Bright upland crater
Copernicus 2	9°50'N, 21°20'W	Jan. 9, 1971	0.150 to 0.159	-27°	5	Large mare crater
Copernicus 6	10°05'N, 19°35'W	Jan. 9, 1971	0.142 to 0.150	-27°	5	Large mare crater
Descarte 2	10°40'S, 16°5'E	Oct. 18, 1970	0.192 to 0.206	46°	3	Bright upland
Descarte 3	11°15'S, 14°50'E	Dec. 15, 1970	0.150 to 0.159	33°	5	Upland
Fra Mauro 6	8°30'S, 15°45'W	Oct. 17, 1970	0.159 to 0.169	33°	2	Bright upland
Fra Mauro 7	6°55'S, 16°34'W	Oct. 17, 1970	0.120 to 0.127	33°	3	Upland
Fra Mauro 15	4°35'S, 21°55'W	Oct. 17, 1970	0.102 to 0.108	33°	7	Mare
Guericke C	11°35'S, 11°30'W	Jan. 11, 1971	0.120 to 0.127	-4°	2	Mare crater
Hesodius B	27°55'S, 17°30'W	Jan. 11, 1971	0.108 to 0.114	-4°	3	Mare crater
Kepler	8°10'N, 37°40'W	Jan. 9, 1971	0.134 to 0.142	-26°	3	Large mare crater
Le Monnier	26°20'N, 30°10'E	Oct. 17, 1970	0.090 to 0.096	35°	3	Mare
Linne	27°40'N, 11°45'E	Jan. 9, 1971	0.108 to 0.114	-26°	4	Mare
Luna 16	0°30'S, 56°40'E	Nov. 12, 1970	0.079 to 0.085	-15°	4	Mare
Sea of Cold 1	57°30'N, 13°0'W	Dec. 12, 1970	0.102 to 0.108	-8°	3	Mare
Sea of Moisture 0	21°15'S, 37°45'W	Oct. 17, 1970	0.079 to 0.085	33°	7	Mare
Sea of Moisture 41	19°30'S, 31°0'W	Oct. 17 to 18, 1970	0.108 to 0.114	33° & 48°	6	Upland
Sea of Moisture 45	24°50'S, 44°55'W	Oct. 17 to 18, 1970	0.108 to 0.114	33° & 48°	6	Mare crater
Sea of Moisture 51	20°40'S, 43°0'W	Oct. 17, 1970	0.085 to 0.090	33°	3	Mare
Sea of Serenity 2	18°40'N, 21°25'E	Standard Spot	0.090 to 0.096			Mare
Sea of Tranquility 1	16°55'N, 22°35'E	Oct. 17, 1970	0.085 to 0.090	32°	6	Mare
Messier A	2°0'S, 46°55'E	Jan. 10, 1971	0.102 to 0.108	-16°	2	Mare crater
Mosting C	1°50'S, 8°5'W	Jan. 10, 1971	0.127 to 0.134	-14°	3	Mare crater
Niccolet	21°55'S, 12°30'W	Jan. 11, 1971	0.108 to 0.114	-4°	4	Mare crater
Plato C	51°30'N, 11°10'W	Dec. 12, 1970	0.085 to 0.090	-8°	4	Mare
Proclus	16°5'N, 47°0'E	Dec. 7, 1970	0.180 to 0.192	-70°	2	Upland crater
Tycho 1	42°55'S, 10°40'W	Nov. 11, 1970	0.159 to 0.169	-26°	3	Upland bright crater
Upland 7	27°45'N, 31°10'E	Oct. 17, 1971	0.114 to 0.120	35°	4	Upland

*From Pohn and Wildey [1970].

spectral reflectivity for the standard lunar area yields the spectral reflectivity for the lunar area *i*.

An additional aid in determining the spectral reflectance of the lunar standard area is the laboratory measurements of Apollo 11 lunar-soil samples. By comparing the telescope and the laboratory measurements, it is possible to refine the telescope reflection spectrum. Uncertainty in the solar and stellar fluxes and in the effects of solar lines on the filter passbands can be reduced in this way.

In this study we have used both standard-star observations and laboratory lunar-soil-sample measurements to develop the spectral reflectivity curve for the standard lunar area in the Sea of Serenity. The standard-star fluxes used are from *Oke* [1964], as modified by *Oke and Schild* [1970]. The solar fluxes are from *Labs and Neckel* [1968], modified to account for solar lines and their effect on the effective wavelength of our filters. The spectral reflectivity curve for the Sea of Serenity site was measured at a phase angle of 20°–30°. Also, the Apollo 11 site was measured relative to the Sea of Serenity standard site. The spectral reflectivity of the Apollo 11 site was then calculated and compared with laboratory curves of Apollo 11 soil samples. The two curves matched within the measurement error. The laboratory data are more precise, and thus the spectral

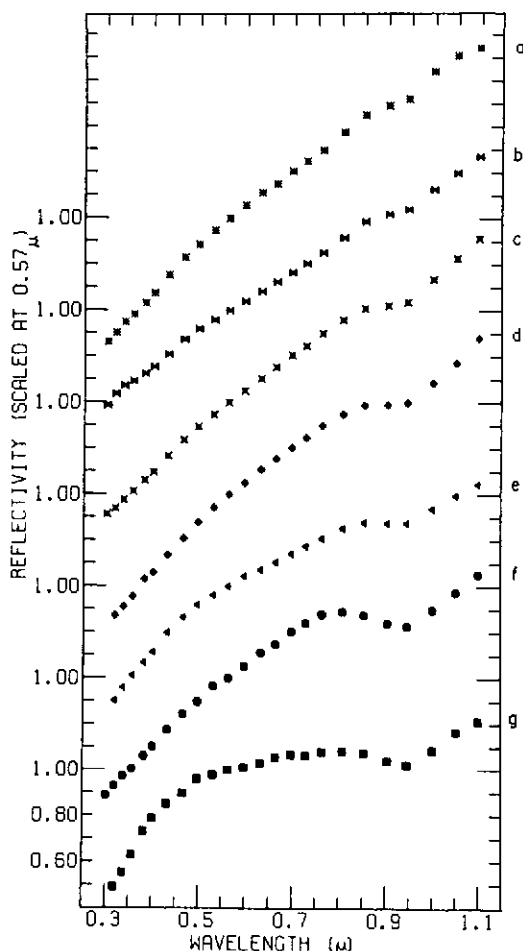


Fig. 1. Spectral reflectivity, scaled to unity at 0.56 μ , for seven lunar areas: (a) Sea of Moisture 41; (b) Sea of Tranquility 1; (c) Sea of Serenity 2; (d) Sea of Cold 1; (e) Tycho 1; (f) Sea of Moisture 45; (g) Aristarchus. Area *a* is upland; areas *b*, *c*, and *d* are mare; areas *e*, *f*, and *g* are bright craters.

TABLE 2. Spectral Reflectivity Values for the Standard Area in the Sea of Serenity 2 Versus Sun (Scaled to unity at 0.564 μ .)

Filter Wavelength, μ	Ratio
0.301	0.5143
0.319	0.5390
0.338	0.5750
0.358	0.6130
0.383	0.6610
0.402	0.6960
0.433	0.7666
0.467	0.8362
0.498	0.8945
0.532	0.9475
0.564	1.0000
0.598	1.0506
0.633	1.1040
0.665	1.1537
0.699	1.2062
0.730	1.2471
0.765	1.3006
0.809	1.3529
0.855	1.4105
0.906	1.4231
0.948	1.4389
1.002	1.5368
1.053	1.6286
1.101	1.7145

reflectance data for the standard lunar area (MS2) were adjusted to agree with them. Table 2 gives the resultant spectral reflectivities.

The normalized spectral reflectivity curves for several lunar areas representing a variety of lunar terrains are shown in Figure 1. The standard area curve (the derivation discussed above) is assumed to be perfect. Thus, the formal error is that for the relative curves.

The normalized relative spectral reflectivity curves for lunar areas discussed in the article are displayed in Figures 2, 3, and 4. The stand-

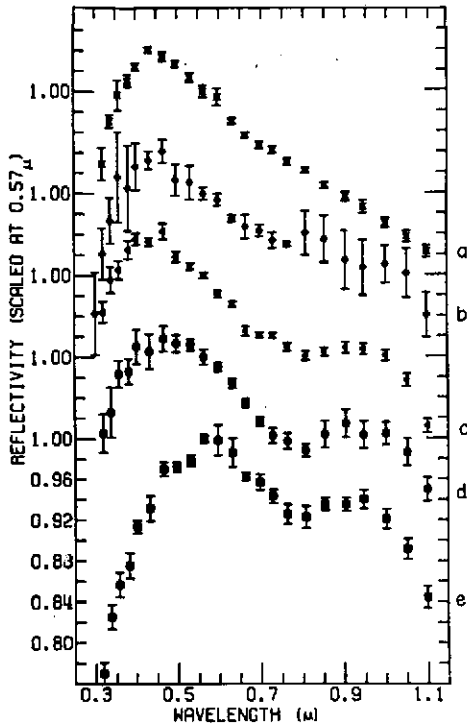


Fig. 2a. Relative spectral reflectivity for (a) Proclus; (b) Censorinus 2; (c) Descartes 2; (d) Fra Mauro 6; (e) Tycho 1. Relative reflectivity is the ratio of the reflectivity of one area to that of the standard area (in this study an area in the Sea of Serenity).

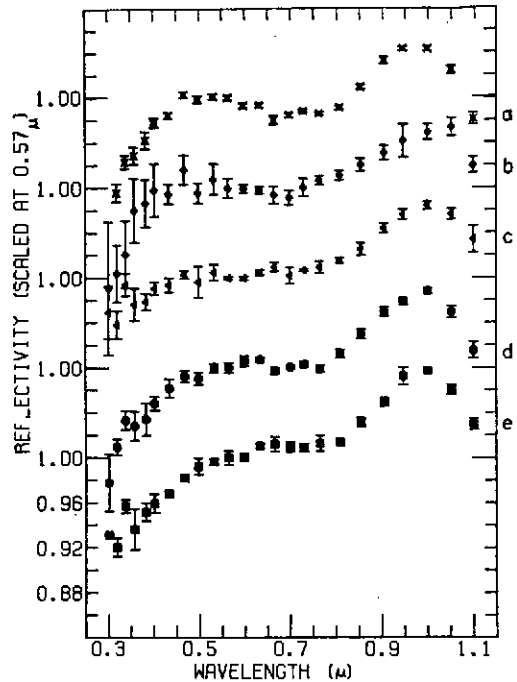


Fig. 2b. Relative spectral reflectivity for (a) Descartes 3; (b) Fra Mauro 7; (c) uplands 7; (d) Sea of Moisture 41; (e) Alphonsus 2.

Figure 2 shows the relative spectral reflectivity for a series of areas in the uplands ranging from bright craters (Tycho 1) to background upland material (Alphonsus 2).

ard area in the Sea of Serenity is used in the relative ratio for all areas. The formal standard deviation for each filter measurement, determined from an average of 3-5 separate measurements of area pairs, is indicated by the error bar.

RESULTS

Spectral reflectivity. The spectral reflectivity curves for all areas of the lunar surface that were measured have a basic similarity (Figure 1). All curves show an increase in reflectivity toward longer wavelengths and an absorption feature near 0.95μ .

A variety of lunar terrains are represented in Figure 1. Curve *a* is for an upland region. Curves *b*, *c*, and *d* represent mare regions, curve *e* represents an upland bright crater, and

curves *f* and *g* represent mare bright craters. In all curves the absorption band appears at 0.95μ . No other absorption band is evident in this spectral region. The curve shapes and continuum slopes vary from curve to curve and are not uniform over this spectral range. The greatest variety of curves occurs between the bright craters and other lunar terrain.

Relative spectral reflectivity. The reflection spectra for lunar areas (Figure 1) have small but significant differences. A sensitive method for studying these small differences is to measure and to plot the ratio of the reflectivities for two lunar areas. This ratio curve is called the relative spectral reflectivity curve. For example, when curve *b* (Sea of Tranquility 1) in Figure 1 is divided by curve *c* (Sea of Serenity 2), the result is the relative curve for Sea of

Tranquility 1 shown at the top of Figure 3. In the present study, the standard area for Sea of Serenity 2 (18.7°N, 21.4°E) was always used in the denominator to calculate the reflectivity ratios.

The short-wavelength end of the spectral re-

gion studied in our earlier work was 0.4μ . In the present study we have extended this range to 0.30μ . There are additional spectral features in this near-ultraviolet spectral region, previously unreported, that are particularly useful in classifying lunar-area spectral types.

The classification of lunar areas into general spectral types that correlate with the lunar-terrain types (maria, uplands, and bright craters) was made earlier [McCord, 1968a, 1969a]. In the present study this classification can be refined. Curves for a series of upland-terrain types ranging from Tycho 1 to Alphonsus 2 are shown in Figure 2. In these figures a peak near 0.40μ and then a rapid decrease of the relative spectral curves toward the ultraviolet for bright upland craters and slope material is clear. This feature helps to distinguish the bright upland material curves from the mare-region curves (Figure 3), which can be similar in other parts of the curve, for example, between 0.4 and 0.7μ . There is a continuous change in the relative spectral curve through a sequence of fresh bright craters (Tycho 1), to less bright craters (Proclus), to older background upland material (Upland 7). For example, the peak near 0.40μ becomes less sharp and shifts toward red wavelengths as the lunar terrain changes from very bright upland material to background upland material. The albedos for the areas discussed in this article are given in Table 1. Also, the slope of the relative spectral reflectivity curve between 0.4 and 1.1μ changes from negative to positive and the absorption-band feature near 1.0μ becomes stronger along the same terrain sequence. The absorption band appears as a positive maximum in these relative curves because the band in spectral reflectivity curves is not so deep for these areas as it is for the standard area.

In earlier work it was suggested that there are distinct lunar spectral types, areas such as bright craters and uplands possessing distinct spectral curves with no overlap between the classes of curve. However, Figure 2 suggests that a spectrum of curve shapes exists between distinct end-members for upland regions, which is related to the freshness of the exposed surface material.

Another series of curve shapes exists for mare regions (Figure 3). The ultraviolet region and the $1.0\text{-}\mu$ region again show the most obvious

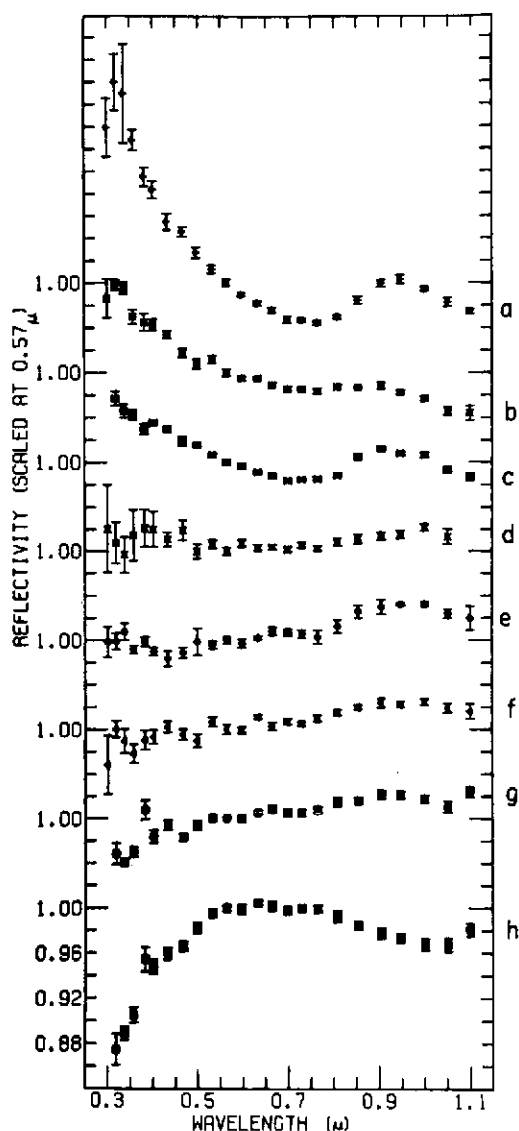


Fig. 3. Relative spectral reflectivity for a series of background mare areas ranging from 'blue' mare (Sea of Tranquility 1) to 'red' mare (Sea of Cold 2). (a) Sea of Tranquility 1; (b) Sea of Cold 2; (c) Sea of Moisture 0; (d) Luna 16 landing site; (e) Fra Mauro 15; (f) Le Monnier; (g) Sea of Moisture 51; (h) Plato C; (i) Sea of Cold 1.

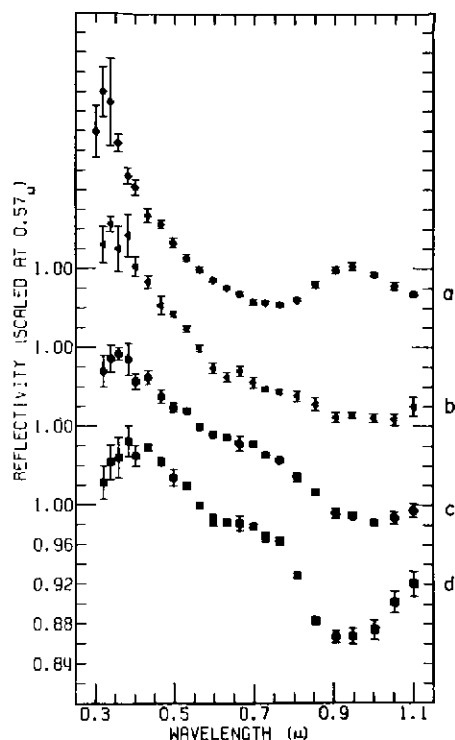


Fig. 4a. Relative spectral reflectivity for (a) Sea of Tranquility 1; (b) Hesodius B; (c) Nicotlet; (d) Guericke C.

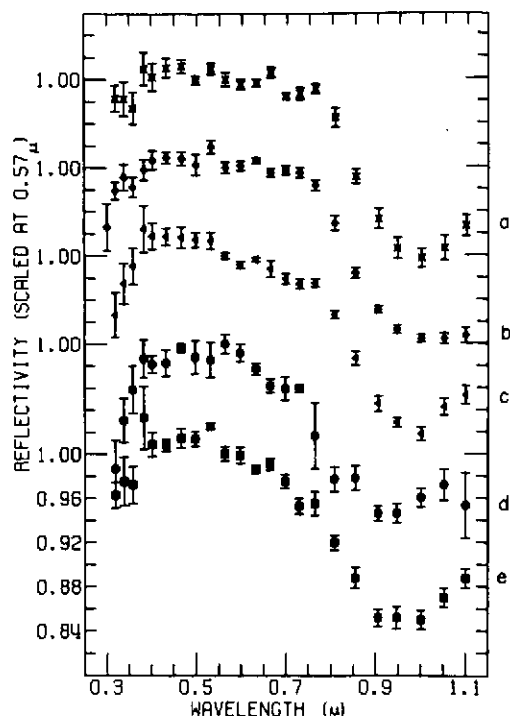


Fig. 4b. Relative spectral reflectivity for (a) Linne; (b) Sea of Moisture 45; (c) Messier A; (d) Kepler; (e) Mosting C.

Figure 4 shows the relative spectral reflectivity for a series of regions in the mare ranging from background mare through old mare craters to young mare craters.

differences. In the maria the relative spectral curve series runs from the bluer regions, such as most of the Sea of Tranquility, to the redder regions, such as the Sea of Serenity and the Sea of Cold.

Within any one mare the spectral characteristics are not uniform. A mare can be composed of material of several spectral types, as has been pointed out [McCord, 1968a, 1969a; Soderblom, 1970]. This composition does not occur in the uplands, where the background upland material is fairly uniform in spectral properties everywhere on the moon. Only the very bright upland regions show different spectral characteristics. These very bright regions are usually fresh craters, but other anomalously bright regions are also included in the uplands.

The effects produced by disturbing the mare regions through cratering are similar to those

found in the uplands. The exposed material is brighter than the surrounding material, and rays are formed. However, the spectral characteristics for most bright craters in the mare (Figure 4) are not the same as the spectral characteristics for the upland craters. The 0.95- μ absorption feature is stronger for most mare bright craters than for other lunar areas studied. The decrease in slope toward shorter wavelengths below about 0.5 or 0.4 μ is present in both the mare bright crater and the upland bright crater relative curves, but the character is different and the variety is much greater. There is evidence for an age-color relation for mare bright craters and for upland bright craters, the spectral properties of the craters becoming similar to those for the background mare material as the crater becomes less bright and more covered with soil (see Figure 4a).

However, partly because of the lack of data on older mare bright craters, this relation cannot be conclusively proven at this time.

Absorption band character. Both the spectral reflectivity curves (Figure 1) and the relative spectral reflectivity curves (Figures 2-4) show evidence of an absorption band in the 0.90- to 1.0- μ spectral region. The wavelength position of this band is of considerable importance because it is a primary indicator of mineralogy. In the relative curves the relative band appears at a variety of positions ranging between 0.90 and 1.00 μ . In all the reflectivity curves shown (Figure 1) the band appears very nearly at 0.95 μ . As has been pointed out by L. T. Silver (personal communication, 1969) and *Conel and Nash* [1970], and as is well known among spectroscopists, the apparent wavelength position of an absorption feature superimposed on a sloping continuum depends partly on the continuum slope. The continuum of the lunar spectrum has a large positive slope; thus, there is a problem in reading absorption-band positions directly from lunar spectra.

Artificial lunar spectra have been calculated by using straight-line sloping continuums and superimposed Gaussian absorption bands. The continuum slope and band depth and position were varied to test resultant relative and 'absolute' curve behavior. The results of these tests were applied to actual lunar curves to remove the effects of the continuum slope on the apparent band position. The relative lunar curves suffer most from band-distortion effects. Apparent shifts in the relative bands in our curves are due to differences in the slopes of the two curves involved and not to differences in the absorption band between the two curves. Artificial relative curves can be produced that duplicate the behavior of actual lunar curves without resorting to absorption-band position shifts. This analysis is, of course, limited by our spectral resolution.

The band position in actual lunar spectral reflectivity curves appears at about 0.95 μ for nearly all curves, according to visual analysis. The band is generally quite shallow and is always superimposed on a positive sloping continuum. The combination of these effects results in almost no difference between actual and apparent band position as determined by visual analysis. An analysis of four lunar spectral

reflectivity curves is shown in Figure 5. The absorption band was extracted from the curve under the assumption that there was a linear continuum in the vicinity of a symmetric absorption band. The continuum required to produce a symmetric band and the resulting band are shown in Figure 5 along with the actual spectrum. Note that the slope of the continuum changes at about 0.90 μ for some curves.

INTERPRETATION

The distinct differences between the spectral curves for the mare and upland regions correlate with the well-known differences in albedo and topography. Differences in bulk composition between uplands and maria are implied, and a contrast in bulk chemistry is supported by Surveyor and Apollo data.

The ability to differentiate surface upland material from mare material by means of the spectral curves becomes important in areas where the usual indicators, albedo, and topography are ambiguous. At the edges of the maria there are places where crater ejecta of one type overlap or are mixed with material of the adjacent terrain. At Davy rille, for example, a mixture of upland and mare materials is indicated by the spectral curves [McCord et al., 1971].

The distinction between upland and mare curves is of particular interest as applied to the large craters Copernicus and Aristarchus. Although the craters are located in the maria, the spectral curves (Figure 6) are those of upland material. We interpret these data to mean that cratering events at Copernicus and Aristarchus penetrated through the mare fill and exposed underlying upland material. Other craters in this mare region, including Kepler (Figure 4b), have mare-type curves. Thus, it is possible to place an upper limit of about 15- and 5-km thickness of the mare fill in the vicinity of these two large craters, if a 1:5 depth-diameter ratio and initial crater diameters of 72 and 32 km are assumed. In the vicinity of Kepler the mare depths must be at least about 5 km for an initial crater diameter of 24 km.

There are transitions in the spectral curves from bright craters to background material for both the uplands and the maria. The changes in the curves correlate with apparent age as

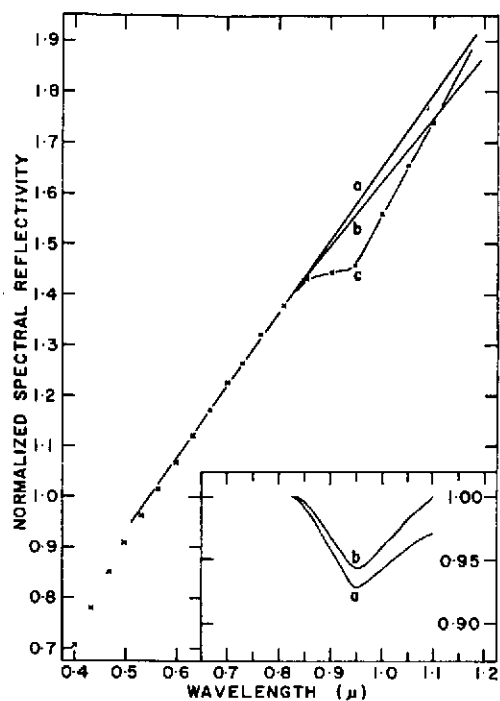


Fig. 5a. Sea of Serenity 2.

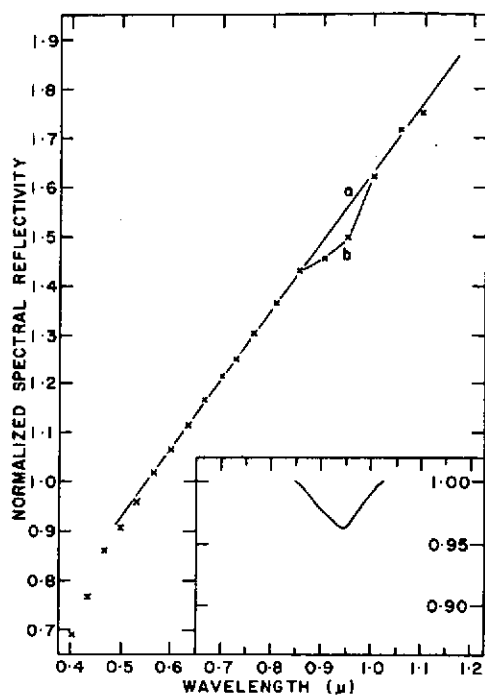


Fig. 5b. Censorinus 2.

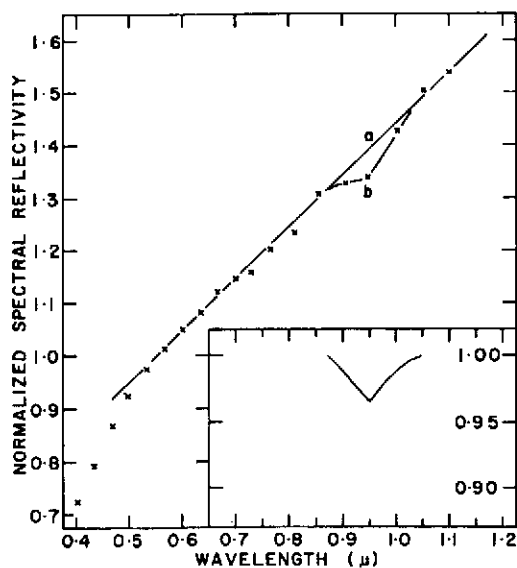


Fig. 5c. Fra Mauro 14.

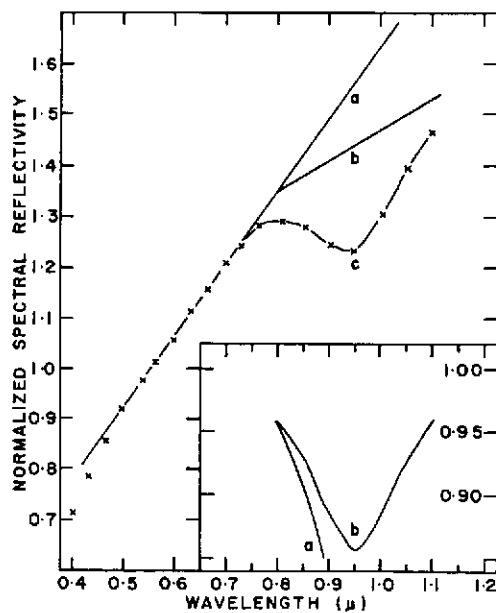


Fig. 5d. Sea of Moisture 45.

Figure 5 shows the spectral reflectivity curves and the absorption band with the continuum removed. For curves in 5a and d the continuum slope changes at about 0.8μ .

deduced by crater form and by stratigraphic relationships. The spectral properties apparently are affected by the aging process in a regular way.

Aging leads to subdued crater outlines and to a loss of contrast between the brighter crater material and the darker background. Darkening of fresh craters and their rays is more pronounced in the maria than in the uplands. In both regions it is necessary to penetrate the darkened surface layer to expose the brighter, fresher material underneath. From the spectral data a clear distinction can be made between bright craters in upland material and bright craters in mare material (although the albedos may be the same), and an estimate can be made of the stage of aging and darkening. Copernicus ranks as upland material in an advanced stage of aging. Therefore, further darkening of Copernican material is limited and would be caused mainly by mixing with the surrounding darker mare soil. Aristarchus, on the other hand, is most closely related to fresh

upland material in spectral type, which implies that in time the crater and its rays will degrade further both by aging and by mixing with the surrounding soil.

Background, dark mare material is not of uniform spectral type. The spectral curves range between the two extremes of 'red' and 'blue' mare, subgroups recognized and discussed by Whittaker [1966], Goetz *et al.* [1971], and others. The mare subgroups are distinguished by differences in the relative curves at the blue end of the spectrum. The curve differences can be explained by the amount of absorption by Ti^{3+} ions in the glass phase of the soil [Burns, 1970; Conel, 1970; Adams and McCord, 1971a, b].

The implied compositional differences in the maria are very slight, and this conclusion is in good agreement with differences in the titanium content in returned samples. It is significant that the lunar spectral types are limited to the compositional groups of uplands and maria, and to a subgroup of types within the maria. Although uplands and maria appear to differ in composition, there is also an implied similarity in that the $0.95\text{-}\mu$ (pyroxene) band, although weaker in the uplands, is common to both regions. Therefore, we conclude that the major compositional differences across the near side of the moon are effectively restricted to the uplands versus the maria and that most other variations in the spectral curves are a function of the degree of aging within the major types of materials. The aging process itself and its effect on spectral properties have been discussed elsewhere, on the basis of studies of returned lunar samples [Adams and McCord, 1971a, b].

Acknowledgment. This research was supported by NASA grants NGR-22-009-350 and NGR-52-083-0030.

REFERENCES

- Adams, J. B., Lunar and Martian surfaces: Petrologic significance of absorption bands in the near-infrared, *Science*, **169**, 1453, 1968.
- Adams, J. B., and A. L. Filice, Spectral reflectance 0.4 to $2.0\text{ }\mu$ of silicate rock powders, *J. Geophys. Res.*, **72**, 5705, 1967.
- Adams, J. B., and R. L. Jones, Spectral reflectivity of lunar samples, *Science*, **167**, 737, 1970.
- Adams, J. B., and T. B. McCord, Remote sensing of lunar surface mineralogy implications from visible and near-infrared reflectivity of Apollo

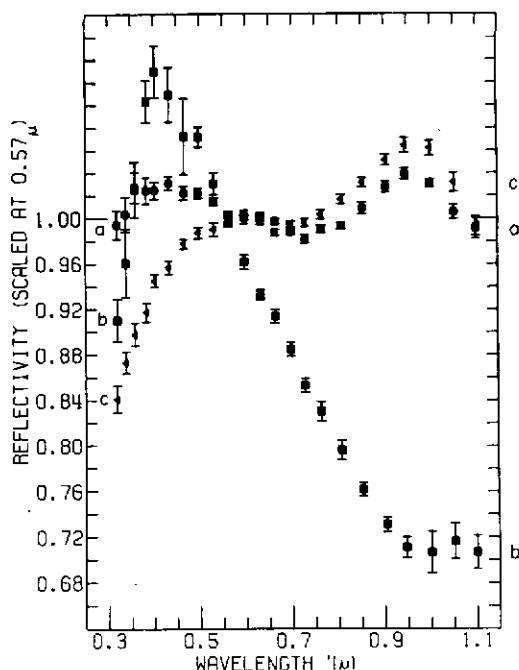


Fig. 6. Relative spectral reflectivity for (a) Copernicus NE floor; (b) Aristarchus; (c) Copernicus W rim. These craters, located in the mare, have curves that belong to the sequence of upland material (Figure 2).

- 11 samples, *Geochim. Cosmochim. Acta*, Suppl. 1, 1937, 1970.
- Adams, J. B., and T. B. McCord, Alteration of lunar optical properties; Age and composition effects, *Science*, 171, 567, 1971a.
- Adams, J. B., and T. B. McCord, Optical properties of mineral separates, glass, and anorthositic fragments from Apollo mare samples, *Geochim. Cosmochim. Acta*, in press, 1971b.
- Burns, R. G., *Mineralogical Applications of Crystal Field Theory*, Cambridge University Press, London, 1970.
- Conel, J. E., Coloring of synthetic and natural lunar glass by titanium and iron, *Jet Propulsion Laboratory Space Program Summary*, vol. 3, pp. 26-31, 1970.
- Conel, J. E., and D. B. Nash, Spectral reflectance and albedo of Apollo 11 lunar samples: Effects of irradiation and vitrification and comparison with telescopic observations, *Geochim. Cosmochim. Acta*, Suppl. 1, 2013, 1970.
- Cruikshank, D. P., Moon: Infrared studies of surface composition, *Science*, 166, 215, 1969.
- Goetz, A. F. H., F. Billingsly, E. Yost, and T. B. McCord, Apollo 12 multispectral photography experiment, Apollo 12 Preliminary Science Report, NASA SP-235, p. 103, 1971.
- Labs, D., and H. Neckel, The radiation of the solar photosphere from 2000 Å to 100 μ , *Z. Astrophys.*, 69, 1, 1968.
- McCord, T. B., Color differences on the lunar surface, Ph.D. dissertation, Calif. Inst. of Technol., Pasadena, 1968a.
- McCord, T. B., A double-beam astronomical photometer, *Appl. Opt.*, 7, 475, 1968b.
- McCord, T. B., Color differences on the lunar surface, *J. Geophys. Res.*, 74, 3131, 1969a.
- McCord, T. B., Time dependence of lunar differential color, *Astron. J.*, 74, 273, 1969b.
- McCord, T. B., and T. V. Johnson, Relative spectral reflectivity 0.4-1 μ of selected areas of the lunar surface, *J. Geophys. Res.*, 74, 4395, 1969.
- McCord, T. B., and T. V. Johnson, Lunar spectral reflectivity (0.3 to 2.50 μ) and implications for remote mineralogical analysis, *Science*, 169, 855, 1970.
- McCord, T. B., and J. A. Westphal, Mars: Narrowband photometry, from 0.3 to 2.5 μ , of surface regions during the 1969 apparition, *Astrophys. J.*, 30, 40, 1971.
- McCord, T. B., M. P. Charette, T. V. Johnson, L. A. Lebofsky, and C. Pieters, Spectrophotometry (0.3 to 1.1 μ) of visited and proposed Apollo lunar landing sites, final report, NASA grant NGR-22-009-496, 1971.
- Okc, J. B., Photoelectric spectrophotometry of stars suitable for standards, *Astrophys. J.*, 140, 689, 1964.
- Oke, J. B., and R. Schild, The absolute spectral energy distribution of Alpha Lyrae, *Astrophys. J.*, 161, 1015, 1970.
- Pohn, H. A., and R. L. Wildey, *A Photographic Study of the Normal Albedo of the Moon*, U.S. Government Printing Office, Washington, D.C., 1970.
- Soderblom, L. A., The distribution and ages of regional lithologies in the lunar maria, Ph.D. dissertation, Calif. Inst. of Technol., Pasadena, 1970.
- Whittaker, E., in Interpretation of Ranger VII records by G. P. Kuiper, *Commun.* 68, pp. 4 and 18, Lunar and Planet. Lab., Univ. of Arizona, 4, Tucson, 1966.

(Received July 30, 1971;
revised November 10, 1971.)

Remote sensing of lunar surface mineralogy: Implications from visible and near-infrared reflectivity of Apollo 11 samples

JOHN B. ADAMS

Caribbean Research Institute, College of the Virgin Islands, St. Croix,
U.S. Virgin Islands 00820
and

THOMAS B. MCCORD

Department of Earth and Planetary Sciences, Massachusetts Institute of Technology,
Cambridge, Massachusetts 02139

(Received 2 February 1970; accepted in revised form 23 February 1970)

Abstract—The reflectivity curve for the Apollo 11 fines closely matches the telescopic curve for an 18 km diameter area that includes the landing site. A laboratory study of four lunar rocks and two samples of fines indicates that the shallow depression at $0.95 \mu\text{m}$ in the telescopic curve is a degraded band arising from electronic absorptions in clinopyroxene and to a minor extent in olivine. Iron- and titanium-rich glass in the lunar fines accounts for the strong blue absorption in the telescopic curve and may be primarily responsible for the low albedo. Bands at approximately $0.95 \mu\text{m}$ in telescopic curves for Kepler, Aristarchus and Plato C indicate the presence of clinopyroxene similar to that found at the Apollo 11 site. The curve for the lunar highlands has a very weak band, implying that clinopyroxene is less abundant there. Variations in the amount of dark glass are suggested by differences in curve slopes for diverse lunar maria areas.

INTRODUCTION

OUR INVESTIGATION of the Apollo 11 lunar samples had the following objectives: (1) to search for electronic or other absorption bands in the visible and near-i.r. portions of the spectrum, and to relate any bands to the mineralogy of the samples, (2) to investigate parameters other than mineralogy that might affect the frequencies or depths of bands, and (3) to relate laboratory spectra and lunar sample mineralogy to earth-based telescopic spectra of the moon and to evaluate the feasibility of obtaining mineralogical information by remote reflectivity measurements. In this paper we expand the preliminary report by ADAMS and JONES (1970) on the Apollo 11 samples and include new interpretations of lunar telescopic measurements.

The basis for interpretation of absorption bands in silicates between $0.3 \mu\text{m}$ and $2.5 \mu\text{m}$ was developed through the application of crystal field theory to mineralogy (BURNS, 1965; WHITE and KEESTER, 1966). Transmission spectra of single oriented crystals, using polarized light, have led to refinements in band assignments (BURNS and FYFE, 1967; BANCROFT and BURNS, 1967; WHITE and KEESTER, 1967). Electronic bands are produced by transition elements, notably iron, in various valence and co-ordination states. Band frequencies are sensitive to distortion of *d*-orbital shells of transition metals by neighboring anions. Because metal-oxygen distances and configurations differ for most minerals, the absorption band frequencies can be used for identification of minerals that exhibit bands.

Absorption bands also appear in diffuse reflectance spectra of minerals and of their powders (WHITE and KEESTER, 1967; ADAMS and FILICE, 1967). The feasibility of making mineral identifications based on reflectivity curves of minerals and rocks has been discussed by ADAMS (1968). Interpretations of bands in lunar and planetary reflectivity curves have been made on the basis of the above arguments. The reflectivity measurements of the Apollo 11 lunar samples provide the first opportunity to test the validity of mineralogical interpretations that were based on reported absorption bands in the telescopic curves. Major uncertainties have been whether the lunar surface has been altered in an unknown way and whether the lunar reflectivity curves can be correctly interpreted in terms of terrestrial mineral and rock curves.

INSTRUMENTATION AND SAMPLE PREPARATION

Preliminary measurements were made with a Cary 14RI ratio-recording spectrophotometer at the Manned Spacecraft Center. The instrument had an MgO-lined integrating sphere, and freshly smoked MgO was used as a standard. Illumination was by a water cooled hydrogen lamp in the spectral range 0.32–0.4 μm and a tungsten lamp between 0.4 and 2.5 μm . Detectors consisted of a No. 6217 photomultiplier in the 0.32–0.6 μm region, and a PbS cell beyond 0.6 μm . The system was purged with dry nitrogen gas.

Spectra were scanned at a constant rate of 50 Å/sec. Data were simultaneously recorded on a strip chart and in digital form on paper tape every 20 Å. Spectral resolution varied from a minimum of 70 Å near the spectral extremes to 12 Å in the visible and near i.r.

All samples subsequently were measured at the Caribbean Research Institute Laboratory using a Beckman Dk-2A ratio recording spectrophotometer. This instrument also was used with an MgO-lined integrating sphere. Sandblasted gold and freshly smoked MgO were standards. Hydrogen and tungsten lamps were employed as described above. A photomultiplier (1P28) was used in the 0.32–0.6 μm range, and a PbS cell beyond. The instrument was purged with dry N₂. Spectra were recorded on a stationary chart and on paper tape for digital processing.

Samples were prepared in the same way for both instruments. Sample 87-13 was packaged under vacuum at the Lunar Receiving Laboratory in a specially constructed copper and glass tube. All other materials were handled and packaged inside N₂-filled glove bags. Particulate samples were placed in polished aluminum cups and covered with $\frac{1}{8}$ in. polished glass plate made from G.E. No. 125 material. Rock chips were seated on aluminum foil inside glass jars having tight sealing lids and glass windows. Samples were held in contact with the glass. Standards were covered with glass cut from the same 4 × 4 in. plate as used for the samples. Our tests indicate that the glass, which has excellent transmission from 0.35 to 2.5 μm , does not affect the ratioed spectra when matched covers are used for both the sample and the standard. The glass does introduce an unwanted specular component to the measurements. This was removed by suitable orientation of the samples and standards in relation to the illuminating beams. All measurements, therefore, are of the diffuse component of the reflectivity.

Both spectrophotometers illuminate an area of approximately 5 by 10 mm on samples and references. The rock chips were of diverse sizes and shapes and where they did not completely fill the illuminating beam (10020-37, 10020-38, 10003-33, 10003-34) a black mask was prepared to eliminate reflection from the aluminum foil.

LABORATORY RESULTS AND INTERPRETATION

We made reflectivity measurements of the following kinds of lunar material. (1) Type A, crystalline rock containing olivine, (2) Type B, crystalline rock without olivine, (3) Type C, breccia (two samples), and (4) Type D, surface fines (two samples) (LSPET, 1969). Each sample of rock and of breccia consisted of three chips taken from the top, interior and bottom parts. One sample of fines was packaged in a

vacuum container. All other samples were kept in an N_2 atmosphere except for a small fraction of fines that was deliberately exposed to air.

Broad absorption bands occur in the diffuse reflectance spectra of all of the lunar samples investigated. There are significant differences in band frequencies and band depths among the samples. All observed bands are attributed to electronic transitions in iron and titanium. No vibrational bands were observed. Conspicuously absent are the OH^- or H_2O bands at 1.4 and $1.9 \mu m$ that occur in many terrestrial minerals and rocks.

Sample 10003-33 illustrates the simplest type of curve (Fig. 1) in which the two main bands, one at $0.94 \mu m$ and the other at $2.0 \mu m$, are contributed by Fe^{2+} in the clino-

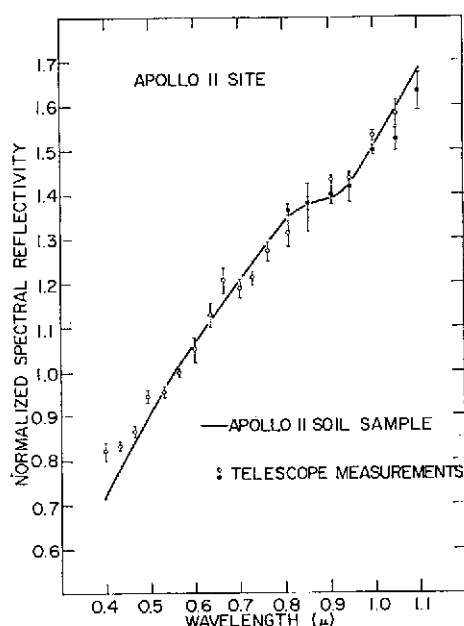


Fig. 1. Spectral reflectance curves of Apollo 11 lunar samples. Reference is MgO . Samples 10003-33 and 10020-38 are crystalline rocks; 10046-39 and 10048-29 are breccias; 10084-66 is surface fines.

pyroxene. The curve is generally similar to polarized absorption spectra and diffuse reflectance spectra of orthopyroxenes (BANCROFT and BURNS, 1967; WHITE and KEESTER, 1967). The common magnesian orthopyroxenes have Fe^{2+} bands at $0.90 \mu m$ and at approximately $1.85 \mu m$. Splitting arises from strong distortion of the M2 site from octahedral symmetry. These two bands shift toward lower frequencies with the substitution of Ca^{2+} for Fe^{2+} on the M2 site (ADAMS, unpublished data). Pigeonite from the Pasamonte basaltic achondrite (DUKE and SILVER, 1967), for example, has bands at $0.93 \mu m$ and at $2.0 \mu m$. A similar shift occurs at the iron-rich end of the orthopyroxene series. BURNS and FYFE (1967) report an orthoferrosilite ($Mg_{0.118}Fe_{0.884}Ca_{0.018}Si_2O_6$) with bands at $0.95 \mu m$ and at approximately $2.1 \mu m$.

The two main bands for sample 10003-33 at $0.94\ \mu\text{m}$ and $2.0\ \mu\text{m}$ are here attributed to Fe^{2+} primarily on the non-centrosymmetric M2 coordination site. The band frequencies clearly distinguish the lunar pyroxene as being more Ca- and/or Fe-rich than the compositional range enstatite-hypersthene which gives bands at 0.90 and $1.85\ \mu\text{m}$, but less calcic than common augite or diopside which have bands at 1.0 and $2.3\ \mu\text{m}$. Band frequencies in 10003-33 do not permit a distinction between pigeonite-subcalcic augite and ferrosilite. However, the absorption coefficient of the ferrosilite is so high that a diffuse reflection spectrum yields only subdued bands even for very fine powders.

Studies of the pigeonites and subcalcic augites from rock 10003 and other lunar rocks demonstrate that the pyroxenes display a range in composition. The optical spectra are necessarily an average of the properties of the several kinds of pyroxenes and of chemical inhomogeneities within kinds. Ross *et al.* (1970), for example, give ratios of augite to pigeonite in single crystals (of rock 10003) of 4:1, 7:3, 1:1, 1:1, 2:3 and 1:4. The degree to which the absorption spectra of these pyroxenes differ is not yet known. Partial answers, at least, will come from transmission measurements on single crystals.

The reflectivity curve for sample 10003-33 also shows a faint (<5 per cent) band at $0.5\ \mu\text{m}$ and a flattening at $1.3\ \mu\text{m}$. The band at $0.5\ \mu\text{m}$ corresponds to the simple d -electron transition in Ti^{3+} [$(t_{2g})^1(e_g)^0$]. The shallow depth of this band may result from the fact that the ratio $\text{Ti}^{3+}:\text{Ti}^{4+}$ is very low. Ross *et al.* (1970) conclude there is little Ti^{3+} in the lunar pyroxenes, based on evidence of coupling of Ti and Al with Si and R^{2+} . Although the lunar pyroxenes contain up to 5% TiO_2 (for example, CHAO *et al.*, 1970) most of it is in the form of Ti^{4+} which has no $3d$ electrons.

The weak band at $1.3\ \mu\text{m}$ we assign to Fe^{2+} and not to Ti as reported earlier (ADAMS and JONES, 1970). The structure may arise from Fe^{2+} on the M1 site in the pyroxene, however, it also occurs for ilmenite powder and for calcic plagioclase containing minor Fe^{2+} . There is no evidence for bands arising from chromium.

Sample 10003-33 is a useful reference for the interpretation of bands in other lunar materials, for it contains essentially no olivine or glass. The other major minerals present, plagioclase and ilmenite, do not contribute any measurable band structure to the rock curve in diffuse reflected light. Sample 10020-38 differs mineralogically from sample 10003-33 in that approximately 5% olivine is present. In diffuse reflected light olivine alone has a single strong absorption band at $1.03\ \mu\text{m}$ that arises from Fe^{2+} in sixfold coordination. In the curve for sample 10020-38 (Fig. 1) the band at $1.00\ \mu\text{m}$ is attributed to a combination-band representing the unresolved $0.94\ \mu\text{m}$ pyroxene and $1.03\ \mu\text{m}$ olivine bands. The band at $2.0\ \mu\text{m}$ is assigned to the pyroxene alone, for olivine has no selective absorption in this wavelength region. The $0.94\ \mu\text{m}$ frequency of the pyroxene band is assumed on the basis that the average pyroxene composition is similar to that in sample 10003-33. We have not yet made mineral separates to allow us to measure the individual curves of the pyroxene and of the olivine; however, using the 10003-33 pyroxene curve and the curve from a terrestrial olivine (Fo_{75}) we calculate a sum that is very similar to the curve for 10020-38. The curve for sample 10020 also shows the titanium band at $0.5\ \mu\text{m}$ and the weak Fe^{2+} band at $1.3\ \mu\text{m}$. The titanium band probably is contributed only by the pyroxene.

HAGGERTY *et al.* (1970) do not record a band at $0.5\ \mu\text{m}$ in their single crystal measurement of olivine from sample 10020. They found a probable Cr^{2+} band at $1.04\ \mu\text{m}$; however, it is too faint to be resolved in the reflectivity spectra.

The samples of fines and breccias also contain pyroxene and traces of olivine, but less olivine than sample 10020. The fines and breccias show a weak (<5 per cent) band at approximately $0.95\ \mu\text{m}$ and only a faint suggestion of a dip near $2\ \mu\text{m}$ (see Fig. 1). The $0.95\ \mu\text{m}$ band is consistent with the observed proportions of pyroxene and olivine and does not require the presence of other minerals. The virtual disappearance of the $2.0\ \mu\text{m}$ band in the fines and breccias is related to the overall darkness of these materials and to their lower pyroxene content.

The fines and breccias are darker, have shallower absorption bands, and have steeper overall curves than the crystalline rocks. We attribute these features to the presence of the dark red-brown glass. Although the glass selectively absorbs shorter wavelengths, it does not contribute measurable closed-band structure to the lunar materials in reflected light. The steepening of the curve probably results from a charge-transfer 'band' in the dark glass. Charge-transfer transitions cause very strong absorption in the ultraviolet and blue regions (BURNS and FYFE, 1967). Our spectra do not reveal the high frequency limb of this 'band', only the low reflectivity in the blue. We suggest that the strong absorption in the glass is caused by the high content of iron and titanium that was derived largely from ilmenite through melting, probably by impact, of the crystalline rock. The decrease in reflectivity from crystalline rock to glass-rich rock or fines can be explained by more efficient use of the available metal ions as light absorbers. In the oxide form, ferrous iron absorbs nearly all incident light in the outer few microns of a mineral grain; hence the interior portion of an ilmenite grain does not further attenuate light. If, however, the ilmenite grain is dissolved in a silicate melt, there is greater opportunity for light absorption by each iron or titanium ion through the charge-transfer mechanism.

Microbrecciation of mineral grains (presumably by impact shock) is observed on the surfaces of many of the Apollo 11 rocks. Micro-fractured silicate minerals reflect more light than undisturbed grains. Each fracture is an optical discontinuity with the potential of reflecting incident light. The effects of microbrecciation are closely analogous to the increase in reflectivity that results from grinding silicate minerals to smaller particle sizes (ADAMS and FILICE, 1967). Comparison of reflectivity measurements of outside and of interior surfaces of the lunar samples shows that although microbrecciated surfaces have up to a 30 per cent higher reflectivity, there is no change in the frequency of any of the absorption bands. This observation is in agreement with theory, for the major band frequencies are determined by Fe—O bond configurations which in turn are little affected by mechanical deformation on a scale larger than the unit cell.

More extreme shock leads to vitrification of mineral grains, and it is expected that absorption bands will shift in frequency when new metal—oxygen bonds are formed. In the samples observed glass-lined pits covered too small an area and the glass was too dark to yield a definitive measurement of any new absorption bands. We observed that in reflected light absorption-band frequencies are unaffected by the presence of glass-lined pits or microbrecciated zones on the surfaces of the Apollo 11 rocks.

We have found no evidence for thick metal coatings or other deposits (other than glass) on the surfaces of mineral grains. If such coatings are present they are not thick enough to cause a measurable attenuation of light and can be disregarded for purposes of interpreting mineral absorption bands from reflection spectra.

Reflectivity measurements also were made of surface fines in vacuum, in N_2 , and in air to test for possible changes arising from removal of the samples from the lunar environment. No differences in reflectivity were observed between 10087-13 in vacuum and 10084-66 which had been exposed to dry nitrogen. In addition, 0.5 g of 10084-66 were exposed to air for 3 weeks at 25°C. No departures from the previous reflectivity measurements were noted.

COMPARISON WITH TELESCOPIC DATA

We have compared the laboratory reflectivity curves of the Apollo 11 rocks with earth-based telescopic measurements of the landing site. (McCord *et al.*, 1969; McCord and Johnson, 1970a). The reflectivity curve (0.4–1.1 μm) for an 18-km dia. area that includes the Apollo 11 site agrees very closely with the laboratory curve for the bulk surface fines (Fig. 2). Extension of the telescopic curve from 1.1–2.5 μm using data from a similar area in Tranquillitatis (Fig. 3) reveals a close fit throughout the spectral region measured. From these data we conclude that: (1) Sample 10084-66 (fines) is representative of the main lunar surface material for at least tens of kilometers around the Apollo 11 site. (2) Crystalline rocks are not abundant enough at and around this site to impose the pyroxene double-band structures on the telescopic reflectivity curves. (3) The single weak band at 0.95 μm in the telescopic curve is the clinopyroxene-olivine combination-band, the contribution from olivine being very minor. The telescopic curves, therefore, are recording mineralogical information. (4) The low albedo of the Mare Tranquillitatis, the steepness of the reflectivity curve, and the weakness of the absorption-band structure can be accounted for at least in large part by the presence of iron- and titanium-rich glass. (5) Interpretation of telescopic curves for other parts of the moon can be expected to yield information on areal differences in mineralogy and on relative proportions of crystalline rock vs. glassy soil and breccia.

It is of considerable interest to consider telescopic curves for other areas on the lunar surface in view of these conclusions. Figure 4 shows comparisons between the reflectivity curve for Mare Serenitatis and six other areas, including Mare Tranquillitatis (McCord and Johnson, 1970b). Curve shapes are generally similar to that for the Apollo 11 fines. Other lunar areas, except Littrow, show a band at approximately 0.95 μm , although for Uplands 7 the band is extremely faint. We conclude that the curves in Fig. 4 (excepting Littrow) arise from materials having approximately the same proportions of pyroxene and olivine as found in the Apollo 11 fines. For example, we exclude as possibilities rocks in which olivine is the major mafic silicate, or rocks in which orthopyroxene is dominant rather than clinopyroxene. The absence of band structure in the Littrow curve may arise from a high content of dark glass. This interpretation is compatible with the steep slope of the curve and with the exceptionally low albedo of this area.

The relatively deep 0.95 μm band in the curves for Kepler and for Aristarchus

suggests a larger ratio of clinopyroxene to dark glass, and perhaps rocks to soil, than at the Apollo 11 site. This interpretation is supported further by the suggestion of bands in the $2\text{ }\mu\text{m}$ region of both curves, and by less intense absorption at the blue end of the spectrum.

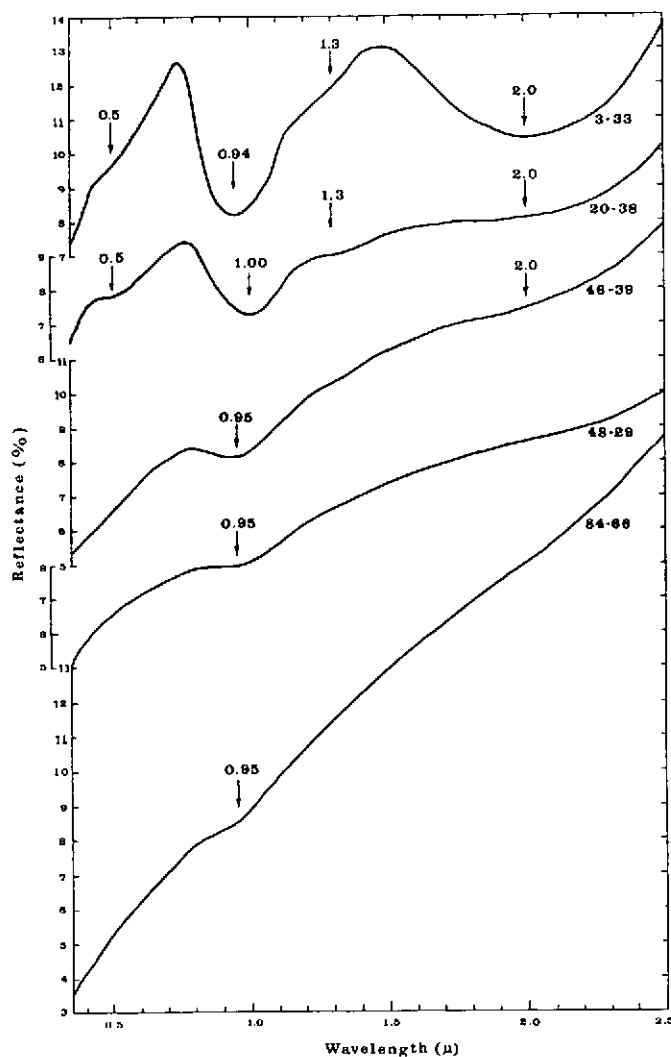


Fig. 2. Comparison of telescopic reflectivity curve (0.4–1.1 μm) for an 18 km area that includes the Apollo 11 site with the curve for sample 10084-66, surface fines.

The faint band in the Uplands 7 curve may mean that there is less clinopyroxene than at the Apollo 11 site, or possibly the band has been degraded by greater microfracturing or comminution. It is unlikely that the band-degradation is due to more abundant dark glass in view of the higher albedo of this region.

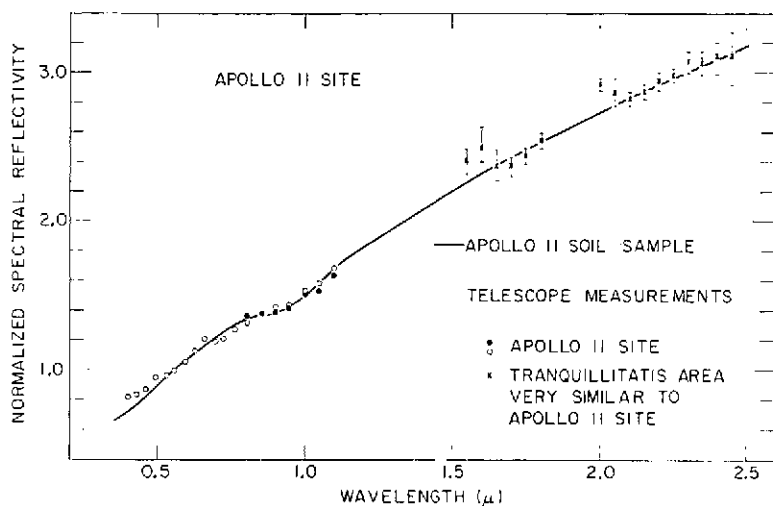


Fig. 3. Comparison of a composite telescopic reflectivity curve (0.4-2.5 μ m) for the Apollo 11 site and an adjacent area, with sample 10084-66, surface fines.

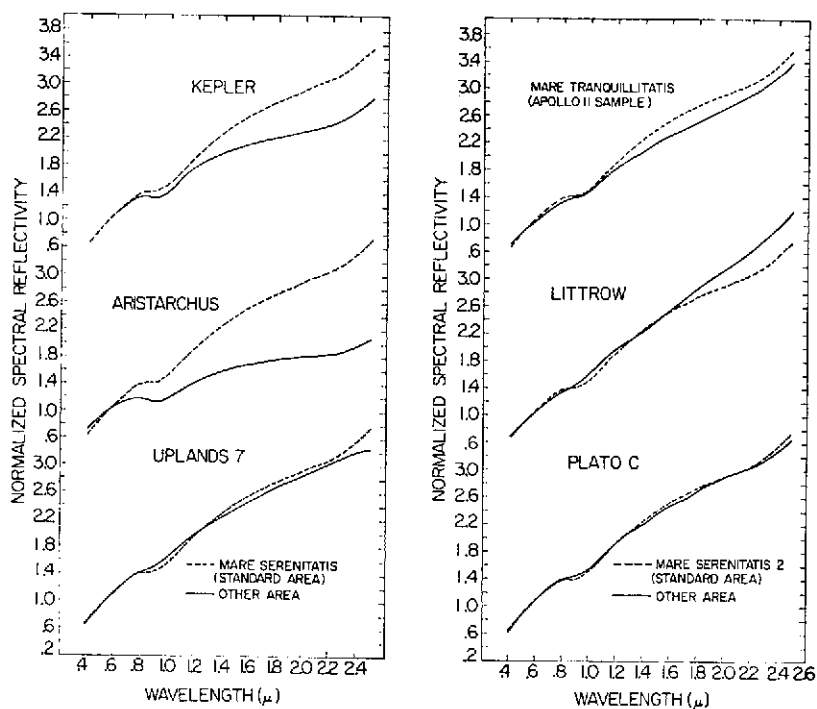


Fig. 4. Normalized spectral reflectivity curves for six lunar areas.

We feel that there is considerable work still to be done to put the spectral reflectivity measurements and interpretations into a geological context. More information is needed on the areal extent of given spectral characteristics to allow correlation with geologic features and other physical properties. We feel, also, that telescopic or orbital measurements at high spatial resolution will permit selection of rocky areas, which, in turn, will give maximum band structure and mineralogical information.

Acknowledgments—We thank ROBERT JONES and JEAN LARSEN for their assistance with the laboratory measurements. This work was supported by NASA (NAS 9-9578 and NGR 22-009-350).

REFERENCES

- ADAMS J. B. (1968) Lunar and martian surfaces: petrologic significance of absorption bands in the near-infrared. *Science* **159**, 1453–1455.
- ADAMS J. B. and FILICE A. L. (1967) Spectral reflectance 0.4 to 2.0 microns of silicate rock powders. *J. Geophys. Res.* **72**, 5705–5715.
- ADAMS J. B. and JONES R. L. (1970) Spectral reflectivity of lunar samples. *Science* **167**, 737–739.
- BANCROFT G. M. and BURNS R. G. (1967) Interpretation of the electronic spectra of iron in pyroxenes. *Amer. Mineral.* **52**, 1278–1287.
- BURNS R. G. (1965) Electronic spectra of silicate minerals: application of crystal-field theory to aspects of geochemistry. Ph.D. Dissertation, University of California, Berkeley.
- BURNS R. G. and FYFE W. S. (1967) Crystal-field theory and the geochemistry of transition elements. In *Researches in Geochemistry*, (editor P. H. Abelson), Vol. 2, 259–285. John Wiley.
- CHAO E. C. T., JAMES O. B., MINKIN J. A., BOREMAN J. A., JACKSON E. D. and RALEIGH C. B. (1970) Petrology of unshocked crystalline rocks and shock effects in lunar rocks and minerals. *Science* **167**, 644–647.
- DUKE M. B. and SILVER L. T. (1967) Petrology of eucrites, howardites and mesosiderites. *Geochim. Cosmochim. Acta* **31**, 1637–1665.
- HAGGERTY S. E., BOYD F. R., BELL P. M., FINGER L. W. and BRYAN W. B. (1970) Iron–titanium oxides and olivine from 10020 and 10071. *Science* **167**, 613–615.
- LSPET (LUNAR SAMPLE PRELIMINARY EXAMINATION TEAM) (1969) Preliminary examination of lunar samples from Apollo 11. *Science* **165**, 1211–1227.
- MCCORD T. B., JOHNSON T. V. and KIEFFER H. H. (1969) Differences between proposed Apollo sites: II. Visible and infrared reflectivity evidence. *J. Geophys. Res.* **74**, 4385–4388.
- MCCORD T. B. and JOHNSON T. V. (1970a) Spectral reflectivity of the moon. In preparation.
- MCCORD T. B. and JOHNSON T. V. (1970b) The spectral reflectivity of the lunar surface (0.30 μm to 2.50 μm) and implications for remote mineralogical analyses. In preparation.
- ROSS M., BENICE A. E., DWORNIK E. J., CLARK J. R. and PAPIKE J. J. (1970) Lunar clinopyroxenes: chemical composition, structural state, and texture. *Science* **167**, 628–630.
- WHITE W. B. and KEESTER K. L. (1966) Optical absorption spectra of iron in the rock-forming silicates. *Amer. Mineral.* **51**, 774–791.
- WHITE W. B. and KEESTER K. L. (1967) Selection rules and assignments for the spectra of ferrous iron in pyroxenes. *Amer. Mineral.* **52**, 1508–1514.

Optical properties of mineral separates, glass, and anorthositic fragments from Apollo mare samples

JOHN B. ADAMS

Caribbean Research Institute, College of the Virgin Islands, St. Croix 00820
and

THOMAS B. MCCORD

Planetary Astronomy Laboratory Department of Earth and Planetary Sciences
Massachusetts Institute of Technology, Cambridge, Massachusetts 02139

(Received 22 February 1971, accepted 29 March 1971)

Abstract—Visible and near-infrared spectral reflectivity measurements of mineral separates from an Apollo 12 basalt demonstrate that pyroxene absorption bands dominate the curves of mare rocks and soil. Plagioclase, ilmenite, olivine, and other minerals have relatively little effect on the shapes of the reflectivity curves, although the proportions of feldspar and of opaques can affect albedo. By adding artificial glass back to the basalt from which it was made, it is shown that progressive vitrification of ilmenite-rich mare rocks causes darkening and masking of the pyroxene absorption bands, without imparting any of the (weak) band structure of the glass. Anorthositic lithic fragments separated from Apollo 11 soil have reflectivity curves that are dominated by low-Ca pyroxene, whereas telescopic curves of the lunar highlands show a band that indicates pyroxene of the same average composition as occurs at the Apollo 11 and Apollo 12 sites.

INTRODUCTION

THIS PAPER PRESENTS the results of laboratory measurements of the spectral reflectivity of Apollo 12 samples and a comparison of the results with Apollo 11 samples and with telescopic measurements of the lunar surface. An interpretation of the telescopic data, taking into account the laboratory studies of lunar samples, is published separately (ADAMS and MCCORD, 1971).

The following Apollo 12 samples were examined: fines 12042,41 and 12070,111; samples from the double core tube 12025,25; 12025,50; and 12028,97; and rocks 12053,23; 12053,29; 12053,30; and 12063,75; 12063,79; 12063,82. The core-tube samples are, respectively, from the following depths (uncorrected for compaction): 0.4–1.2 cm, 6.0–7.0 cm, 19.7–20.8 cm. The two rocks each consist of chips from top, interior, and bottom surfaces. Reflectivity measurements were made with a Beckman DK2-A ratio-recording spectrophotometer. The instrument and sample-handling procedures are discussed by ADAMS and MCCORD (1970). In the present study all samples were handled in air after it was determined that no changes in reflectivity resulted from exposure to dry air at room temperatures.

In our reports on the Apollo 11 samples (ADAMS and JONES, 1970 and ADAMS and MCCORD, 1970), we called attention to the differences between the spectral reflectivity curves for crystalline rocks and those for breccias and fines. The rock curves have well-developed absorption bands, whereas the breccias and the fines have only faint vestiges of bands. The main absorption bands in the rocks were attributed to Fe^{2+} in

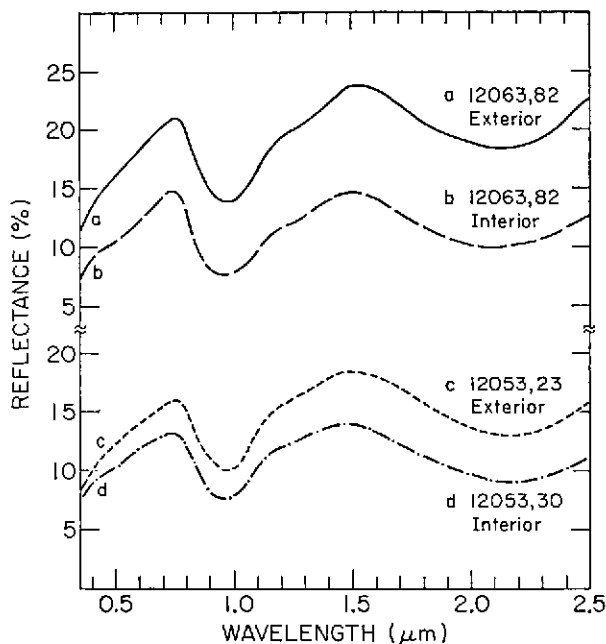


Fig. 1. Spectral reflectivity curves of exterior and interior surfaces of chips of Apollo 12 basalts 12063 and 12053. All measurements are relative to MgO.

pyroxene. The progressive degradation of these bands from rocks to breccias to fines was correlated with an increase in the percentage of dark glass.

The Apollo 12 samples are generally similar to those from the Apollo 11 site in their optical properties. The rocks (Fig. 1) exhibit strong absorption bands whereas the surface fines (Fig. 2) have weak bands. Our samples of Apollo 12 fines included light and dark material from the double core tube. These samples provided important additional evidence on the factors controlling the strength of the optical absorption bands. We have obtained further information on the origin of the bands in the Apollo 12 materials by analyzing mineral separates (Fig. 3). We have, in addition, fused Apollo 12 crystalline rock and investigated the optical properties of the glass and of glass-crystal mixes (Fig. 4). The results of these analyses lead to a consistent explanation for the main optical properties of the lunar samples at the Apollo 11 and 12 sites and correlate well with the telescopic measurements.

LABORATORY RESULTS

The optical properties of the moon as seen from an earth-based telescope are dominated by the fine soil at the surface. The Apollo 11 and 12 soils are made up of a complex assortment of silicate minerals, oxides, and glasses, with very minor sulfides and metals. To understand the optical properties of the bulk soil it is useful to start with the properties of individual mineral species and work toward multiphase assemblages.

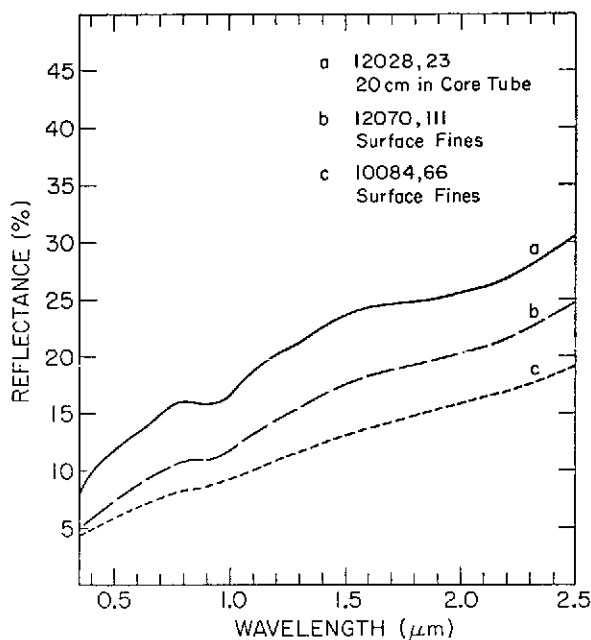


Fig. 2. Spectral reflectivity of Apollo 11 surface fines, Apollo 12 surface fines, and Apollo 12 fines from 20 cm deep in the double-core tube.

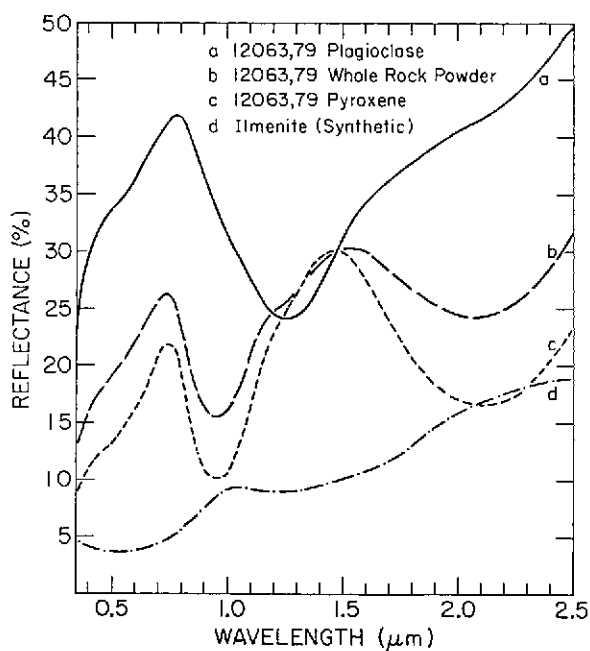


Fig. 3. Spectral reflectivity of Apollo 12 basalt powder 12063, and plagioclase and pyroxene separates from the same rock. Ilmenite is a synthetic sample.

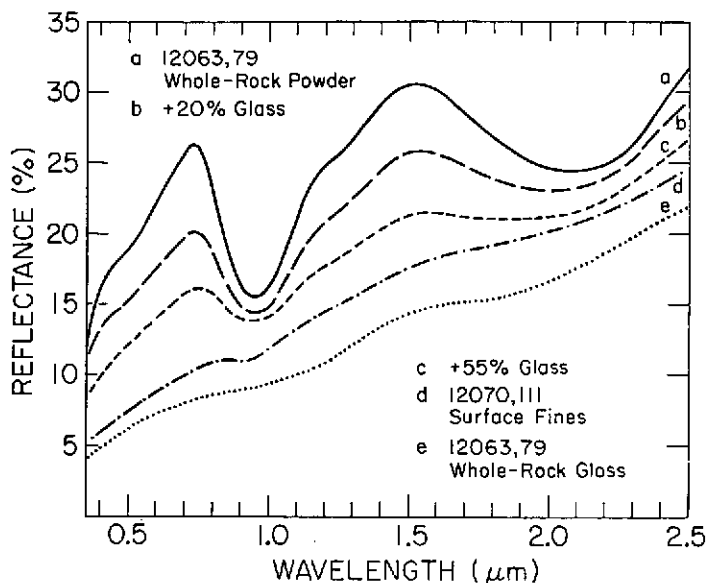


Fig. 4. Spectral reflectivity of glass made from 12063 whole-rock powder; mixtures of rock powder plus 20% glass and plus 55% glass; compared with curve of Apollo 12 surface fines.

Mineral separates were made from 0.5 gms of rock 12063 using a combination of magnetic techniques and hand-picking under the microscope. The rock consists of 51% pyroxene and 27% plagioclase, with 8% olivine and 11% opaques, mostly ilmenite (WARNER, 1970). It was possible to obtain only nearly pure separates of pyroxene and of feldspar owing to the limited amount of starting material. Figure 3 shows spectral reflectivity curves for the whole rock, the plagioclase separate, and the pyroxene separate, all sized to particles between 125 μm and 500 μm . Also shown for reference is a curve for synthetic ilmenite powder (< 44 μm).

The pyroxene has two strong absorption bands at 0.95 μm and at 2.1 μm . These bands are produced by Fe^{2+} on a highly distorted (M2) octahedral site, and their assignments have been treated in detail elsewhere (BANCROFT and BURNS, 1967 and ADAMS and McCORD, 1970). A weak Ti^{3+} band occurs at 0.5 μm , and there is the suggestion of a band at 1.25 μm , which probably arises from Fe^{2+} on the M1 site.

The curve for plagioclase is characterized by a strong Fe^{2+} band centered at 1.25 μm and by strong absorption at the blue end of the spectrum. Comparison with curves of terrestrial calcic feldspars suggests that our lunar specimen still includes a component of pyroxene. This is seen in the flattening at 0.5 μm , the shallow depression near 1 μm , and in the faint band at 2.1 μm . Tiny inclusions (seen under the microscope) of the strongly absorbing pyroxene in the relatively clear plagioclase account for the above features.

To conserve sample, no attempt was made to separate ilmenite from rock 12063. The main spectral features are illustrated by a synthetic stoichiometric ilmenite. The

band at $0.5\ \mu\text{m}$ is assigned to Ti^{3+} , and the broad depression between $1.0\ \mu\text{m}$ and $1.5\ \mu\text{m}$ is assigned to Fe^{2+} . Note that the curve in Fig. 3 is from a $< 44\ \mu\text{m}$ powder that allows light to pass through individual particles without being totally absorbed. For larger particle sizes, the absorption bands become less distinct and the overall reflectivity decreases.

Olivine, which makes up $< 10\%$ of rock 12063 was not separated—again, to conserve sample. The optical properties of olivine are well known (ADAMS, 1968), and we would expect a broad Fe^{2+} band at $1.02\ \mu\text{m}$.

It is evident from Fig. 3 that the curve of the whole rock is overwhelmingly dominated by the spectral features of the pyroxene. Only the weak band at $1.25\ \mu\text{m}$ in the rock curve is derived largely from plagioclase, as was suggested by CONEL and NASH (1970), although it overlaps the Fe^{2+} bands in pyroxene and in ilmenite, as was pointed out by ADAMS and MCCORD (1970). Ilmenite, olivine, and other minor minerals do not contribute significantly to the spectral reflectivity of rock 12063. Rock chips (Fig. 1), although slightly darker than the whole rock powders, show the same main spectral features. All curves are dominated by pyroxene. Freshly broken surfaces of the two Apollo 12 samples are slightly darker and have flatter curves than those for the natural outer surfaces of the specimens. We found a similar relationship for Apollo 11 rock samples. The natural outer surfaces of the rocks are highly microfractured. These optical discontinuities cause more light to be reflected, in the same way that crushing the rock to progressively finer particle sizes increases the albedo (ADAMS and FILICE, 1967). Although the exterior surfaces also contain glassy pits, there is no apparent effect on the spectral curves from the small amount of glass. Significantly, the "space weathering" of the rocks does not shift the positions of the absorption bands.

The spectral curves of the fines (Fig. 2) are different from those of the rocks. The two pyroxene bands are present, but they are very weak, and the integral reflectivity is about one-half that of the rock powder. Of the five Apollo 12 samples of fines that we measured, all had identical spectral curves except the light gray fines from 20 cm in the core tube. The other four samples available to us were from the surface or within the top 7 cm of the core tube, and have a curve given by 12070,111 in Fig. 2. Our 20 cm core-tube sample has a higher overall reflectivity and stronger absorption bands than the surface fines. NASH and CONEL (1971) reported on a different set of samples from the core tube and showed that albedo does not vary as a simple function of depth. They found, however, that the brighter materials have deeper absorption bands.

The most striking difference between lunar soil and rocks is the presence of abundant glass in the soil. Although the glass is highly varied in composition and therefore in color and refractive index, the most abundant type is a dark reddish brown.

We are still separating glasses from the lunar soil in an attempt to make a direct measurement of their optical properties. Separation of a sufficient quantity of glass is, however, a very slow procedure. Meanwhile, we have made artificial glass from crystalline rock (12063). The spectral curve for this glass and for mixtures of crystalline rock powder and glass powder are shown in Fig. 4.

Glass was made from 40 mg of the whole-rock powder of rock 12063. The charge

was held in a platinum tube at 1300°C for 1.5 hours. The furnace was purged with dry N₂ during the run to prevent oxidation of the sample. The fused product is very dark brown. This glass was crushed and the powder was measured with the spectrophotometer. The curve for the glass has two broad absorption bands at approximately 1.1 μm and 1.9 μm . These bands are from Fe²⁺ on highly distorted sites. The curve and the bands are closely similar to those of terrestrial basaltic glasses that we have measured in our laboratory. The results are also in agreement with CONEL and NASH (1970) (see also CONEL, 1970).

To simulate the production of lunar soil by partial vitrification of crystalline rock, we added glass powder back to the same rock powder from which the glass was made (Fig. 4). Three points are significant: (1) The addition of dark glass lowers the albedo of the overall powder. (2) The absorption bands of the glass (1.1 μm and 1.9 μm) do not appear when the glass is mixed with the crystalline powder. (3) The absorption bands in the curve of the rock powder are progressively weakened as more glass is added. The disappearance of the glass bands in the mixed powder is not surprising in view of the absence of ilmenite (and plagioclase) bands in the rock-powder curve (Fig. 3). The weakening of the pyroxene bands in the rock-powder curve with the addition of glass is caused by the overall darkening of the mix, which leads to a lessening of differential absorption. The same effect can be produced by adding carbon-black or any other very dark material.

Figure 4 also shows the curve for Apollo 12 surface fines. We conclude that the curves of the natural mare soils can be explained in terms of crystalline rock powders (in which pyroxene dominates the optical properties), that have been partially melted to yield a mixture of dark glass and crystalline phases. As more glass is produced by micrometeoroid bombardment at the lunar surface, the soil should become darker and the pyroxene bands become less distinct. There is evidence for this effect in Fig. 2. The 20 cm core tube sample contains about 10% glass (our estimate), the Apollo 12 surface fines have about 20% glass (LSPET 1970), and the Apollo 11 soil (10084) contains approximately 50% glass (LSPET 1969). These curves show that as the glass content increases, the albedo decreases and the pyroxene bands become fainter.

Although our experiments with artificial glass illustrate the importance of glass for the lunar optical properties, there are differences between our laboratory mix and the natural lunar fines. Notably, our crushed glass consists wholly of chips and splinters that transmit more light than the spherical or equant grains of lunar glass which trap light by multiple internal reflections. Even very small (< 20 μm) spheres of the lunar brown glass are dark under the microscope. When we grind the artificial glass to particle sizes approaching the lunar material, the albedo is too high owing to the decreased mean path length of light in the irregular grains. The most important difference, however, is that none of the dark glass sticks to the other mineral grains. Therefore, a greater surface area of light particles is exposed in the laboratory mix than in the natural mare soil. The lack of sticking and the marked difference in particle shape may explain why the addition of 20% artificial glass does not reduce the albedo to that of the Apollo 12 soil containing 20% natural glass. It may also explain why CONEL and NASH (1970) found a higher albedo for their artificial glass than for the Apollo 11 soil. We also note that rock 12063 from which we made glass contains about

10% ilmenite. This percentage may not be representative of the ilmenite content of the average local basalt. Higher concentrations of ilmenite will yield darker glasses.

GOLD *et al.* (1970) and O'LEARY and BRIGGS (1970) reported that sputter-deposited metal coatings on Apollo 11 soil particles cause the low albedo of the soil. The presence of ubiquitous metal coatings, however, is contradicted by other evidence from electron microscopy, Mössbauer studies, magnetic properties, and electrical properties. (See, for example, GOLDSTEIN *et al.*, 1970; MCKAY *et al.*, 1970; FRONDEL *et al.*, 1970; HERZENBERG and RILEY, 1970; STRANGWAY *et al.*, 1970; GOLD *et al.*, 1970.)

HAPKE *et al.* (1970) drew attention to possible sputter-deposited opaque coatings on Apollo 11 fines, and HAPKE *et al.* (1971) presented evidence, based on an acid-leaching technique, for impact-produced vapor-deposited glassy coatings (approximately 2 μm thick) on the Apollo 12 fines. It is well known that glass cements particles in the breccias and soils, and that glass partially or even completely coats some grains. The occurrence and formation of glass, however, are highly complex and do not fit a simple vapor deposition model (MCKAY *et al.*, 1970; MCKAY *et al.*, 1971; FREDRIKSSON *et al.*, 1970). We agree with HAPKE *et al.* (1970) that dark glass in the mare soil lowers the albedo; however, it is important to emphasize that glass does not coat all grains and, in fact, occurs in many forms such as local splashes, interstitial "cement," spherules, and irregular fragments. The ability of glass to stick to other particles strongly affects the optical properties as we pointed out earlier. In the mare soils sticking apparently has occurred over a range of temperatures, from the softening point of a glass through the liquid and vapor phases.

Using high voltage transmission electron microscopy, BORG *et al.* (1971) found amorphous rinds 0.1 μm thick on 1 μm diameter particles of Apollo 12 soil. These rinds appear to be a radiation-damaged outer portion of the crystalline material rather than a surface-deposited layer. BORG *et al.* (1971) also reported that the damaged particles have a lower albedo than the undamaged ones. A definitive test, however, requires classifying and separating otherwise similar 1 μm lunar soil particles according to whether they have damaged outer layers or not. Albedo measurements of the two classes of particles would require the separation of at least 50 mg of each class. This is a formidable task in view of the difficulties in handling (and classifying) such small particles. Until such separates can be made, without bias as to percentages of mineral and glass species, or until albedo can be measured on single 1 μ particles, the reported effect of the damaged layers on albedo must remain in doubt. If the 0.1 μm rinds do lower the albedo, it must be determined that such damaged layers also occur for the wide size range of larger particles before a generalization can be made about the lunar soil as a whole. We note that the exteriors of rocks are in fact brighter than their interiors (Fig. 1). Any darkening effect on the rocks is lost in the brightening due to microbrecciation. In like manner, any darkening of the soil by radiation damage is overwhelmed by the readily visible darkening due to the production of glass.

Based on the existing data we do not rule out the possibility that radiation damage lowers the albedo of lunar soil, but further work is necessary to determine the magnitude of any effects. Our results indicate that such effects on albedo must be minor, if they occur at all, and that they are not required to explain the optical properties of the mare soil samples.

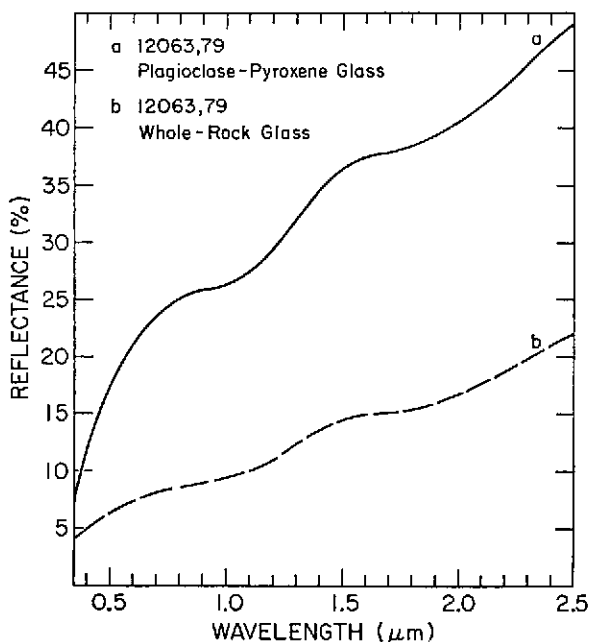


Fig. 5. Comparison of spectral reflectivity of glass made from Apollo 12 basalt (12063) containing about 10% ilmenite (lower curve), and glass made from a 1:1 by weight mixture of plagioclase and pyroxene from the same rock (upper curve).

In our study of the Apollo 11 soil (ADAMS and JONES, 1970; ADAMS and McCORD, 1970) we proposed that the strong optical absorption in the glass was caused by iron and titanium that had been derived largely from ilmenite. Our glass experiments with Apollo 12 samples support this idea. We used portions of our mineral separates of plagioclase and of pyroxene to prepare a mixture that simulated a mare basalt that was free of ilmenite. Pure plagioclase and pure pyroxene powders were mixed 1:1 by weight and fused in a platinum tube, as previously described. The resulting glass is light tan, as contrasted with the very dark brown of the glass derived from the whole rock. Spectral reflectance curves of the two types of glass are shown in Fig. 5. The plagioclase-pyroxene glass has a higher overall reflectivity than the whole-rock powder (12063).

We conclude that ilmenite in the mare basalts is essential to the production of the dark glass, which, in turn, accounts primarily for the low albedo of the soil. Rocks without ilmenite (or other opaque phases) would be expected to undergo little or no darkening at the lunar surface as a result of vitrification.

ANORTHOSITIC ROCKS COMPARED WITH LUNAR HIGHLANDS

We turn now to the feldspathic component of the Apollo 11 and 12 soils. We separated anorthositic fragments from the Apollo 11 soil and measured the spectral reflectivity (Fig. 6). We took care to exclude all pieces of coarse basalt from our

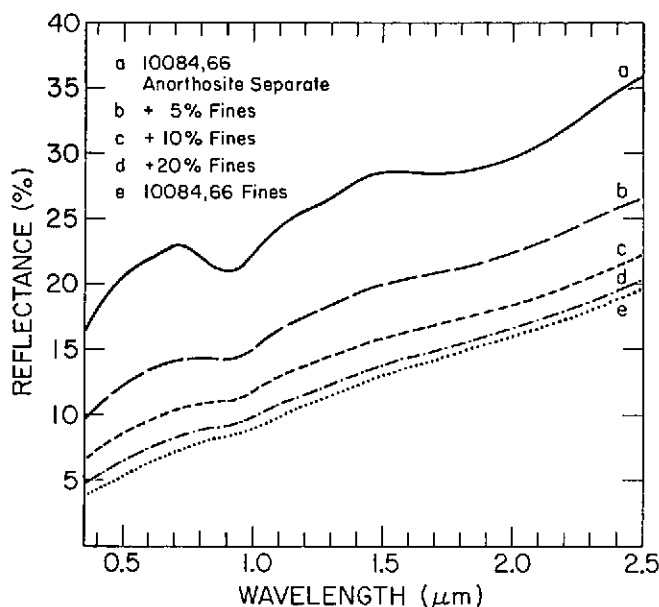


Fig. 6. Spectral reflectivity of anorthositic lithic fragments from Apollo 11 soil; compared with curves of the same material plus 5%, 10%, and 20% of fines from Apollo 11 soil (10084).

anorthositic sample, following the criteria of WOOD *et al.* (1970). There are two striking features of the curve for the anorthositic separate: (1) The curve is dominated by pyroxene features rather than by the plagioclase, even though pyroxene makes up < 10% of the sample. This can be understood in terms of our previous discussion of mineral separates (Fig. 3). (2) The pyroxene bands are at $0.91 \mu\text{m}$ and at $1.8 \mu\text{m}$. These band frequencies correspond to pigeonite or orthopyroxene. Low calcium pyroxenes are characteristic of the anorthositic fragments as has been verified by optical and microprobe analyses (WOOD *et al.*, 1970).

We did not have a large enough sample of Apollo 12 soil to separate out the "foreign" feldspathic component. However, reports on the mineralogy of, for example, "Luny Rock 1" (10085, ALBEE *et al.*, 1970), rock 12013 (DRAKE *et al.*, 1970), "KREEP" (GAST and HUBBARD, 1971), "Norite" (WOOD *et al.*, 1971) refer consistently to feldspathic rock containing minor low-calcium pyroxene. Although we have not yet made direct measurements on these Apollo 12 feldspathic rocks, we expect, based on the mineralogy, that the reflectivity curves will be very similar to the Apollo 11 anorthositic separate (Fig. 6). The band positions should be very near $0.91 \mu\text{m}$ and $1.8 \mu\text{m}$.

The Apollo 11 and 12 feldspathic rocks have far less ilmenite (typically $\ll 5\%$) than the basalts. Anorthositic glasses from the Apollo 11 soil have about the same albedo as the crystalline fragments, and we expect that, in general, the Apollo 11 and 12 feldspathic materials alone darken little, if at all, by impact vitrification at the lunar surface. If comparable feldspathic rocks comprise the lunar highlands (WOOD *et al.*,

1970), an interesting problem arises as to how highland bright craters and rays with albedo ~ 0.25 darken with time to an albedo of ~ 0.13 . ADAMS and McCORD (1971) pointed out that the optical properties of the highlands may imply contamination by a few % of the dark mare soil. We will not review here the arguments supporting the contamination hypothesis. We have, however, added Apollo 11 fines back to our Apollo 11 anorthositic separate to observe the change in spectral reflectivity. Figure 6 illustrates that addition of 5% to 10% of the dark fines degrades the absorption bands of the anorthositic material and depresses the albedo.

There are two important differences between the laboratory curve for the Apollo 11 anorthositic rock and the telescopic curves of the lunar highlands (ADAMS and McCORD, 1970; McCORD *et al.*, 1971; and Figs. 7 and 8): The pyroxene band is (1) faint to absent for most of the highlands, (2) except for bright craters and rays where the band is at $0.95 \mu\text{m}$ (rather than at 0.91 for the anorthositic sample).

ADAMS and McCORD (1971) presented evidence that the bright craters and rays have a higher crystal/glass ratio than the surrounding areas. The absorption band at $0.95 \mu\text{m}$ indicates that highland "rocky" areas have an average pyroxene composition similar to that found in the mare basalts, in contrast to the low calcium pyroxene of the feldspathic rocks recovered from the Apollo 11 and 12 sites.

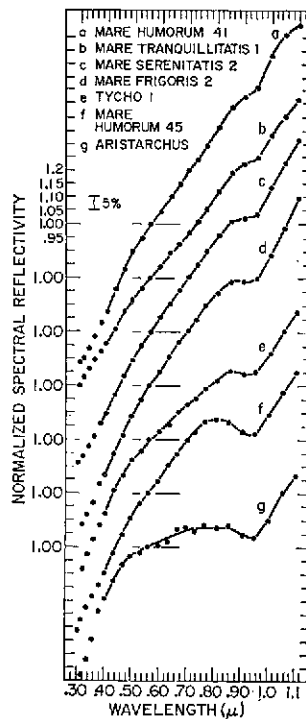


Fig. 7. Normalized spectral reflectivity curves of 18 km-diameter areas on the lunar surface (McCord *et al.*, 1971). (a) highland area near edge of Mare Humorum, (b) dark mare area (Tranquillitatis), (c) standard mare area (Serenitatis), (d) mare area (Frigoris), (e) highland bright crater (floor of Tycho), (f) mare bright crater (Mare Humorum), (g) mare bright crater (Aristarchus).

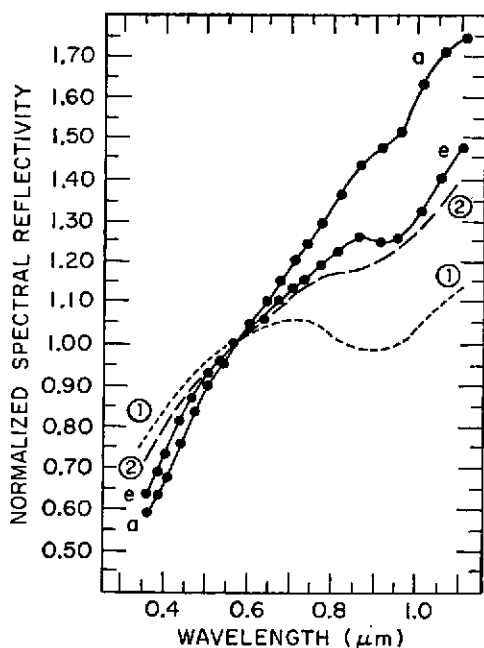


Fig. 8. Normalized spectral reflectivity curves of (1) anorthositic separate from Apollo 11 soil, (2) anorthositic material plus 10% fines from Apollo 11 soil, and telescopic curves of (a) highland area, and (e) highland bright crater (Tycho).

The telescopic curves of "background" highland areas (other than bright craters and rays) have only a slight change of slope in the $0.9\text{ }\mu\text{m}$ to $1\text{ }\mu\text{m}$ region. The alteration of highland bright crater and ray material to "background" soil is accompanied by an almost complete degradation of the pyroxene band. Contamination by mare fines (or any other dark material), although it lowers the albedo, does not cause this much degradation of the pyroxene band (see Fig. 8). It is unlikely that the highland regolith is devoid of a pyroxene component, as the pyroxene band appears wherever (subsurface) bright-crater material is exposed. The disappearance of the band, instead, may be due to disordering of the pyroxene structure by extensive impact melting and shock alteration of the soil. Complete melting of the soil, however, probably would produce the weak Fe^{2+} band at $1.1\text{ }\mu\text{m}$, which is not observed.

Acknowledgments—We thank Professor DAVID WONES of M.I.T. for making possible the vitrification experiments. Mr. JEAN LARSEN and Miss CLAUDIA GELLERT assisted with the laboratory measurements at C.R.I. This work was supported by NASA grants and contracts (NGR-22-009-350, NGR-52-083-003, and NAS 9-9478).

REFERENCES

- ADAMS J. B. (1968) Lunar and martian surfaces: Petrologic significance of absorption bands in the near-infrared. *Science* **159**, 1453–1455.
- ADAMS J. B. and FILICE A. L. (1967) Spectral reflectance 0.4 to 2.0 microns of silicate rock powders. *J. Geophys. Res.* **72**, 5705–5715.
- ADAMS J. B. and JONES R. L. (1970) Spectral reflectivity of lunar samples. *Science* **167**, 737–739.
- ADAMS J. B. and MCCORD T. B. (1970) Remote sensing of lunar surface mineralogy: Implications from visible and near-infrared reflectivity of Apollo 11 samples. *Proc. Apollo 11 Lunar Sci. Conf., Geochim. Cosmochim. Acta Suppl.* 1, Vol. 3, pp. 1937–1945. Pergamon.

- ADAMS J. B. and McCORD T. B. (1971) Alteration of lunar optical properties: Age and composition effects. *Science* **171**, 567-571.
- ALBEE A. L., BURNETT D. S., CHODOS A. A., EUGSTER J. C., HUNEKE D. A., PAPANASTASSIOU F. A., PODOSEK G., PRICE RUSS, III, SANS H. G., TERA F., and WASSERBURG G. J. Ages, irradiation history, and chemical composition of lunar rocks from the Sea of Tranquility. *Science* **167**, 463-466.
- BANCROFT G. M. and BURNS R. G. (1967) Interpretation of the electronic spectra of iron in pyroxenes. *Amer. Mineral.* **52**, 1278-1287.
- BORG J., DURRIEU L., JOURET C., and MAURETTE M. (1971) The ultramicroscopic irradiation record of micron-sized lunar dust grains. Second Lunar Science Conference (unpublished proceedings).
- CONEL J. E. (1970) Coloring of synthetic and natural lunar glass by titanium and iron. *Jet Propulsion Laboratory Space Programs Summary* 37-62. Vol. 3, pp. 26-31.
- CONEL J. E. and NASH D. B. (1970) Spectral reflectance and albedo of Apollo 11 lunar samples: Effects of irradiation and vitrification and comparison with telescopic observations. *Proc. Apollo 11 Lunar Sci. Conf., Geochim. Cosmochim. Acta Suppl.* 1, Vol. 3, pp. 2013-2023. Pergamon.
- DRAKE M. J., McCALLUM I. S., MCKAY G. A., and WEIL D. F. (1970) Mineralogy and petrology of Apollo 12 sample no. 12013: A progress report. *Earth Planet. Sci. Lett.* **9**, 103-123.
- FREDRIKSSON K., NELEN J., and MELSON W. G. (1970) Petrography and origin of lunar breccias and glasses. *Proc. Apollo 11 Lunar Sci. Conf., Geochim. Cosmochim. Acta Suppl.* 1, Vol. 1, pp. 419-432. Pergamon.
- FRONDEL C., KLEIN C., JR. ITO J., and DRAKE J. C. (1970) Mineralogical and chemical studies of Apollo 11 lunar fines and selected rocks. *Proc. Apollo 11 Lunar Sci. Conf., Geochim. Cosmochim. Acta Suppl.* 1, Vol. 1, pp. 445-474. Pergamon.
- GAST P. W. and HUBBARD N. J. (1971) Rare earth abundances in soil and rocks from the Ocean of Storms. Second Lunar Science Conference (unpublished proceedings).
- GOLD T., CAMPBELL M. J., and O'LEARY B. T. (1970) Optical and high-frequency electrical properties of the lunar sample. *Proc. Apollo 11 Lunar Sci. Conf., Geochim. Cosmochim. Acta Suppl.* 1, Vol. 3, pp. 2149-2154. Pergamon.
- GOLDSTEIN J. I., HENDERSON E. P., and YAKOWITZ H. (1970) Investigation of lunar metal particles. *Proc. Apollo 11 Lunar Sci. Conf., Geochim. Cosmochim. Acta Suppl.* 1, Vol. 1, pp. 499-512. Pergamon.
- HAPKE B. W., COHEN A. J., CASSIDY W. A., and WELLS E. N. (1970) Solar radiation effects on the optical properties of Apollo 11 samples. *Proc. Apollo 11 Lunar Sci. Conf., Geochim. Cosmochim. Acta Suppl.* 1, Vol. 3, pp. 2199-2212. Pergamon.
- HAPKE B. W., CASSIDY W. A., and WELLS E. N. (1971) The albedo of the Moon: Evidence for vapor-phase deposition processes on the lunar surface. Second Lunar Science Conference (unpublished proceedings).
- HERZENBERG C. L. and RILEY D. L. (1970) Analysis of first returned lunar samples by Mössbauer spectrometry. *Proc. Apollo 11 Lunar Sci. Conf., Geochim. Cosmochim. Acta Suppl.* 1, Vol. 3, pp. 2221-2241. Pergamon.
- LSPET (Lunar Sample Preliminary Examination Team) (1969) Preliminary examination of the lunar samples from Apollo 11. *Science* **165**, 1211-1227.
- LSPET (Lunar Sample Preliminary Examination Team) (1970) Preliminary examination of the lunar samples from Apollo 12. *Science* **167**, 1325-1339.
- McCORD T. B., CHARETT M., JOHNSON T. V., LEBOSKY L., and PIETERS C. (1971) *Lunar Spectral Types*. In preparation.
- MCKAY D. S., GREENWOOD W. R., and MORRISON D. A. (1970) Origin of small lunar particles and breccia from the Apollo 11 site. *Proc. Apollo 11 Lunar Sci. Conf., Geochim. Cosmochim. Acta Suppl.* 1, Vol. 1, pp. 673-694. Pergamon.
- MCKAY D., MORRISON D., LINDSAY J., and LADLE G. (1971) Second Lunar Science Conference (unpublished proceedings).
- NASH D. B. and CONEL J. E. (1971) Luminescence and reflectance of Apollo 12 samples. Second Lunar Science Conference (unpublished proceedings).
- O'LEARY B. T. and BRIGGS F. (1970) Optical properties of Apollo 11 moon samples. *J. Geophys. Res.* **75**, 6532.

- STRANGWAY D. W., LARSON E. E., and PEARCE G. W. (1970) Magnetic studies of lunar samples—breccia and fines. *Proc. Apollo 11 Lunar Sci. Conf., Geochim. Cosmochim. Acta Suppl.* 1, Vol. 3, pp. 2435–2451. Pergamon.
- WARNER J. (compiler) (1970) Apollo 12 Lunar-sample information. *NASA Technical Report R-353*.
- WOOD J. A., DICKEY J. S., MARVIN U. B., and POWELL B. N. (1970) Lunar anorthosites and a geophysical model of the moon. *Proc. Apollo 11 Lunar Sci. Conf., Geochim. Cosmochim. Acta Suppl.* 1, Vol. 1, pp. 965–988. Pergamon.
- WOOD J. A., MARVIN U. B., REID J. B., TAYLOR G. J., BOWER J. F., POWELL B. N., and DICKEY J. S., JR. (1971) Relative proportions of rock types, and nature of the light-colored lithic fragments in Apollo 12 soil samples. Second Lunar Science Conference (unpublished proceedings).